

ATMOS Research & Consulting

ANNE STONER and KATHARINE HAYHOE



Climate Impact Assessment for the City of Houston

AUGUST 2020



Table of Contents

LIST OF FIGURES	3
ACRONYMS AND ABBREVIATIONS	4
PREFACE	5
ABOUT THIS ASSESSMENT	6
EXECUTIVE SUMMARY	7
INTRODUCTION	9
ONE. GLOBAL CLIMATE CHANGE: PAST, PRESENT AND FUTURE.....	9
TWO. OBSERVED CHANGES IN THE U.S. AND GULF COAST	12
THREE. PROJECTED FUTURE CHANGES IN THE U.S. AND GULF COAST REGION	17
CLIMATE TRENDS AND PROJECTIONS	21
ONE. PROJECTED CHANGES IN AVERAGE TEMPERATURE, THE LENGTH OF SUMMER, AND HEATING AND COOLING DEGREE-DAYS.....	21
TWO. CHANGES IN EXTREME TEMPERATURES	31
THREE. CHANGES IN ANNUAL AND SEASONAL PRECIPITATION AND DRY DAYS	37
FOUR. CHANGES IN EXTREME PRECIPITATION.....	42
FIVE. REGIONAL VARIABILITY.....	46
SIX. CONCLUSIONS AND SUMMARY	48
DATA, MODELS, AND METHODS	52
ONE. OBSERVED DATA.....	52
TWO. CLIMATE INDICATORS.....	52
THREE. FUTURE SCENARIOS.....	54
FOUR. GLOBAL CLIMATE MODELS AND EMPIRICAL-STATISTICAL DOWNSCALING	55
FIVE. SOURCES OF UNCERTAINTY IN FUTURE PROJECTIONS	58
PRODUCTS	61
ONE. DAILY STATION-BASED CLIMATE PROJECTIONS - DATA	61
TWO. ANNUAL STATION-BASED CLIMATE INDICATORS - DATA.....	61
THREE. MULTI-MODEL MEAN AND RANGES OF STATION-BASED CLIMATE INDICATORS FOR THE HIGHER AND LOWER FUTURE SCENARIOS – DATA AND TIME SERIES PLOTS	61
APPENDICES	64
APPENDIX A: CLIMATE INDICATOR TIME SERIES FOR WEATHER STATIONS	64
APPENDIX B: CLIMATE INDICATOR BAR CHARTS FOR WEATHER STATIONS	64
APPENDIX C: CLIMATE INDICATOR BAR CHARTS FOR WEATHER STATIONS – RETURN FREQUENCY OF THE 24-HOUR 100-YEAR PRECIPITATION EVENT	64
REFERENCES	65

List of Figures

Figure 1 Human and natural factors influencing Earth's climate	11
Figure 2 Historical billion dollar weather and climate disasters	12
Figure 3 Observed changes in US annual, winter, and summer temperature	14
Figure 4 Observed changes in US annual and seasonal precipitation.....	15
Figure 5 Observed local relative sea level trends	16
Figure 6 Projected changes in US annual average temperatures	17
Figure 7 Projected change in total seasonal precipitation.....	18
Figure 8 Projected sea level in the Houston area under 4°C (7.2°F) and 2°C (3.6°F) of global warming	20
Figure 9 Projections in the timing of the first day, the last day, and the length of summer (time series).....	25
Figure 10 Projections in the timing of the first day, the last day, and the length of summer (bar charts)	26
Figure 11 Projections in cooling degree days (time series).....	27
Figure 12 Projections in cooling degree days (bar charts).....	28
Figure 13 Projections in heating degree days (time series)	29
Figure 14 Projections in heating degree days (bar charts).....	30
Figure 15 Projections in days above 100°F and nights above 80°F (time series).....	33
Figure 16 Projections in days above 100°F and nights above 80°F (bar charts)	34
Figure 17 Projections in temperature of the hottest day and week, and length of the longest heatwave (time series).....	35
Figure 18 Projections in temperature of the hottest day and week, and length of the longest heatwave (bar charts).....	36
Figure 19 Projections in annual precipitation and number of dry days (time series)	38
Figure 20 Projections in annual precipitation and number of dry days (bar charts).....	39
Figure 21 Projections in seasonal precipitation (time series).....	40
Figure 22 Projections in seasonal precipitation (bar charts).....	41
Figure 23 Projections in the wettest 3-day precipitation amounts and the number of events per year above 4 inches (time series)	44
Figure 24 Projections in the wettest 3-day precipitation amounts and the number of events per year above 4 inches (bar charts).....	45
Figure 25 Projections in the 12-month SPEI drought index.....	46
Figure 26 Map of the 11 weather stations.....	53
Figure 27 Historical and future carbon emissions.....	55
Figure 28 Downscaling: importance of spatial scale.....	57
Figure 29 Projected changes in four different climate indicators	63

Acronyms and Abbreviations

CDDs:	Cooling Degree-Days
CMIP5:	The Coupled Model Intercomparison Project version 5
GCM:	Global Climate Model
GHCN:	Global Historical Climatology Network
HDDs:	Heating Degree-Days
IPCC:	Intergovernmental Panel on Climate Change
NCA4:	Fourth U.S. National Climate Assessment
NOAA:	National Oceanic and Atmospheric Administration
RCP4.5:	Representative Concentration Pathway 4.5 is a lower scenario where human-caused increases in radiative forcing reach 4.5 W/m ² by the year 2100
RCP8.5:	Representative Concentration Pathway 8.5 is a higher scenario where human-caused increases in radiative forcing reach 8.5 W/m ² by the year 2100
SPEI:	Standardized Precipitation-Evapotranspiration Index
WMO:	World Meteorological Organization

Preface

Houston's Climate Impact Assessment was a collaboration between the City's Chief Resilience Officer and Chief Sustainability Officer and was made possible through generous funding from C40 Cities, a network of the world's megacities committed to addressing climate change. The Climate Impact Assessment was identified in 2019 by both teams as a critical component to creating a safer, more resilient and sustainable Houston. This Assessment further links the City's first resilience strategy, *Resilient Houston*, released in February 2020 and the City's first climate action plan, *Houston Climate Action Plan*, released on the 50th Earth Day in April 2020. The climate science and data within will help inform, guide, and prioritize the implementation of both plans and engage Houstonians in climate mitigation and adaptation education and action.

About This Assessment

Global climate is changing due to human activities and at a rate unprecedented in modern times. These changes have important and, in some cases, unique implications for human systems and society. “Human society is built on the implicit assumption that climate is largely stationary: that historical records can be used with confidence to determine the energy loads of our buildings, the hundred-year floodplains of our cities, and the growing zones for the crops that power our economy and feed our world. What happens when that assumption is no longer valid?” ask Hayhoe and Kopp (2016).

In 2020, the City of Houston released its first Resilient Houston strategy and Houston's Climate Action Plan. Together, these form a framework for the city to adapt to and mitigate climate change. As called for in Resilient Houston, this Climate Impact Assessment is a necessary next step for better understanding the heat, drought, and precipitation risks associated with climate change as well as the clear need to reduce and capture emissions of carbon dioxide, methane, and other heat-trapping gasses through energy transition, transportation, building optimization and materials management.

This assessment quantifies how climate is changing across the U.S., the Gulf Coast region, and for Houston in particular. It summarizes observed and projected changes in temperature and precipitation for 11 long-term weather stations across the greater Houston area, and translates these into 25 different climate indicators, from the temperature of the hottest day of the year to projected changes in heavy precipitation. This information will be used by the City and partners in the next phases of the Climate Impact work, including:

- Implementation of *Resilient Houston* focused on a healthy place to live, and equitable, inclusive and affordable city, a leader in climate adaptation, a city that grows up, not out, and a transformational economy that builds forward. Using this Climate Impact Assessment to inform City policies and programs is specifically called for by Action 32.
- Implementation of Houston's *Climate Action Plan* focused on transportation, energy transition, building optimization, and materials management.

Executive Summary

Houston's climate is already changing and many of the observed changes are projected to continue and even accelerate over the rest of this century. This report summarizes observed and projected changes in temperature and precipitation for 11 weather stations across the greater Houston area from 1950 through 2100. Temperature and precipitation projections are shown for a lower and higher future scenario that encompass a range of likely futures as a result of human choices and resulting greenhouse gas emissions.

Since 1950, the city of Houston has experienced significant increases in **annual average temperature**, in the number of **hot days** with temperature above 100°F, in the number of **warm nights** with temperature above 80°F, and in **cooling degree-days**, a measure of air conditioning needs. In addition, summer now begins earlier and ends later in the year.

Over the rest of this century, projected future changes for Houston include:

- Increases in the average temperature of all seasons
- Lengthening of summer, with summer beginning earlier and ending later
- Increases in energy demand for cooling buildings for the spring, summer, and fall seasons
- Increases in the number of hot days per year (defined here as maximum temperature above 100°F) and the number of warm nights per year (defined here as minimum temperature above 80°F)
- Increases in the temperature of the hottest days experienced each year
- Longer multi-day heatwaves
- Little change in total annual precipitation but a decrease in summer precipitation and increase in fall precipitation
- Greater variability in day-to-day precipitation that includes both slight increases in number of dry days and increasing risk of drought due to soil moisture decreases resulting from higher temperatures, as well as increases in the precipitation falling during extreme precipitation events such as the wettest three-day period each year.

Projected changes have important implications for future planning with respect to Houston's infrastructure, its energy and water resources, its public services, and the health and welfare of its inhabitants. For both temperature and precipitation, the changes reported here are consistent with those projected to occur throughout the Gulf Coast region in response to human-induced climate change. The projections are appropriate for use in scientific analyses to quantify the impacts of climate change on both human and natural systems across the region, and to inform long-term planning, education, and outreach regarding climate adaptation and resilience in the region.

This assessment does not analyze observed or projected changes in hurricanes, coastal storms, or sea level. Instead, it provides a brief summary based on the scientific literature and the Fourth U.S. National Climate Assessment (NCA4) [Volume 1](#) and [Volume 2](#).

Assessment Outline

The **Introduction** to this report introduces the topic of climate change and its causes, both human and natural. It describes historical extreme weather events that have impacted Houston and the attribution of extreme events to human-induced climate change. It concludes by summarizing findings from NCA4 and from the scientific literature on observed and projected changes in temperature, precipitation, hurricanes and sea level across the U.S. and the Gulf Coast region in general.

The **Climate Trends and Projections** section focuses in on the city of Houston, analyzing historical and projected temperature and precipitation trends in 25 different climate indicators, from the temperature of the hottest day of the year to projected changes in heavy precipitation, at 11 long-term weather stations across the greater Houston area. Historical trends are based on daily observations collected at these weather stations. Future projections are based on simulations from an ensemble of global climate models (GCMs) from the Coupled Model Intercomparison Project version 5 (CMIP5). Future projections are based on two different scenarios: the lower Representative Concentration Pathway (RCP) scenario RCP4.5 and the higher RCP8.5. The lower RCP4.5 scenario represents a future where the majority of the world follows the stated goal of the city of Houston to meet its Paris Agreement targets, transitioning to clean energy sources and reducing carbon emissions. In contrast, the higher RCP8.5 scenario represents a future where fossil fuel use and carbon emissions continue to increase through the end of the century, tracking historical trends to date. Global climate model output for each scenario statistically downscaled to each of 11 Houston weather stations is compared to observations for two historical periods (1971-1990, 2001-2020) and used to calculate projected values for three future 20-year periods (2021-2040, 2051-2070, 2081-2100).

The **Data, Models and Methods** section describes the observational data used, how the climate indicators were defined, how historical trends were calculated, and how the future projections were generated. It also describes the global climate models, scenarios, and empirical-statistical downscaling models used. It concludes by discussing the sources of uncertainty in future projections and how these were addressed in this report.

The **Products** section describes the outputs that are available for use in scientific analyses, impact modeling, long-term planning, education, and outreach. They include data files, bar charts, and time series.

The **Appendices** contain figures and data for all of the 11 stations included in the study. Sample figures are included in this report to illustrate projected changes for a single weather station (Houston Hobby Airport). The complete set of observed and projected future indicator values for individual weather stations by year is available in PDF format in *Appendix A: Climate Indicator Time Series for Weather Stations*, the complete set of bar charts of observed and projected future indicator values is available in PDF format in *Appendix B: Climate Indicator Bar Charts for Weather Stations*, and a complete set of bar charts of the 24-hour 100-year precipitation events showing projections for individual global climate models is available in PDF format in *Appendix C: Climate Indicator Bar Charts for Weather Stations - Return Frequency of the 24-hour 100-year Precipitation Event*.

Introduction

ONE. Global Climate Change: Past, Present and Future

Climate is changing. Since 1900, global mean temperature has increased by about 1.8°F (1°C) and global mean sea level has risen by about 7-8 inches (16-21 cm; Hayhoe et al. 2018). In addition, sea ice in the Arctic is decreasing, ice loss from Greenland and Antarctica is accelerating, permafrost is thawing, and heavy rainfall and extreme heat is becoming more frequent in many locations (Hartmann et al. 2013; Knutson et al. 2017; Vose et al. 2017; Easterling et al. 2017; Sweet et al. 2017; Taylor et al. 2017). The *Fourth U.S. National Climate Assessment* (NCA4) describes these and other observed changes that are occurring across the Gulf Coast region, North America and the world.

This change is unprecedented in the history of modern civilization. Over the last two thousand years, climate changed relatively little at the global scale. Relative to the long-term average, global temperature varied by less than $\pm 0.9^\circ\text{F}$ ($\pm 0.5^\circ\text{C}$; Masson-Delmotte et al. 2013). As a result, many human systems, including infrastructure, agriculture, and the allocation and use of natural resources, are based on the assumption of a relatively stable climate. In other words, it is assumed that past conditions experienced over long-term, climatic time scales provide a reliable guide for planning for the future. This assumption underlies building codes, urban plans, infrastructure design and maintenance, agricultural methods, long-term water plans, flood zone delineation, and more.

Today, however, the global climate is changing at a rate that is unprecedented over the history of human civilization. NCA4 concludes, “global climate continues to change rapidly compared to the pace of the natural variations in climate that have occurred throughout Earth’s history,” and “global annual averaged temperatures for 1986–2015 are likely much higher, and appear to have risen at a more rapid rate during the last 3 decades, than any similar period possibly over the past 2,000 years or longer” (Wuebbles et al. 2017).

Climate is defined as the statistics of weather averaged over a relatively long period of time. The World Meteorological Organization (WMO) uses a 30-year period to define *climate normals*, “reference points used by climatologists to compare current climatological trends to that of the past or what is considered 'normal'.” Thirty years is typically used for historical trends because this period has historically been “long enough to filter out any interannual variation or anomalies, but also short enough to be able to show longer climatic trends.” (WMO, 2014) This report uses climatic periods of 20 years, a shorter period better able to capture the changes in climate that are occurring while still averaging over a period sufficient to encompass a broad range of natural variability.

Although a 1.8°F increase in the global mean temperature may not sound significant, this change has already increased the magnitude and/or the frequency of many different types of extreme events (Hayhoe et al. 2018); it is driving the migration or invasion of plants and animals into areas they did not inhabit previously (Lipton et al. 2018); and it is affecting many aspects of human society, from water and energy resources to food production to the integrity of infrastructure and public services (Gowda et al. 2018; Lall et al. 2018; Maxwell et al. 2018; Zamuda et al. 2018). If observed and future changes are not accounted for in future planning, many human and natural systems may become stressed or even fail.

Humans are responsible. Climate has historically varied due to natural causes including the internal variability of the climate system and changes in solar output, orbital cycles, volcanic eruptions and other geologic activity. Natural factors still influence climate today. However, as can be clearly seen in Figure 1, human emissions of greenhouse gases from combustion of fossil fuels and land use change now overwhelm their influence on Earth's climate.

In reference to observed warming since 1900, NCA4 concludes, “there are no convincing alternative explanations [other than human agency] supported by the extent of the observational evidence” (Wuebbles et al. 2017) and expands on this, stating, “observational evidence does not support any credible natural explanations for this amount of warming; instead, the evidence consistently points to human activities, especially emissions of greenhouse or heat-trapping gases, as the dominant cause” (Hayhoe et al. 2018).

Regarding natural factors, NCA4 states: “We find no convincing evidence that natural variability can account for the amount of global warming observed over the industrial era. Solar output changes and internal variability can only contribute marginally to the observed changes in climate over the last century, and we find no convincing evidence for natural cycles in the observational record that could explain the observed changes in climate” (Wuebbles et al. 2017). Instead, the dominant factor causing climate to change today is human activities, specifically human emissions of carbon dioxide and other heat-trapping gases released during fossil fuel combustion, deforestation, agriculture and other activities.

Human choices will determine how much more climate changes. Some additional amount of future change is inevitable, due to human choices that have already been made and human emissions that have already occurred. This is the result of two different types of lags. The first lag is in the physical climate system, in responding to human emissions of heat-trapping that have already occurred. This is analogous to the lag in the response of the human body to, for example, poor lifestyle choices such as diet or smoking. The second lag is in the energy sector, in transitioning from traditional fossil-based energy to low or zero-carbon energy. Although policies may be put in place near-term, it takes some time for the infrastructure and for heat-trapping gases to be altered in response.

A significant amount of future change, however, can be avoided by reducing and eventually eliminating carbon emissions from human activities, compared to continuing to rely on fossil fuels. NCA4 emphasizes the importance of human choices in determining the magnitude of future change, stating, “beyond the next few decades, the magnitude of climate change depends primarily on cumulative emissions of greenhouse gases and aerosols and the sensitivity of the climate system to those emissions (high confidence).” (Hayhoe et al. 2017) It is estimated that, “with significant reductions in emissions, global temperature increase could be limited to 2°C [3.6°F] or less compared to preindustrial temperatures [but] without significant reductions, annual average temperatures could increase by 5°C [9°F] or more by the end of this century compared to preindustrial temperatures.” (Hayhoe et al. 2018)

Our future is in our hands. This report tracks observed changes in the greater Houston area that are consistent with those occurring at the regional, state, and national scale. It also summarizes projections corresponding to a higher and a lower possible future, depending on the choices the world makes. This information can be used to prepare for or adapt to future change, as well as to quantify the benefits of policies like the City of Houston's Climate Action Plan to reduce heat-trapping gas emissions and avert future impacts. More information on the future scenarios used in this report, which are also used in the *Fourth U.S. National Climate Assessment*, and the Intergovernmental Panel on Climate Change's *Fourth* and *Fifth Assessment Reports*, is provided in the **Data, Models, and Methods** section.

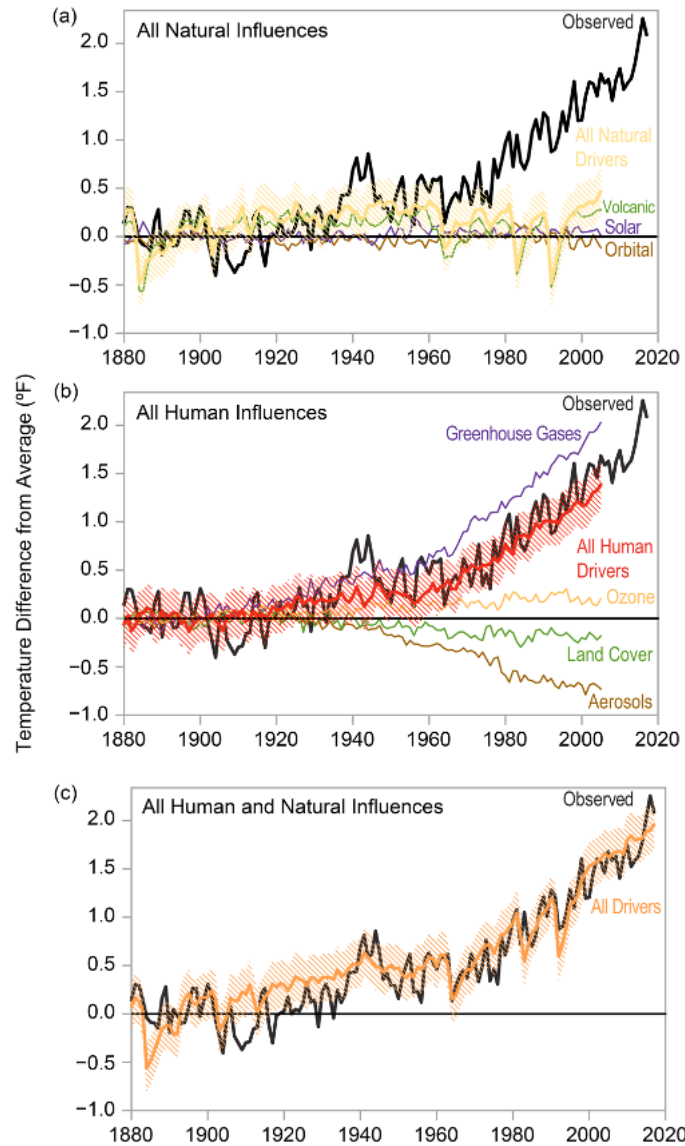


Figure 1 Both human and natural factors influence Earth's climate, but the long-term global warming trend observed over the past century can only be explained by the effect that human activities have had on the climate.

(a) The temperature changes simulated by a climate model when only natural factors (yellow) are considered. The other lines show the individual contributions to the overall effect from observed changes in Earth's orbit (brown), the amount of incoming energy from the sun (purple), and changes in emissions from volcanic eruptions (green). Note that no long-term trend in globally averaged surface temperature over this time period would be expected from natural factors alone.

(b) The simulated changes in global temperature when considering only human influences (dark red), including the contributions from emissions of greenhouse gases (purple) and small particles (referred to as aerosols, brown) as well as changes in ozone levels (orange) and changes in land cover, including deforestation (green). Changes in aerosols and land cover have had a net cooling effect in recent decades, while changes in near-surface ozone levels have had a small warming effect. These smaller effects are dominated by the large warming influence of greenhouse gases such as carbon dioxide and methane. Note that the net effect of human factors (dark red line) explains most of the long-term warming trend.

(c) The temperature change (orange) simulated by a climate model when both human and natural influences are included. The result matches the observed temperature record closely, particularly since 1950, making the dominant role of human drivers plainly visible. Researchers do not expect climate models to exactly reproduce the specific timing of actual weather events or short-term climate variations, but they do expect the models to capture how the whole climate system behaves over long periods of time. The simulated temperature lines represent the average values from a large number of simulation runs. The orange hatching represents uncertainty bands based on those simulations. For any given year, 95% of the simulations will lie inside the orange bands. Source: Fourth U.S. National Climate Assessment, Volume 2, Chapter 2, Figure 2.1 (Hayhoe et al. 2018).

TWO. Observed Changes in the U.S. and Gulf Coast

Southern Great Plains and the Gulf Coast have a highly variable climate with frequent weather extremes. Average temperature across Texas can vary by about 3°F from one year to the next and annual precipitation by as much as 25 inches from year to year. The region also experiences a wide array of extreme weather and climate events, including heatwaves, prolonged droughts, intense rainfall events, hurricanes, and flood. According to NOAA, as of July 2020 the state of Texas had experienced 119 climate and weather events since 1980 that caused at least one billion dollars' worth of damage each (Figure 2, Smith et al. 2020). This is more than any other state.

1980-2020* Billion-Dollar Weather and Climate Disasters (CPI-Adjusted)

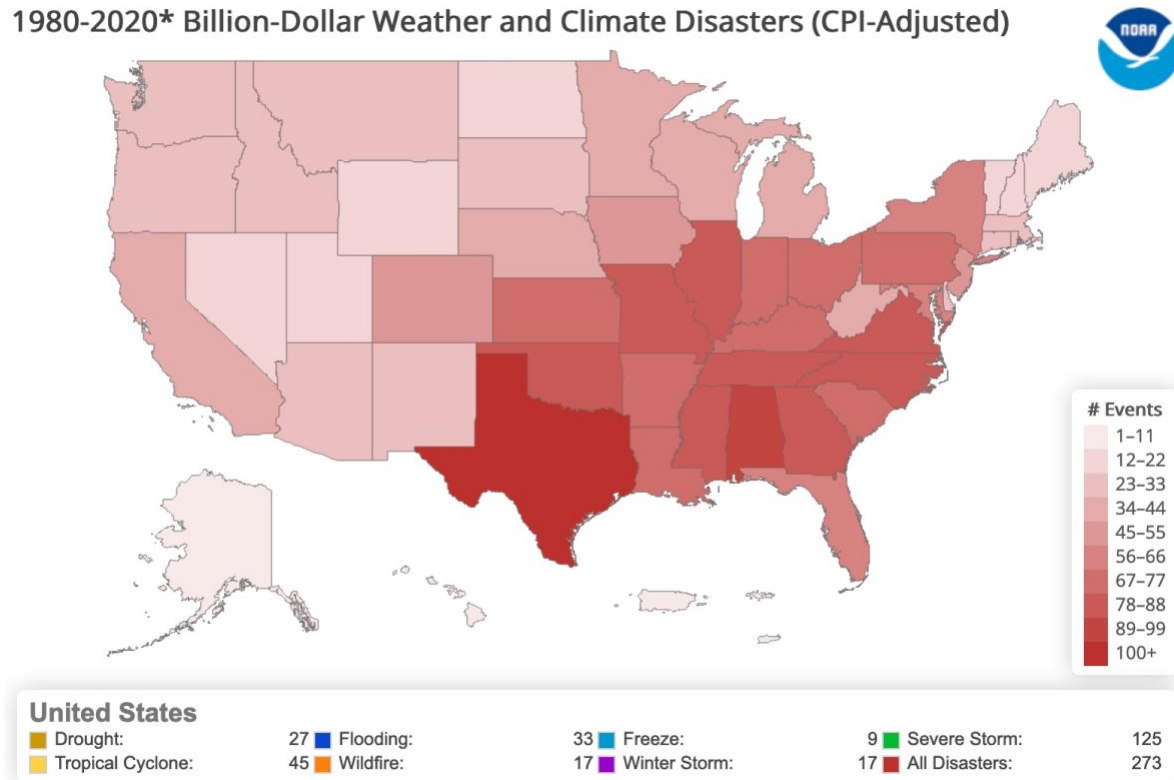


Figure 2 From 1980-2020 (as of July 8, 2020), there have been 273 weather/climate disaster events with losses exceeding \$1 billion (CPI-Adjusted) each to affect the United States. These events included 27 drought events, 33 flooding events, 9 freeze events, 125 severe storm events, 45 tropical cyclone events, 17 wildfire events, and 17 winter storm events (source: NOAA National Centers for Environmental Information (NCEI) U.S. Billion-Dollar Weather and Climate Disasters (2020), Smith et al., 2020).

The Houston area has been impacted by many of these climate and weather extremes. In 2011, for example, Texas experienced a record-breaking drought. According to the Texas A&M Forest Service, the 2011 drought killed over 300 million trees across Texas, including about half the trees in Houston's Memorial Park. Referring to over 1,000 leaks in Houston's water lines that occurred during the drought, a Texas Public Comptroller of Accounts report stated that "the 2011 drought caused considerable damage to infrastructure (Combs, 2012). Much of Texas is covered in clay-rich soils that swell when wet and shrink when soil moisture evaporates. That shrinkage can cause the soil to buckle, damaging foundations, roads and water and sewer lines."

Extreme precipitation events have also caused significant flood-related damages to the city of Houston and surrounding area. The Harris County Flood Control District was originally founded in response to a devastating 1935 flood. More recently, the 2015 Memorial Day floods occurred when some locations received as much as 11 inches of rain in less than a day in some locations, causing \$460M in damages. During the 2016 Tax Day Flood, Harris County averaged nearly 8 inches of rain. Some locations received between 12 to 16 inches of rain in two days, and it's estimated that damages to water control infrastructure alone totaled \$65 million. More recently, the 2018 Independence Day flood resulted in damages of \$84 million in water control infrastructure.

Houston is also vulnerable to hurricanes and tropical storms. The Galveston hurricane of 1900 was responsible for an estimated 6,000 to 12,000 deaths, making it the deadliest natural disaster in U.S. history. The Greater Houston area were severely damaged by Hurricane Alicia in 1983, which caused \$2.6 billion in damages and 13 deaths. In 2001 Hurricane Allison made landfall near Freeport and stalled for several days causing severe flooding in the Houston area and an estimated \$4.8 billion in damages and 23 deaths. Hurricane Rita made landfall on the border between Texas and Louisiana in September 2005 and caused severe flooding northeast of Houston in Beaumont and Port Arthur, widespread power outages, damage to offshore oil platforms, and 59 deaths. Throughout Hurricane Rita's path through Texas and Louisiana the storm caused \$18.5 billion in damages.

The most destructive hurricane in Southeast Texas' recent past was Hurricane Harvey, which made landfall near Rockport in August 2017. The storm stalled in the region for several days producing unprecedented catastrophic flooding in Houston and Harris County and surrounding counties, with some areas receiving more than 40 inches of rain over a four-day period. The storm caused damages estimated around \$126 billion, making it the costliest tropical cyclone worldwide. Another tropical storm that caused widespread and record-breaking rainfall and flooding was Hurricane Imelda, which made landfall near Freeport in September 2019, causing damages estimated to have exceeded \$5 billion.

The region's temperature is changing. Annual average temperature has increased across the Gulf Coast region by 0.76°F over the past 30 years (1986-2016) compared with the first half of the century (1901-1960), with nighttime temperatures increasing faster than daytime temperatures, by 0.96°F and 0.56°F, respectively, over the same period (Vose et al. 2017).

The temperature trend for the Southern Great Plains is smaller than the average for the contiguous U.S., which has seen an increase of 1.23°F in the annual average temperature (Figure 3). However, it is still significant relative to the long-term average and it is consistent with the observed trends that are occurring at the regional to global scale as a result of human-caused climate change. Although less than a degree of warming may not sound like much, over the typical human lifetime and that of much of our infrastructure the long-term average temperature of a region is historically as stable as the temperature of the human body. Even a one-degree increase can have a noticeable impact.

Nationwide, the number of heat waves per year has increased from an average of 2 per year in the 1960s to an average of 6 per year in the 2010s and the average length of the heat wave season has increased from 3 weeks per year in the 1960s to 10 weeks per year in the 2010s (USGCRP [Heatwaves](#)).

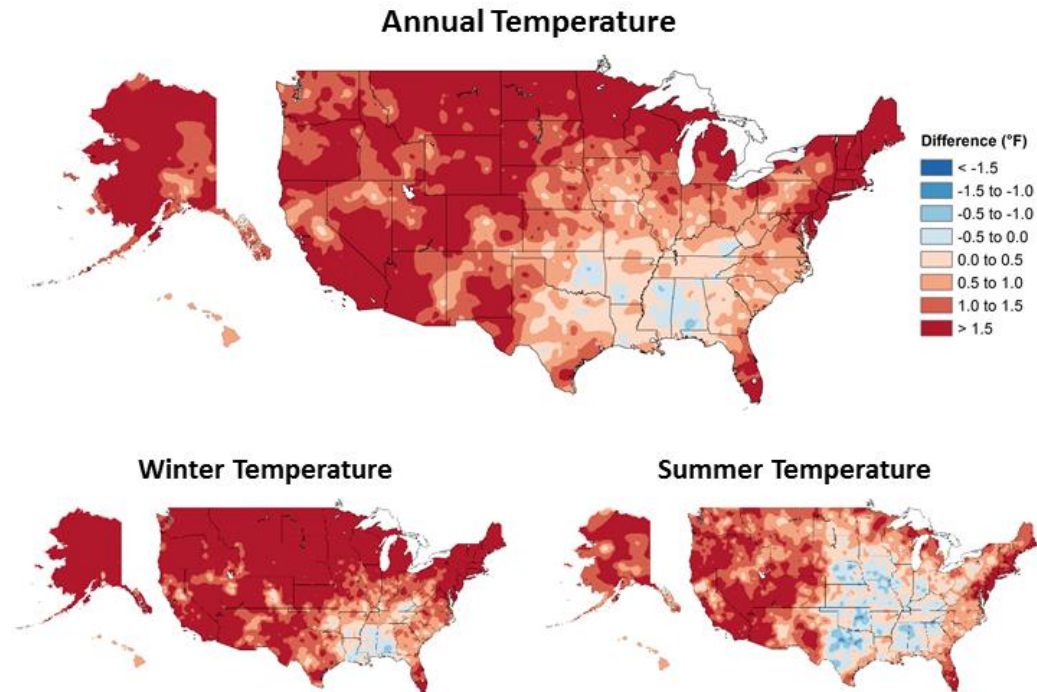


Figure 3 Observed changes in annual, winter, and summer temperature (°F). Changes are the difference between the average for present-day (1986–2016) and the average for the first half of the last century (1901–1960 for the contiguous United States, 1925–1960 for Alaska and Hawai'i) Source: Fourth U.S. National Climate Assessment, Volume 1, Chapter 6, Figure 6.1 (Vose et al. 2017).

The region's precipitation is changing. Annual precipitation has increased over the central U.S. including eastern Texas (Easterling et al. 2017). However, this increase varies by season. The largest increases in precipitation for the Gulf Coast have occurred in fall, followed by winter and summer (see Figure 4, Easterling et al. 2017).

Extreme precipitation has also increased across the mid-latitudes in general and the contiguous U.S. specifically. This is also the result of the observed increase in temperature, as warmer air holds more water vapor. All else being equal, this increases the amount and the intensity of precipitation associated with a given storm, as temperature increases.

The Southern Great Plains has seen an increase of 12% in the amount of precipitation that fell within the 1% heaviest events between 1958–2016, and a 40% increase in the number of most extreme two-day rain events in five years (Easterling et al. 2017). Over the greater Houston area, observational data since 1880 shows that the intensity of extreme precipitation has increased by 12 to 22 percent (van Oldenborgh et al. 2017).

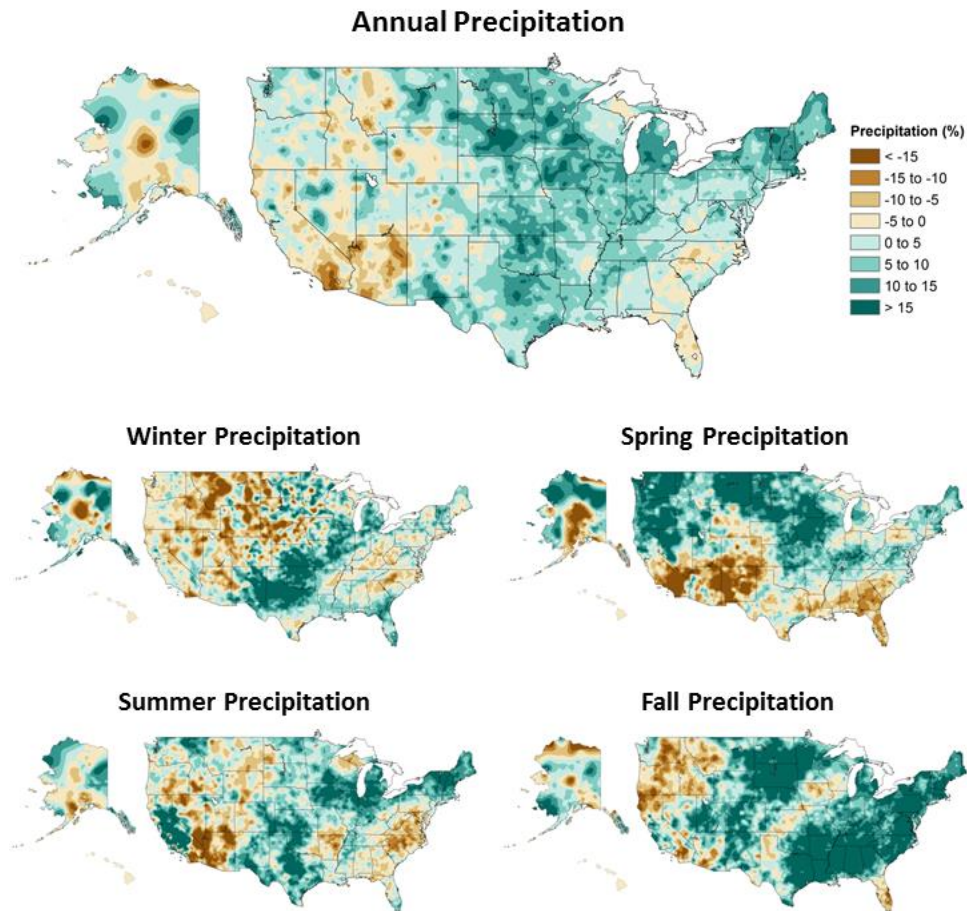


Figure 4 Annual and seasonal changes in precipitation over the United States. Changes are the average for present-day (1986–2015) minus the average for the first half of the last century (1901–1960 for the contiguous United States, 1925–1960 for Alaska and Hawai‘i) divided by the average for the first half of the century. Source: Fourth U.S. National Climate Assessment, Volume 1, Chapter 7, Figure 7.1 (Easterling et al. 2017).

Storms and hurricanes are being affected. Long-term, hurricanes are not becoming more frequent. However, they are being altered by increasing temperatures in other important ways. Observational data shows that hurricanes are intensifying faster; that they are becoming stronger, on average; and that they are also becoming bigger and slower (Kossin et al. 2017; Kloessel et al. 2018).

Warmer temperatures are also increasing the amount and the intensity of precipitation associated with a given storm. Hurricane Harvey was a record-breaking storm, with over 3 inches of rain per hour being recorded in some locations (Brauer et al. 2020), and total accumulation exceeding 50 inches in several locations in Galveston and Harris Counties (NWS 2017) and cutting-edge climate attribution studies have quantified the extent to which human-induced climate change may have contributed to its impact.

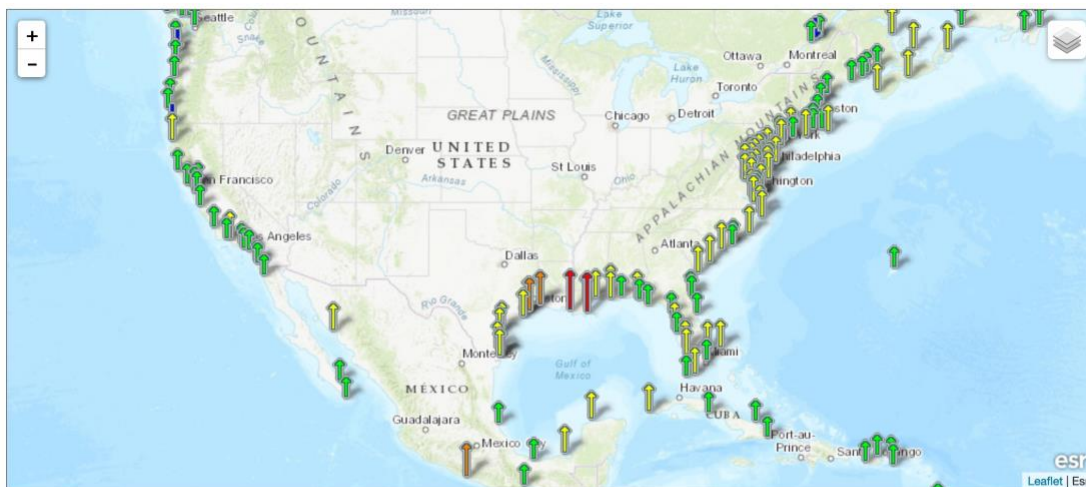
The intensity of precipitation during Hurricane Harvey was likely increased by about 15% and was about three times more likely as a result of a changing climate (van Oldenborgh et al. 2017). A slightly different analysis found that climate change increased the chances of that much precipitation occurring by about 3.5 times and that the total precipitation that occurred during the storm was increased by at least 19% with a best estimate of 38% compared to what would have happened if the same storm had occurred over background conditions that had

not been altered by human-induced climate change (Risser and Wehner 2017). The reason for this increased precipitation is clear: “Record high ocean heat values not only increased the fuel available to sustain and intensify Harvey but also increased its flooding rains on land. Harvey could not have produced so much rain without human-induced climate change,” Trenberth et al. (2018) conclude. And a new analysis on the economic costs of Hurricane Harvey estimates that at minimum, human-induced climate change was responsible for one-third of the economic damages associated with the storm, and more likely with two-thirds of them (Frame et al. 2020).

It is important to note that the impact of extreme weather and climate events can be exacerbated by local factors, many of them under human control, and Hurricane Harvey was no exception. Urbanization exacerbated the flood response and total rainfall, making floods as large as those observed during Hurricane Harvey 20 times more likely, Zhang et al. (2018) find.

Sea level is rising. Global mean sea level has risen by 8 to 9 inches since 1900 (Sweet et al. 2017, Lindsey 2020) and the rate of sea level rise has doubled as Greenland and Antarctica are melting six times faster than they did in the 1990s (Shepherd et al. 2020). The frequency of “nuisance” or sunny-day flooding at many locations along the U.S. coastline has increased by 5 to 10 times since the 1960s (Sweet et al. 2017).

Regional sea level change is a combination of global sea level rise, changes in ocean circulation that alter local sea levels, and the uplift or subsidence of the coastline. Along the Gulf Coast the land is primarily sinking and much of that subsidence is due to local human activities. According to the U.S. Geological Survey Texas Water Science Center Gulf Coast Program (USGS: [Subsidence](#)), “in the Houston-Galveston region, land subsidence is caused by compaction of fine-grained aquifer sediments (silts and clays) below the land surface due to groundwater withdrawals.” As a result, the relative rate of sea level rise in the Houston area is among the highest in North America, second only to Louisiana (Figure 5, NOAA: [Tides & Currents](#)).



The map above illustrates relative sea level trends, with arrows representing the direction and magnitude of change. Click on an arrow to access additional information about that station.

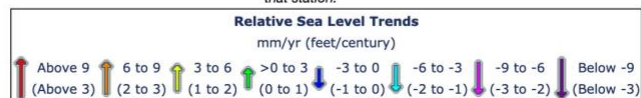


Figure 5 Observed local relative sea level trends measured by tide gauges with respect to local fixed reference on land. Source: NOAA: [Tides & Currents](#)).

THREE. Projected Future Changes in the U.S. and Gulf Coast Region

Temperature will continue to increase. Over coming decades, average temperatures across North America are projected to increase, more so for the higher scenario than the lower and temperature changes will be higher at higher latitudes (Figure 6).

The magnitude of future change depends on human emissions of heat-trapping gases and the response of the climate system to those emissions. Under a lower scenario, average annual temperature across the Gulf Coast region is projected to increase by 2-3°F by mid-century and 3-4°F towards the end of the century. Under a higher scenario, average annual temperature is projected to increase by 3-4°F by mid-century and 6-7°F towards the end of the century (Hayhoe et al. 2018). These projections are for the greater Gulf Coast region and can be moderated by topography, including proximity to large bodies of water, as well as by human development, such as urbanization. Houston-specific projections for average temperature are presented in the next section.

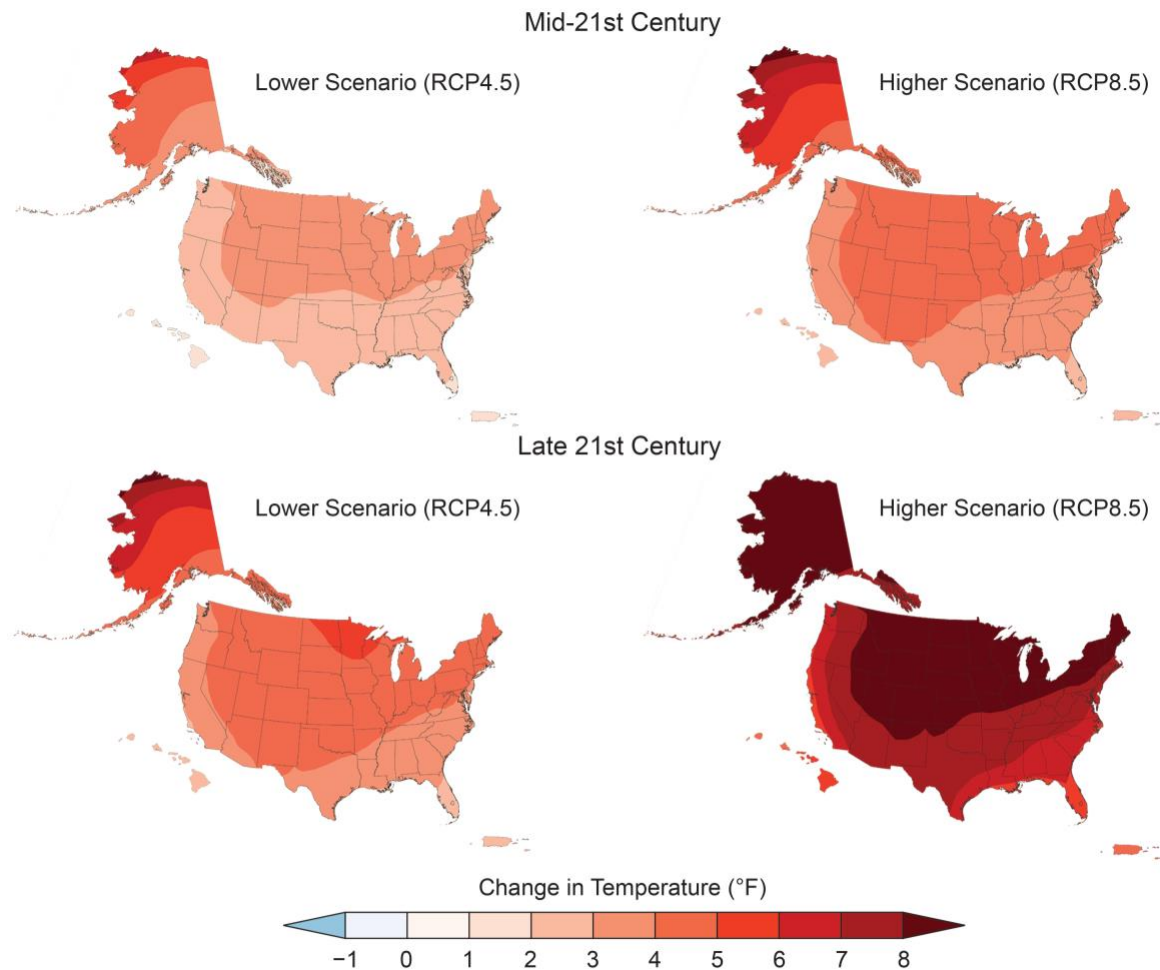


Figure 6 Projected changes in annual average temperatures (°F). Changes are the difference between the average for mid-century (2036–2065; top) or late-century (2070–2099, bottom) and the average for near-present (1986–2015). Each map depicts the weighted multi-model mean. Increases are statistically significant in all areas (that is, more than 50% of the models show a statistically significant change, and more than 67% agree on the sign of the change). Source: Fourth U.S. National Climate Assessment, Volume 2, Chapter 2, Figure 2.4 (Hayhoe et al. 2018).

Precipitation is projected to continue to change. As the climate changes, precipitation patterns are also expected to shift. In general, wetter areas are projected to become wetter and drier areas, drier, particularly during winter and spring (Figure 7). Precipitation may decrease by 10 to 15% in winter and spring across the Southern Great Plains and Gulf Coast region but the trends are not projected to be any larger or necessarily significant. Rather, larger and more significant trends are projected to occur in soil moisture as a result of increasing temperatures and evaporation (Wehner et al. 2017). Houston-specific projections for seasonal precipitation are presented in the next section.

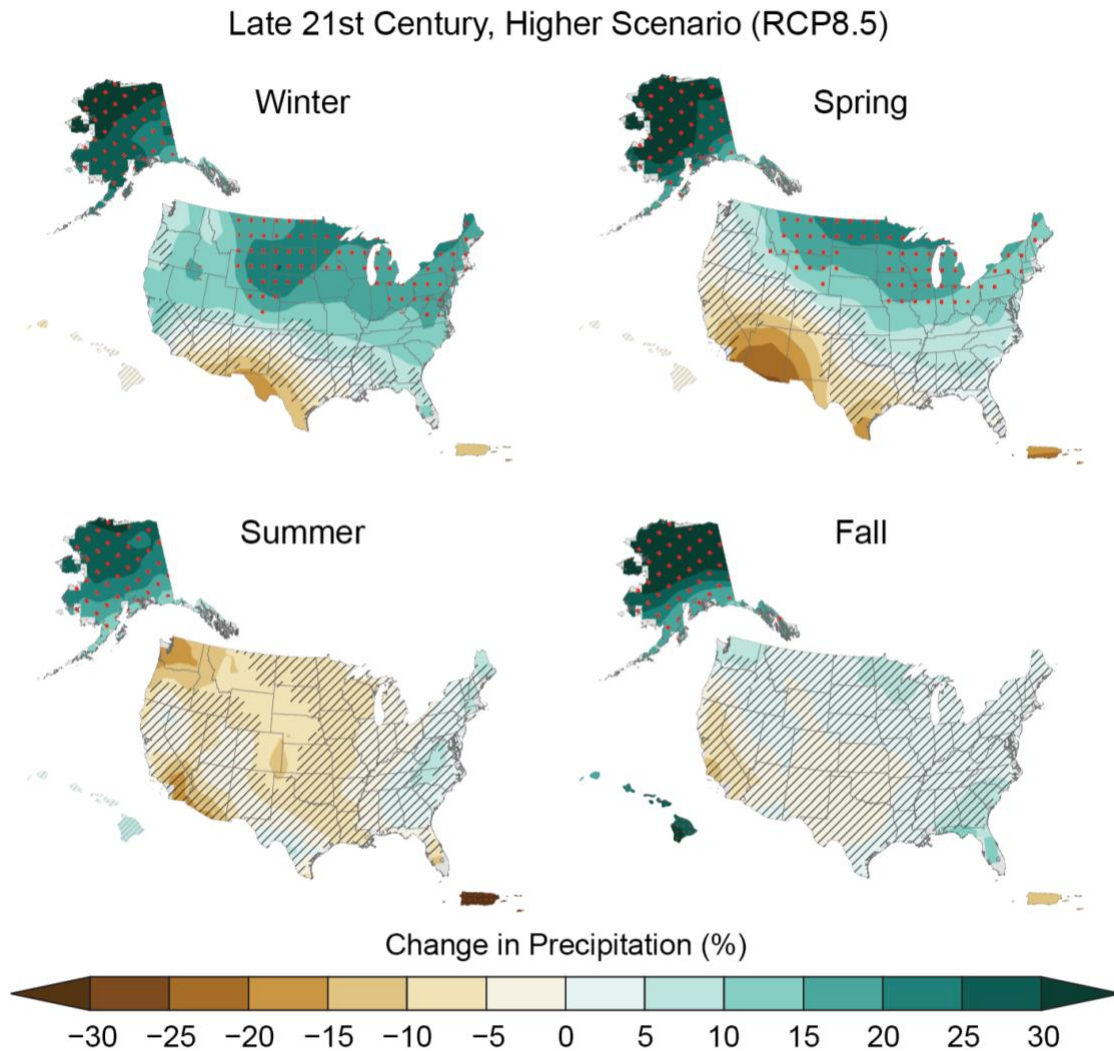


Figure 7 Projected change in total seasonal precipitation from CMIP5 simulations for 2070–2099, in percent. The values are weighted multi-model means and expressed as the percent change relative to the 1986–2015 average. These are results for the higher scenario (RCP8.5). Red dots indicate that changes are assessed to be large compared to natural variations. Diagonal hatching indicates that changes are assessed to be small compared to natural variations. Blank regions (if any) are where projections are assessed to be inconclusive. Source: Fourth U.S. National Climate Assessment, Volume 2, Chapter 2, Figure 2.5 (Hayhoe et al. 2018).

Climate and weather extremes may become more frequent or more intense. The temperature of the coldest and warmest day of the year is projected to increase across the whole U.S., by 2-4°F for the coldest and 4-6°F for the warmest temperature towards the end of the century under a higher scenario in the Gulf Coast region (Vose et al. 2017).

Heavy precipitation is projected to continue to increase across the U.S. as a whole and the Gulf Coast region specifically. For the Southern Great Plains, daily 20-year extreme precipitation is projected to increase by 9% and 13% under a lower and higher scenario by mid-century. Towards the end of the century, it is projected to increase by 12 to 20% under a lower and higher scenario (Easterling et al. 2017).

Additional analysis of the atmospheric circulation patterns responsible for drought over the greater Texas region suggest that climate change may also bring more frequent hot, dry summers to the region (Ryu et al. 2018). Houston-specific projections for selected indicators of extreme temperature and precipitation are presented in the next section.

Hurricanes are likely to be stronger, with more rainfall. Consistent with observed trends, future projections do not suggest a significant increase in the number of landfalling hurricanes. However, warmer ocean temperatures will continue to drive increases in tropical storm intensity as well as an increase in very intense tropical hurricanes worldwide (Kossin et al. 2017). The intensity of the rainfall associated with hurricanes is also likely to increase. For the rainfall associated with Hurricane Harvey, Emanuel (2017) estimates that human-induced climate change had already increased its probability from about 1% during the period 1981-2000 to 6% by 2017, and the probability could increase to over 18% before the end of the century under a higher scenario.

This assessment *does not* analyze projections of changes in hurricane events for the greater Houston region; for regionally-specific modeling of future hurricane characteristics, see studies such as Marsooli et al. (2019). Instead, this analysis focuses on projected changes in temperature and rainfall associated with non-tropical storms, although some of these storms (e.g. the Memorial Day and Tax Day floods) can produce rainfall amounts that resemble those of a hurricane.

Sea level will continue to rise and is likely to continue to accelerate. Over this coming century, global mean sea level is likely to rise 0.3-0.6 feet (9-18 cm) by 2030, 0.5-1.2 feet (15-38 cm) by 2050, and 1.0-4.3 feet (30-130 cm) by 2100 (Sweet et al. 2017). Due to the uncertainty in predicting the rate at which Antarctica and Greenland are melting, Sweet et al. (2017) also warn that, under a higher future scenario such as the one examined in this assessment, sea level rise exceeding 8 feet (2.4 m) by 2100 is “physically possible, although the probability of such an extreme outcome cannot currently be assessed.”

Given that the land around Houston is currently subsiding and likely to continue to do so, it is likely that the relative sea level rise experienced in the region will be greater than the global mean. Sea level rise will increase the frequency of nuisance and sunny-day or high-tide flooding as well as leading to permanent inundation of low-lying areas. Combining sea level rise with changes in hurricane intensity, Marsooli et al. (2019) estimate that the historic 100-year flood could occur anywhere from once a year to once every thirty years across the southeast Atlantic and Gulf Coast regions towards the end of the century.

This assessment *does not* analyze projections of relative sea level rise for the greater Houston region. For regionally specific projections of sea level rise and inundation, see Climate Central's Surging Seas (Figure 8) which compares inundation areas for the lower scenario used in this assessment (right) and the higher scenario (left).

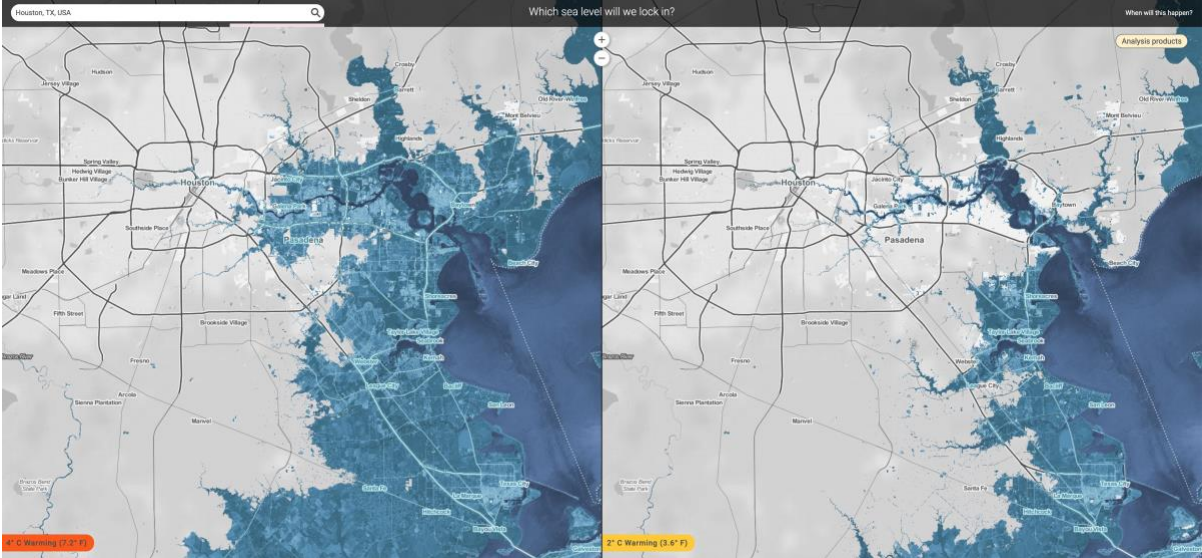


Figure 8 Projected sea level in the Houston area under 4°C (7.2°F) (left) and 2°C (3.6°F) (right) of global warming. Source: Climate Central Surging Seas.

Climate Trends and Projections

The observed trends described in this section are based on long-term observations of daily maximum and minimum temperature at 11 individual long-term weather stations across the Greater Houston area. The observed dataset is described in more detail in the **Data, Models and Methods** section of this report. The figures in this report show changes in indicators for the Houston William P. Hobby Airport weather station; trends at the other long-term weather stations are similar and can be found in the **appendices**.

The future changes described in this section are based on climate projections generated by global climate models from the Coupled Model Intercomparison Project version 5 (CMIP5), for two possible futures: a higher forcing scenario (RCP8.5), where carbon emissions continue to grow as the world continues to depend primarily on fossil fuels, and a lower forcing scenario (RCP4.5), where carbon emissions peak and then begin to decline as the world transitions to non-carbon energy sources. Daily maximum and minimum temperature and precipitation projections from the 22 global climate models have been statistically downscaled to the 11 individual long-term weather stations. These models and scenarios are also described in more detail in the **Data, Models and Methods** section of this report.

Climate indicators are calculated for each global climate model and scenario individually, then averaged over the 22 climate models to calculate an ensemble average. Figures in this section show time series of each indicator that illustrates the spread due to model and scenario uncertainty, as explained in more detail in the **Data, Models and Methods** section of this report, as well as bar charts that show average values for five different 20-year periods. Values given in the text are ensemble averages of the 22 global climate models for each scenario, except for the 2021-2040 period, where values are averaged across both scenarios because the difference between the two scenarios is insignificant during this period. This is due to the lag in the response of the climate system to human emissions described in the Introduction.

ONE. Projected Changes in Average Temperature, the Length of Summer, and Heating and Cooling Degree-Days

Temperatures in the Greater Houston area have already increased, especially for wintertime (Figure 1) and temperatures for all seasons are expected to continue to increase over the remainder of this century and beyond (Figure 6). This drives changes in the timing and length of the seasons as well as changes in the amount of heating and cooling needed to keep homes and workplaces comfortable.

While all seasons are projected to become warmer, this analysis focused specifically on summer. "Summer" is defined as the warmest quarter of the historical period. The temperature threshold for summer is the 75th percentile daily average temperature of the historical period; for William P. Hobby Airport that threshold is 81.5°F. The first day of summer is defined as the first time each year that the average temperature of 10 consecutive days reach the threshold and the last day of summer is defined as the last day of the year when the average of 10 consecutive days are at or above the threshold.

The **beginning of summer** is occurring earlier in the year and the **end of summer** later in the year, resulting in **longer summers**. Observations show that summers have already become longer in recent decades and projections show this trend will continue under both the lower (RCP4.5) and higher (RCP8.5) future scenarios, but with greater change under the higher scenario toward the end of the century (Figure 9 and Figure 10). Figure 10 shows that, on

average, the first day of summer during the 1971-1990 period occurred around June 13th and lasted until around September 18th. By 2001-2020, the first day of summer was already occurring about 9 days earlier, on average, around June 4th and ending 9 days later around September 27th. Over the coming two decades, summer is projected to be slightly longer, on average beginning around May 28th and ending around October 2nd. By the middle of the 21st century, summer is expected to begin around May 22nd for the lower scenario and around May 14th for the higher scenario and ending around October 7th for the lower scenario or around October 13th for the higher scenario. By the end of the century, the beginning of summer is projected to occur around May 19th for the lower scenario or May 1st for the higher scenario and ending in fall around October 9th for the lower scenario or October 26th for the higher scenario.

Compared to the earlier observed period (1971-1990), the length of summer is projected to increase by a month for the coming two decades and by the middle of the century by around 40 days for the lower scenario and 55 days for the higher scenario, whereas by the end of the century summer is projected to be around 50 days longer for the lower scenario and 80 days longer, lasting almost half of the year, for the higher scenario (Figure 10c).

A longer and warmer summer season will increase energy demand for air-conditioning for both residential and commercial purposes. This can be expressed in terms of **cooling degree-days** (CDDs), which is the cumulative number of degrees each day's average temperature is above the 65°F threshold, which is generally when homes and buildings need cooling (see box on page 27). The higher each month's cooling degree-day total is, the warmer that month is and the greater the need for cooling. CDD projections can be used by energy companies to plan for increases in future electricity demand for cooling during the warmer months absent significant increases in efficiency, energy conservation, or other consumer-based changes.

Figure 11 and Figure 12 show the projected changes in cumulative cooling degree-days for Houston William P. Hobby Airport for spring, summer, and fall relative to observations. All three seasons are expected to see increases in CDDs with the greatest changes projected for summer, which has already seen increases of around 140 CDDs between the 1971-1990 and 2001-2020 periods, compared to increases of about 90 CDDs in spring and 110 CDDs in fall. Over the coming two decades, cooling demand is projected to increase by about 170 CDDs in spring, 250 CDDs in summer, and 200 CDDs in fall, compared to the 1971-1990 period, due to warmer temperatures and longer summers.

Toward the middle and end of the century, greater changes are projected under the higher scenario compared to the lower scenario with projections by the middle of the century showing increases in spring cooling degree-days of about 255 CDDs for the lower and 375 CDDs for the higher scenario. For summer, increases are projected to be about 350 CDDs for the lower and 490 CDDs for the higher scenario, while fall is projected to have increases of about 275 CDDs for the lower scenario and 400 CDDs for the higher scenario.

By the end of the century, the projected increase in cooling demand for all three seasons is larger; spring is projected to see increases in cooling degree-days of about 315 CDDs for the lower scenario and 575 CDDs for the higher scenario, summer is projected to see increases of about 395 CDDs for the lower and 730 CDDs for the higher scenario, and fall cooling degree-days are projected to increase by about 325 CDDs and 640 CDDs for the lower and higher scenarios, respectively. For the higher scenario by the end of the century, cooling degree-days almost double during the spring and fall seasons relative to the 1971-1990 period, suggesting that if the world follows the higher scenario, electricity managers and planners would have to consider additional or alternative sources of electricity to be able to align supply with demand.

While warmer temperatures are projected to dramatically increase the demand for cooling during the warmer parts of the year, some offset in energy demand for heating is projected during the colder months due to warmer winter temperatures. Measures of the energy needed for heating is expressed in terms of **heating degree-days** (HDDs), which is the cumulative number of degrees each day's average temperature is below 65°F (see the box below), which is typically when people turn on their furnaces to heat homes and businesses. The higher the heating degree-day value is for a day or a period, the colder it is and the higher the demand for heating.

Figure 13 and Figure 14 show the projected changes in cumulative heating degree-days for fall, winter, and spring, as well as the annual total. All three cooler seasons are projected to see a decrease in the energy demand for heating, with winter projected to experience the largest decrease in demand. The change is projected to be greater for the higher scenario and toward the end of the century.

Annual changes in heating degree-days show that heating demand has decreased by approximately 160 HDDs between the 1971-1990 and 2001-2020 periods, with a decrease of about 40 HDDs in fall, 95 HDDs in winter, and 25 HDDs in spring. Over the coming two decades, annual heating degree-days are projected to decrease by about 295 HDDs, on average, with an average decrease of about 60 HDDs in fall, 185 HDDs in winter, and 45 HDDs in spring, compared to the 1971-1990 period.

By mid-century, annual heating degree days are projected to decrease by about 395 HDDs for the lower scenario, with a decrease of around 75 HDDs in fall, 250 HDDs in winter, and 70 HDDs in spring, compared to the 1971-1990 average. For the higher scenario, annual heating degree-days are projected to decrease by about 535 HDDs by mid-century, with heating degree-days projected at about 105 HDDs less in fall, 340 HDDs less in winter, and 90 HDDs less in spring, compared to 1971-1990.

Cooling degree-days are calculated by subtracting 65 °F from each day's average temperature (T) and adding only positive values for the period of interest (negative values mean the day's average temperature was below 65 °F and no cooling is needed). The higher the CDD value for a day, or period, is, the hotter that day was and the higher the demand for air-conditioning.

$$1 \text{ day:} \quad \text{CDD} = T - 65 \text{ }^{\circ}\text{F}$$

$$2 \text{ days:} \quad \text{CDD} = (T_{\text{day } 1} - 65 \text{ }^{\circ}\text{F}) + (T_{\text{day } 2} - 65 \text{ }^{\circ}\text{F})$$

$$N \text{ days:} \quad \text{CDD} = (T_{\text{day } 1} - 65 \text{ }^{\circ}\text{F}) + (T_{\text{day } 2} - 65 \text{ }^{\circ}\text{F}) + \dots + (T_{\text{day } N} - 65 \text{ }^{\circ}\text{F})$$

Similarly, **heating degree-days** are calculated by subtracting each day's average temperature from 65 °F to calculate how much lower each day's average temperature was than the threshold where heating is needed. Again, only positive values are added because no heating is generally needed when the average temperature is above 65 °F. The lower the HDD value for a day, or period, is, the colder that day was and the higher the demand for heating.

$$1 \text{ day:} \quad \text{HDD} = 65 \text{ }^{\circ}\text{F} - T$$

$$2 \text{ days:} \quad \text{HDD} = (65 \text{ }^{\circ}\text{F} - T_{\text{day } 1}) + (65 \text{ }^{\circ}\text{F} - T_{\text{day } 2})$$

$$N \text{ days:} \quad \text{HDD} = (65 \text{ }^{\circ}\text{F} - T_{\text{day } 1}) + (65 \text{ }^{\circ}\text{F} - T_{\text{day } 2}) + \dots + (65 \text{ }^{\circ}\text{F} - T_{\text{day } N})$$

By the end of the century, heating degree-days are projected to decrease even further, with the global climate model average for the lower scenario, indicating a decrease by about 460 HDDs annually, with seasonal decreases of 90 HDDs in fall, 290 HDDs in winter, and 80 HDDs in spring, compared to 1971-1990. For the higher scenario the annual average is projected to decrease by around 740 HDDs, with decreases of about 135 HDDs in fall, 485 HDDs in winter, and 115 HDDs in spring. For the fall and spring seasons, heating degree-days are more than halved by the end of the century, for the higher scenario, compared to 1971-1990, and winter values are almost halved.

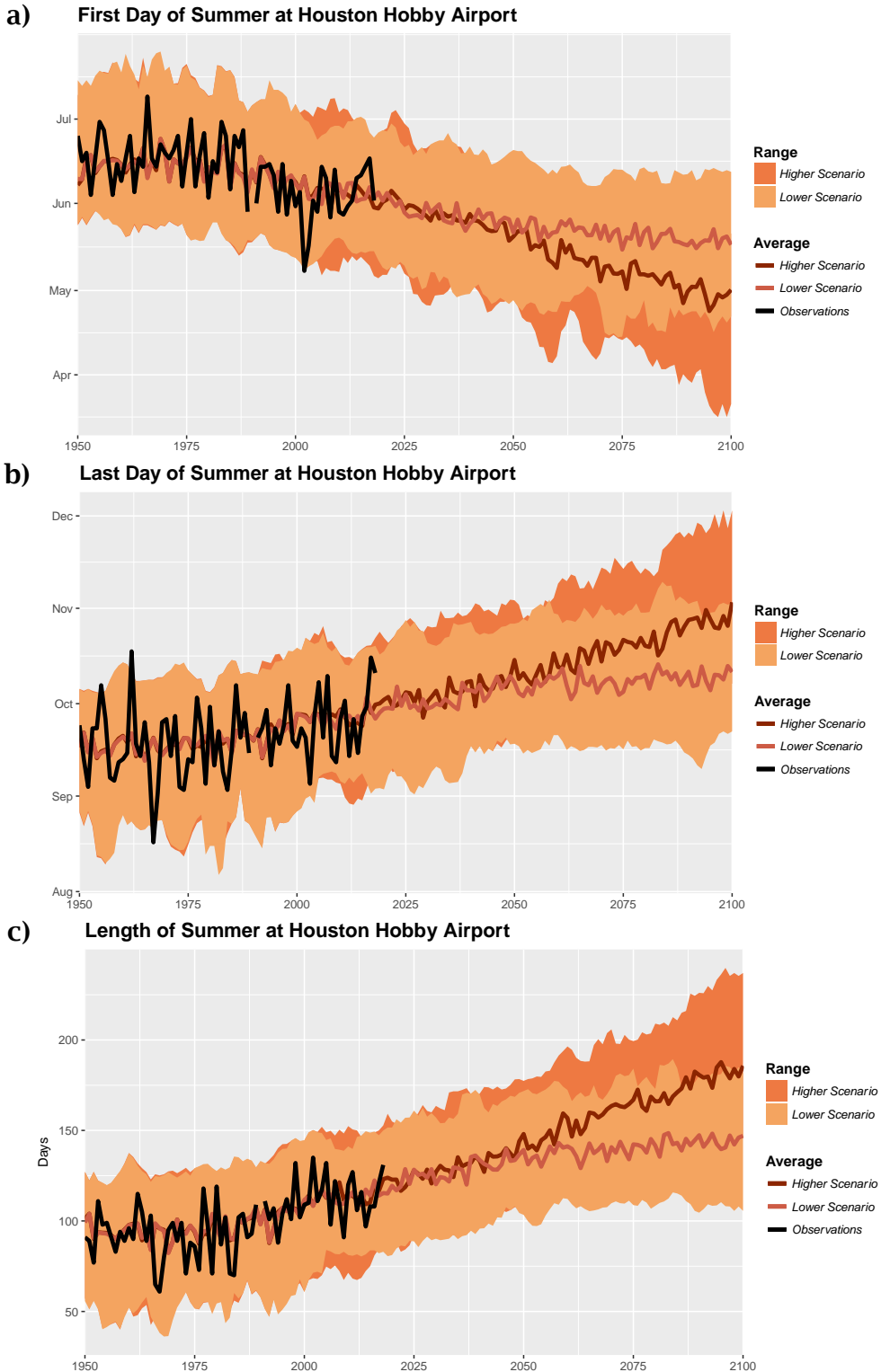


Figure 9 Observed and projected changes in the timing of a) the first day of summer, b) the last day of summer, and c) the length of summer at Houston William P. Hobby Airport. The black line shows observations, the orange and brown lines are the means of 22 GCMs for the lower (RCP4.5) and higher (RCP8.5) scenarios, respectively, and the shaded areas are the ranges among the 22 GCMs for the lower (light orange) and higher (dark orange) scenarios.

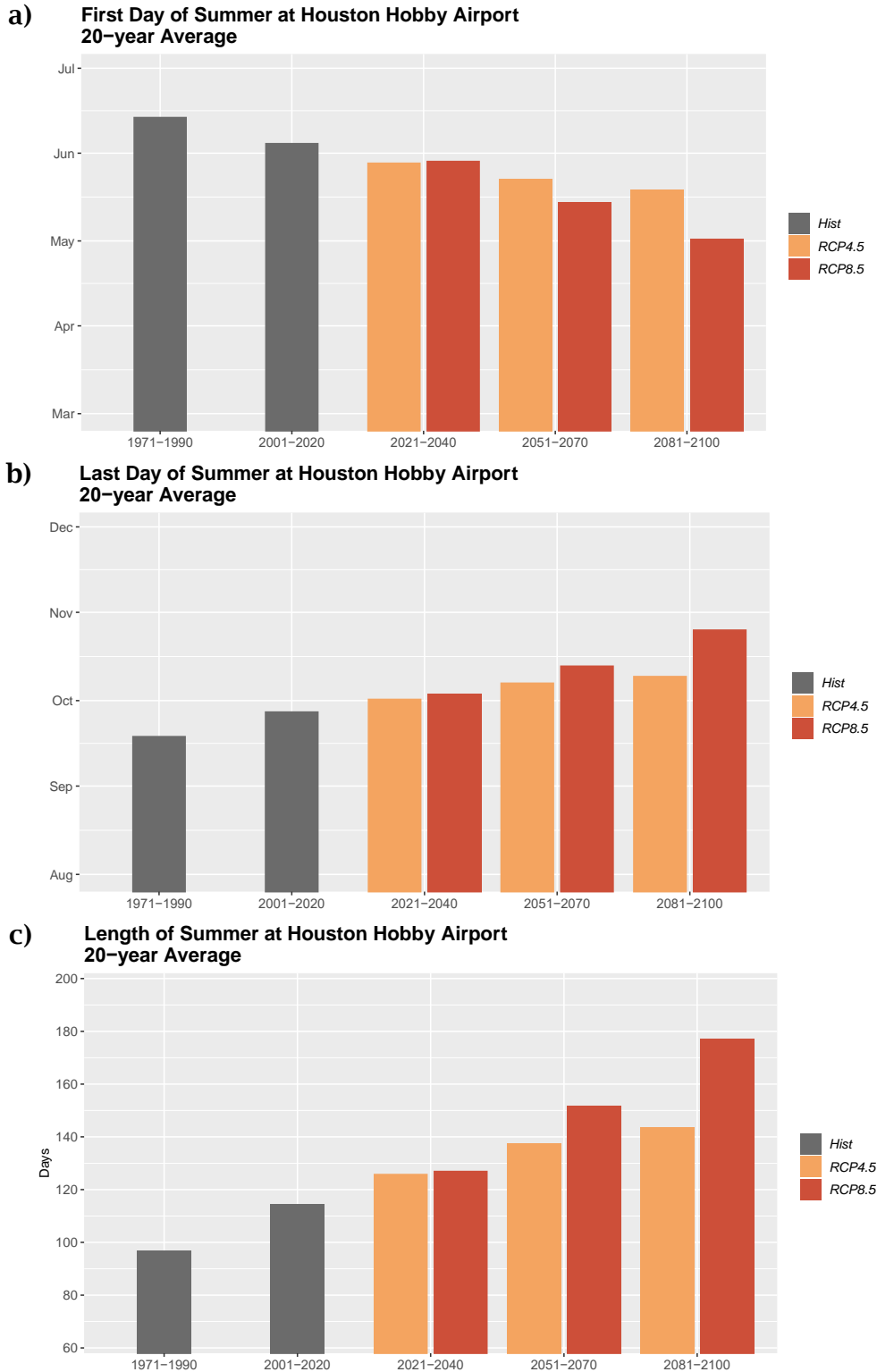


Figure 10 Observed and projected changes in the timing of a) the first day of summer, b) the last day of summer, and c) the length of summer at Houston William P. Hobby Airport for five 20-year periods. The gray bars show the average historical values, the orange and red bars are the means of 22 GCMs for the lower (RCP4.5) and higher (RCP8.5) scenarios, respectively.

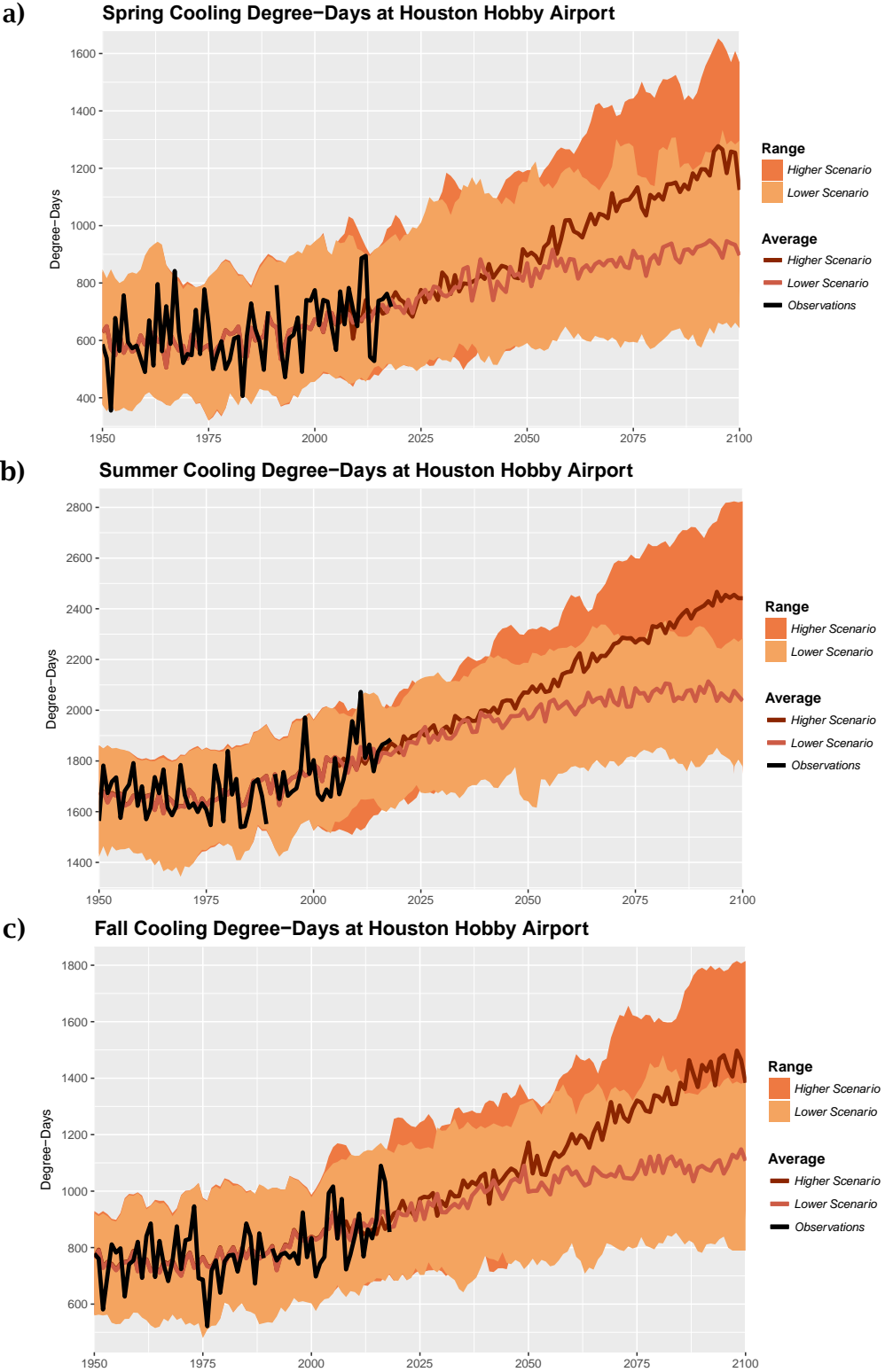


Figure 11 Observed and projected changes in a) spring, b) summer, and c) fall cooling degree days at Houston William P. Hobby Airport. The black line shows observations, the orange and brown lines are the means of 22 GCMs for the lower (RCP4.5) and higher (RCP8.5) scenarios, respectively, and the shaded areas are the ranges among the 22 GCMs for the lower (light orange) and higher (dark orange) scenarios.

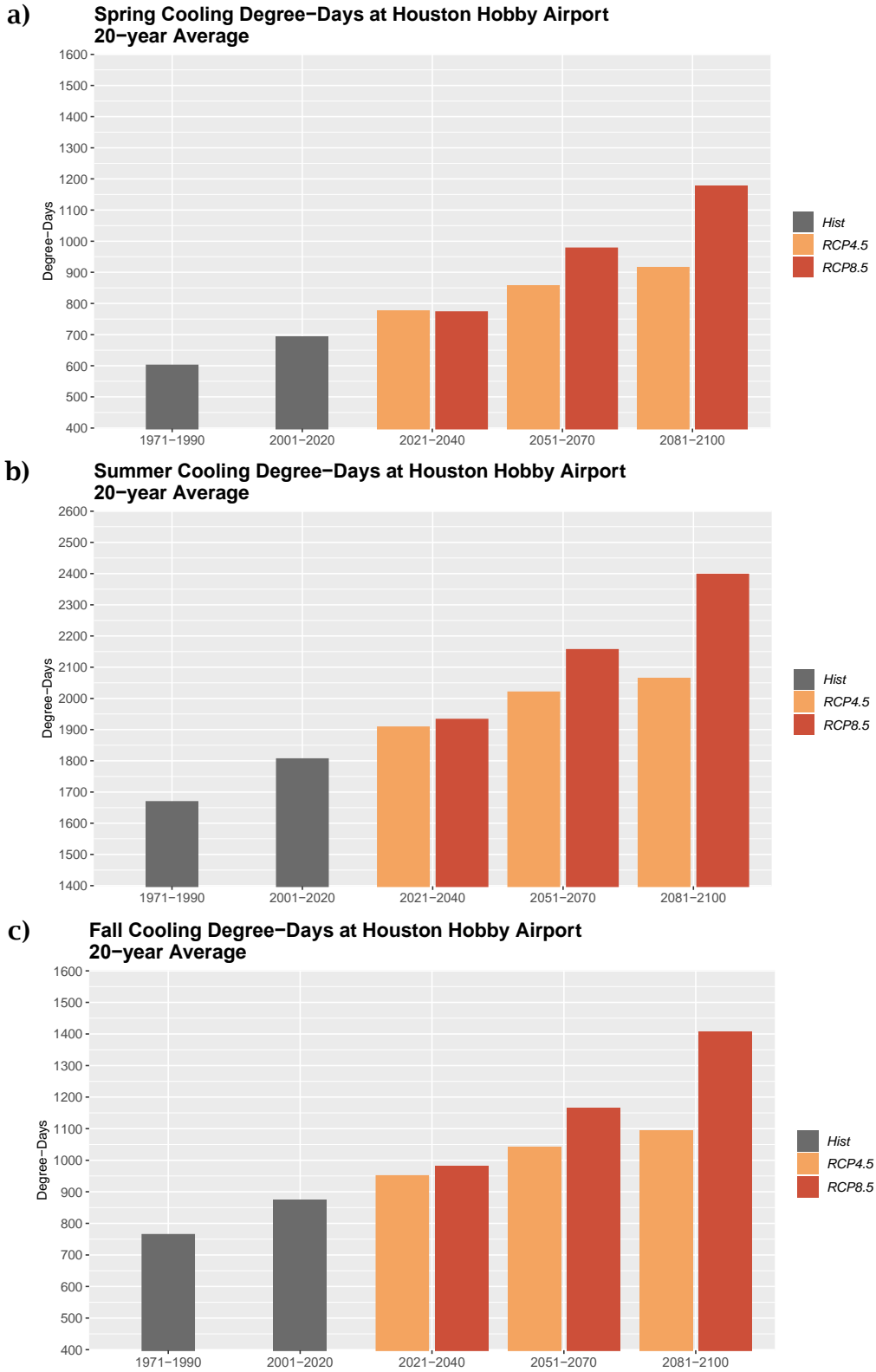


Figure 12 Observed and projected changes in a) spring, b) summer, and c) fall cooling degree days at Houston William P. Hobby Airport for five 20-year periods. The gray bars show the average historical values, the orange and red bars are the means of 22 GCMs for the lower (RCP4.5) and higher (RCP8.5) scenarios, respectively.

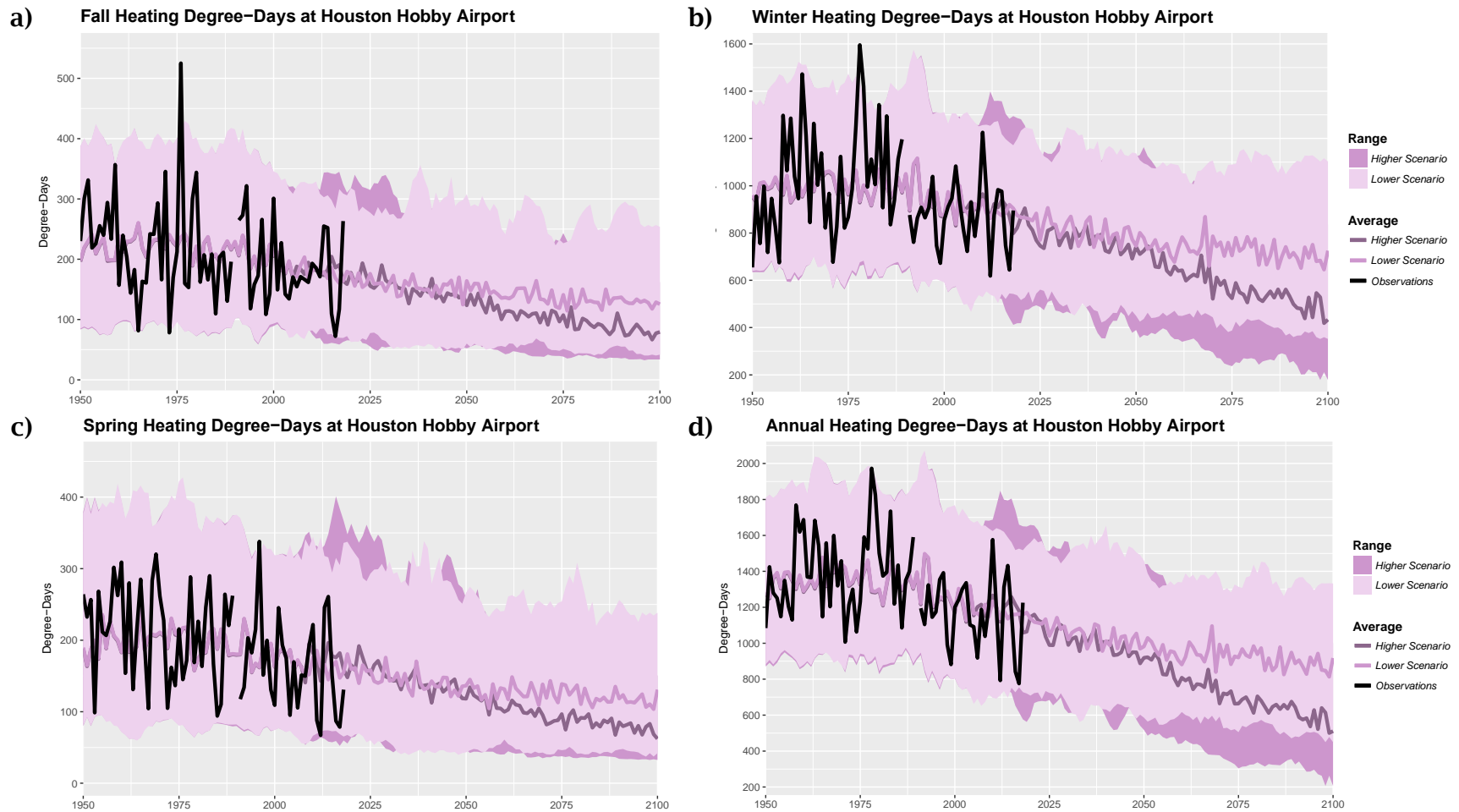
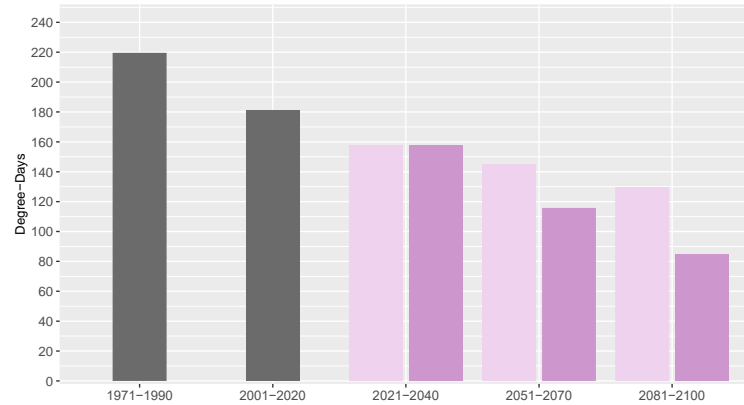
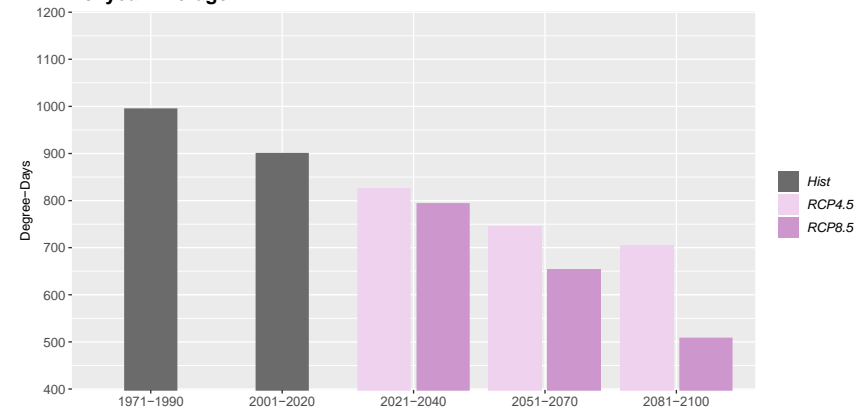


Figure 13 Observed and projected changes in a) fall, b) winter, c) spring, and d) annual heating degree days at Houston William P. Hobby Airport. The black line shows observations, the light and dark purple lines are the means of 22 GCMs for the lower (RCP4.5) and higher (RCP8.5) scenarios, respectively, and the shaded areas are the ranges among the 22 GCMs for the lower (light purple) and higher (dark purple) scenarios.

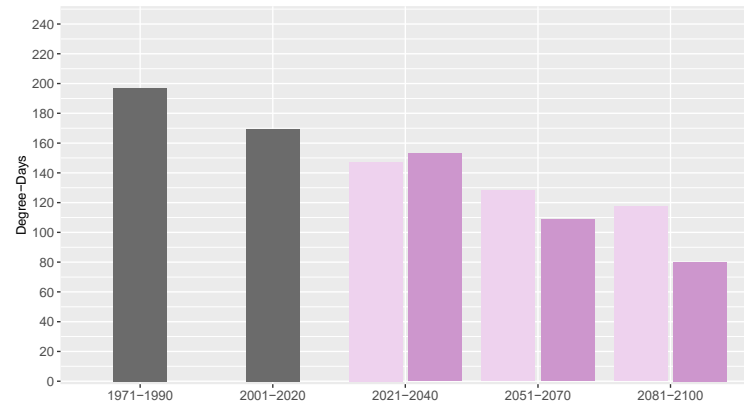
**a) Fall Heating Degree-Days at Houston Hobby Airport
20-year Average**



**b) Winter Heating Degree-Days at Houston Hobby Airport
20-year Average**



**c) Spring Heating Degree-Days at Houston Hobby Airport
20-year Average**



**d) Annual Heating Degree-Days at Houston Hobby Airport
20-year Average**

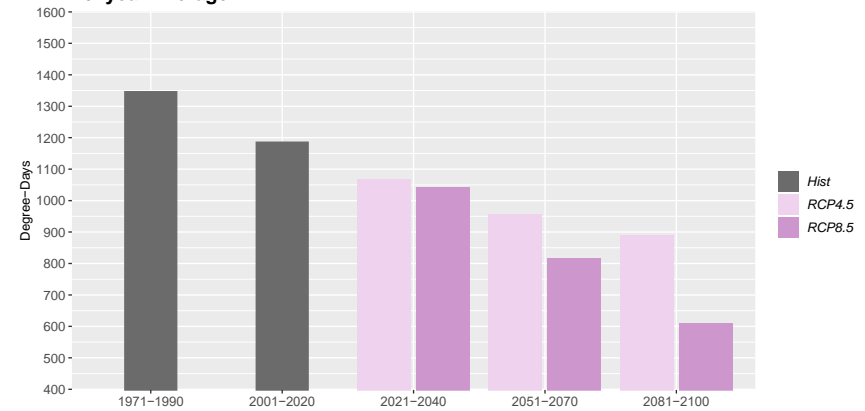


Figure 14 Observed and projected changes in a) fall, b) winter, c) spring, and d) annual heating degree days at Houston William P. Hobby Airport for five 20-year periods. The gray bars show the average historical values, the light and dark purple bars are the means of 22 GCMs for the lower (RCP4.5) and higher (RCP8.5) scenarios, respectively.

TWO. Changes in Extreme Temperatures

Temperature extremes are also changing. The number of very hot days and nights per year are increasing, as is the temperature of the hottest day of the year. The longest heat wave of the year has already nearly doubled in length, and in the future heatwaves are expected to become hotter and longer.

The number of **hot days per year with temperature at or above 100°F** is projected to increase under both the lower and higher scenarios with significantly greater changes expected for the higher scenario. For the earlier (1971-1990) period the average number of days per year above 100°F was less than 1, increasing to just above 3 days per year, on average, for the most recent 20-year period (2001-2020). Over the coming two decades (2021-2040) we can expect to experience approximately 7 days per year above 100°F. By the middle of the century, model projections show an average of 12 days per year above 100°F for the lower scenario and 23 days per year for the higher scenario, and the numbers increase by the end of the century to 14 days under the lower scenario and about 55 days, or nearly 8 weeks, under the higher scenario (Figure 15a and Figure 16a).

Nights are also projected to continue to warm, including **warm summer nights at or above 80°F**. During the 1971-1990 period there were rarely any nights per year above that threshold, with an average of less than one night per year above 80°F, averaged over the 20 years. In the most recent 20-year period that number has increased to an average of just above 3 nights per year. Projections indicate that Houston can expect more warm nights, with about 10 warm nights per year, on average, over the next 20 years, about 20 nights per year by the middle of the century for the lower scenario and about 50 nights per year above 80°F for the higher scenario, and by end of the century, projections show an average of about 30, or one month, of warm nights per year under the lower scenario and as much as 95 warm nights per year, or three entire months, under the higher scenario (Figure 15b and Figure 16b).

The numbers given above are for the average of 22 global climate models. However, Figure 15 also shows the *range* in the projections from the 22 global climate models, which is considerable. Some models project up to 120 days per year above 100°F and over 140 nights per year above 80°F for some years by the end of the century. Generally, the average of many global climate models is a more reliable projection than a single model's projection; however, it is important to be aware of the wide range in model projections, which suggests that there is higher uncertainty for these more extreme temperature indicators.

Not only are the number of extreme hot days expected to increase dramatically, especially in the second half of the century, but the **temperature of the hottest day** and **hottest week** of the year are projected to increase as well, along with the length of the **longest heatwave**. Figure 17 and Figure 18 show the projected changes in these indicators. Until the middle of the century there is not much difference between the lower and higher scenario, but toward the end of the century the higher scenario shows accelerated heating with hotter extreme temperatures and longer heatwaves, especially for the higher scenario. Observations show that during the earlier of the historical periods, 1971-1990, the hottest day was, on average, 99°F, while the hottest week had an average temperature of 96°F. More recently, during the 2001-2020 period, the temperature of the hottest day has increased to 101°F and average temperature of the hottest week to 98°F.

Projections show that this trend will continue, with the model average temperature of the hottest day increasing to about 103°F in the next 20 years, with the hottest week averaging at 99°F. By the middle of the century, the projected model ensemble average shows an increase of the hottest day to 104°F for the lower scenario and 106°F for the higher scenario with average temperatures of the hottest week of 100°F for the lower scenario and 102°F for the

higher scenario. By the end of the century the average temperature of the hottest day is projected to stay at around 104°F for the lower scenario and increase to 109°F for the higher scenario, with average temperatures of the hottest week projected to be about 101°F for the lower scenario and 105°F for the higher scenario. The spread between the models is relatively narrow, indicating the climate models generally are in agreement of the magnitude of the trend of both the temperature of the hottest day and week (Figure 17a and b).

Heatwaves are getting hotter and longer as well (Figure 17c and Figure 18c). Here we use the definition of heatwave from Shiva et al. (2019) where a heatwave consists of at least 2 consecutive days and nights above a locally relevant temperature threshold; here we use the 95th percentile of the historical observed daily minimum and maximum temperature, which is categorized as a severe heatwave. For William P. Hobby Airport that means at least two consecutive days above 94.8°F with nights above 77.2°F.

The length of the observed average annual **longest heatwave** was 2.5 days in the earliest of the historical periods (1971-1990). This increased to 5.5 days, on average, during the most recent two decades and is expected to increase to about 10 days within the next two decades. By the middle of the century, climate models project that the longest heatwave, on average, will last about 15 days for the lower scenario and 27 days for the higher scenario and by the end of the century, the longest heatwave is projected to last 19 days, or two and a half weeks, under a lower scenario and 47 days, or nearly 7 weeks, by the end of the century. For this indicator there is a wide range in global climate model projections, suggesting that the uncertainty is larger for this indicator (Figure 17c).

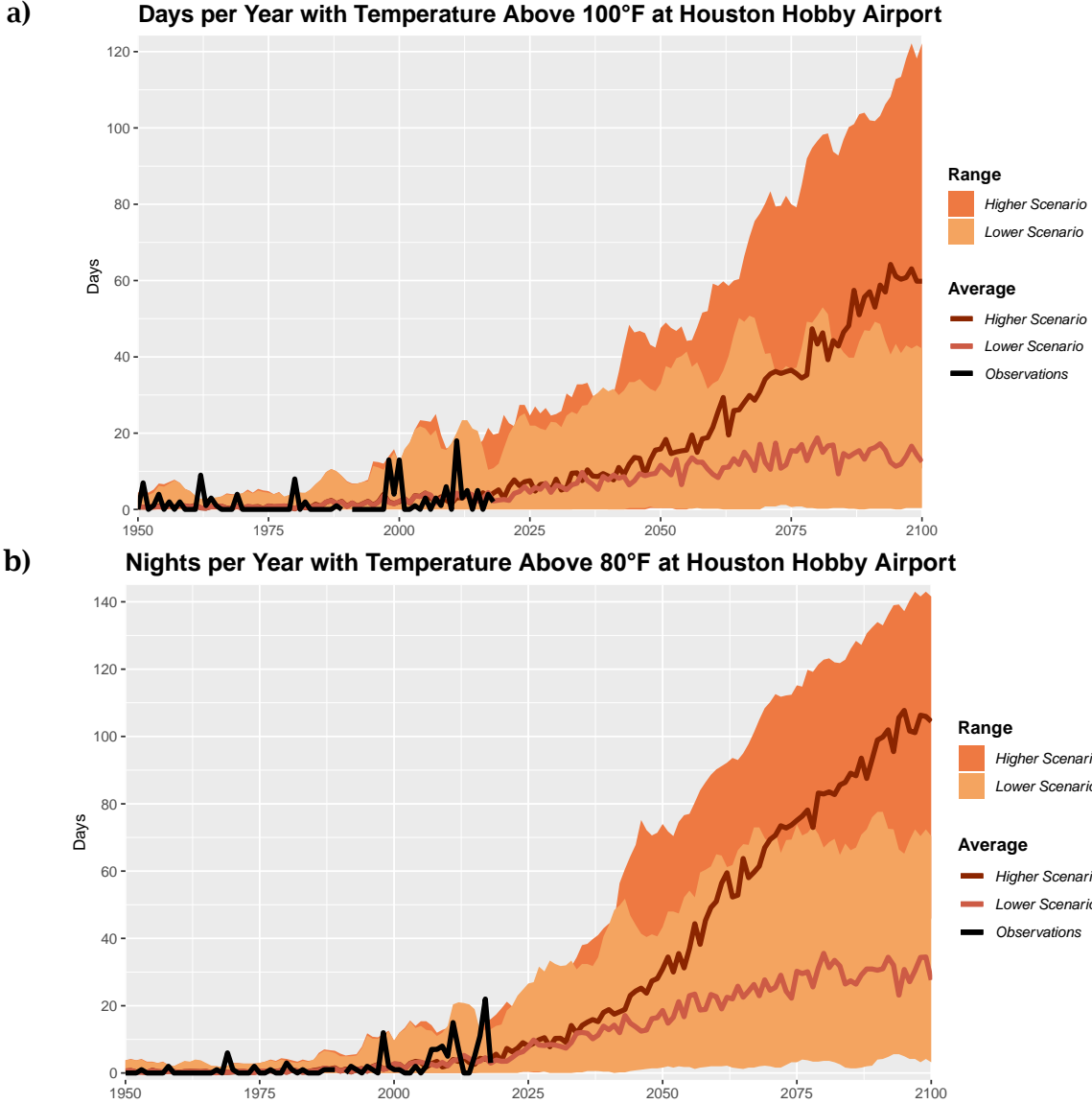


Figure 15 Observed and projected changes in a) days per year with temperature above 100°F and b) nights per year with temperature above 80°F at Houston William P. Hobby Airport. The black line shows observations, the orange and brown lines are the means of 22 GCMs for the lower (RCP4.5) and higher (RCP8.5) scenarios, respectively, and the shaded areas are the ranges among the 22 GCMs for the lower (light orange) and higher (dark orange) scenarios.

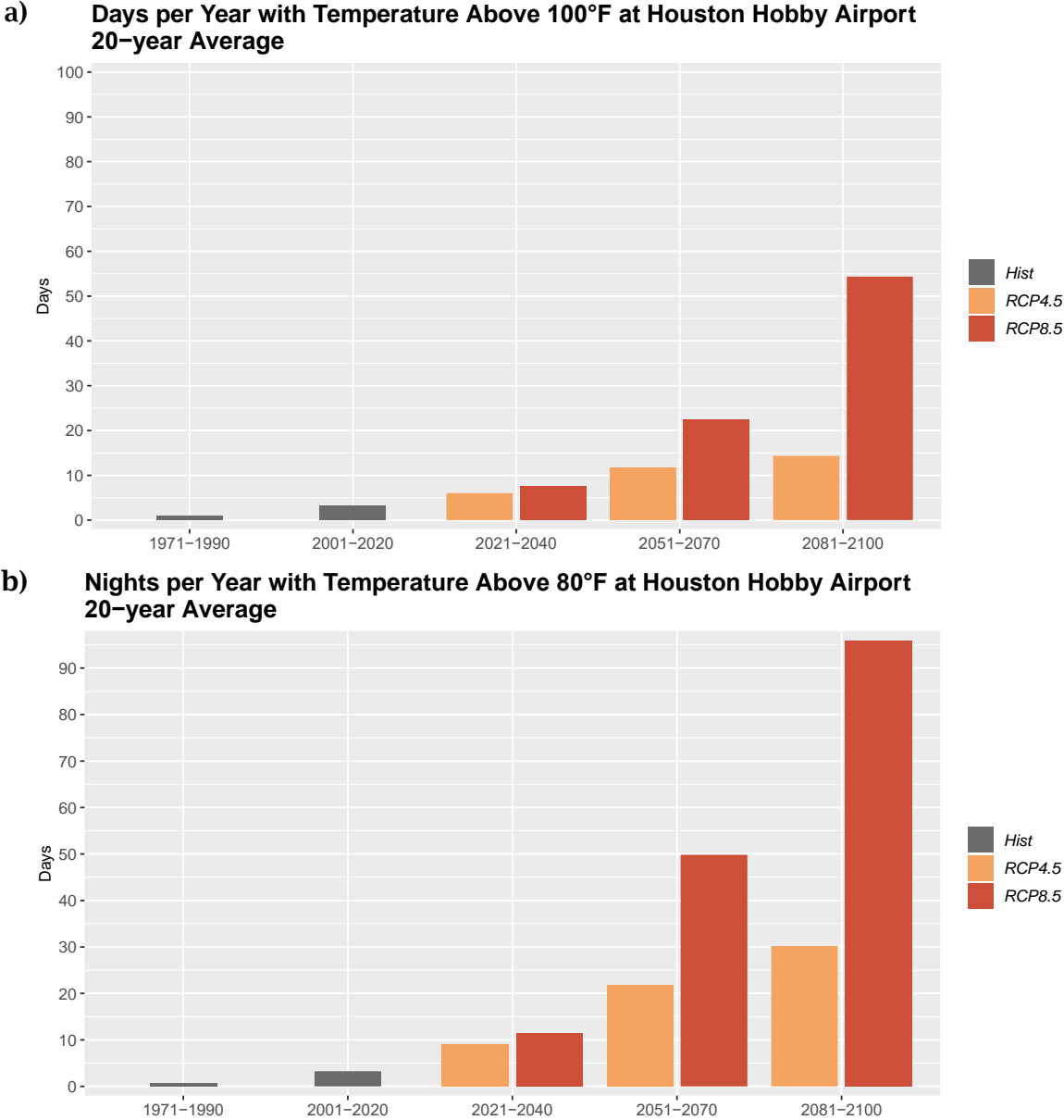


Figure 16 Observed and projected changes in a) days per year with temperature above 100°F and b) nights per year with temperature above 80°F at Houston William P. Hobby Airport for five 20-year periods. The gray bars show the average historical values, the orange and red bars are the means of 22 GCMs for the lower (RCP4.5) and higher (RCP8.5) scenarios, respectively.

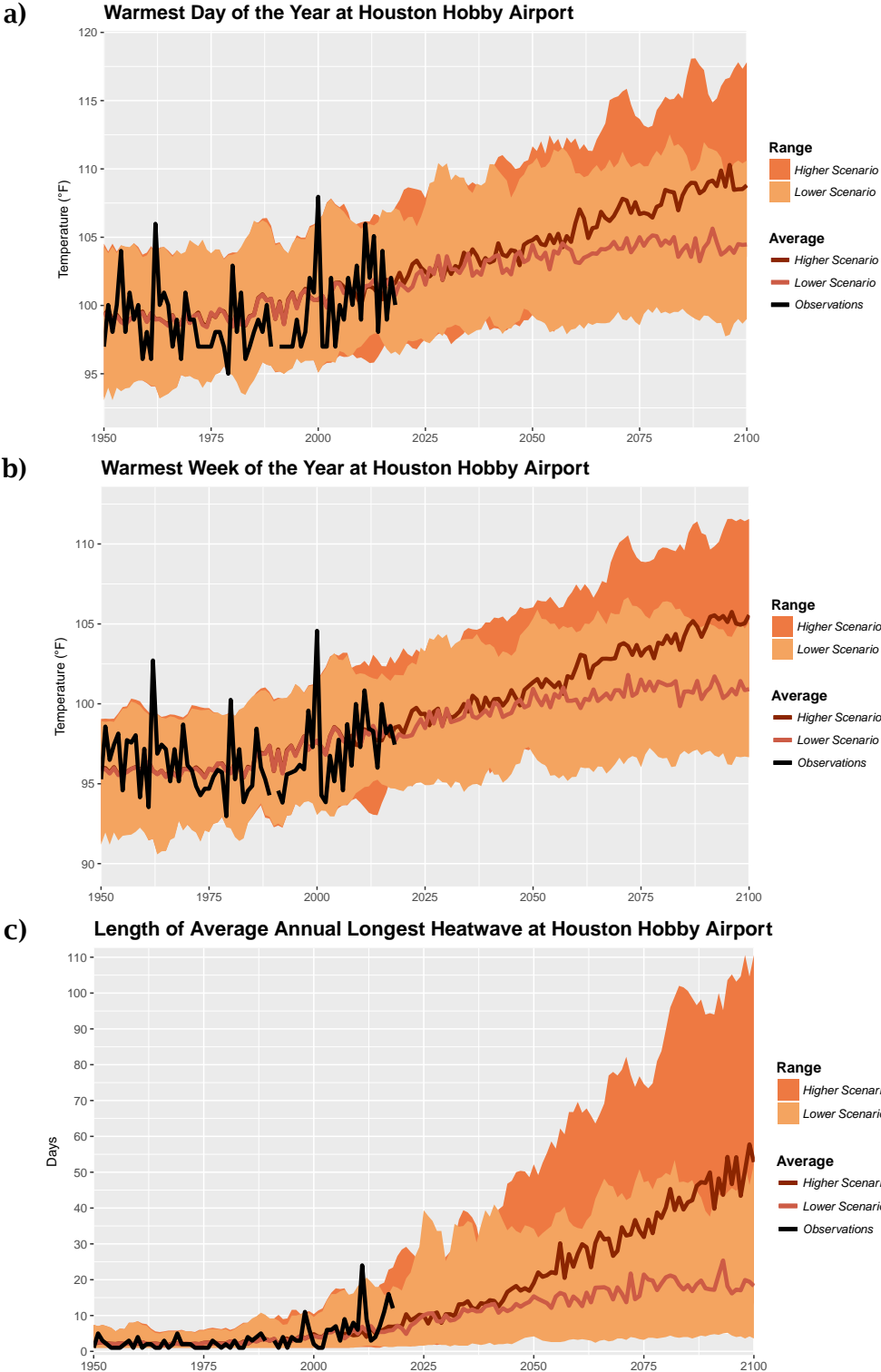


Figure 17 Observed and projected changes in a) temperature of the hottest day of the year, b) temperature of the hottest week of the year, and c) length of the average annual longest heatwave at Houston William P. Hobby Airport. The black line shows observations, the orange and brown lines are the means of 22 GCMs for the lower (RCP4.5) and higher (RCP8.5) scenarios, respectively, and the shaded areas are the ranges among the 22 GCMs for the lower (light orange) and higher (dark orange) scenarios.

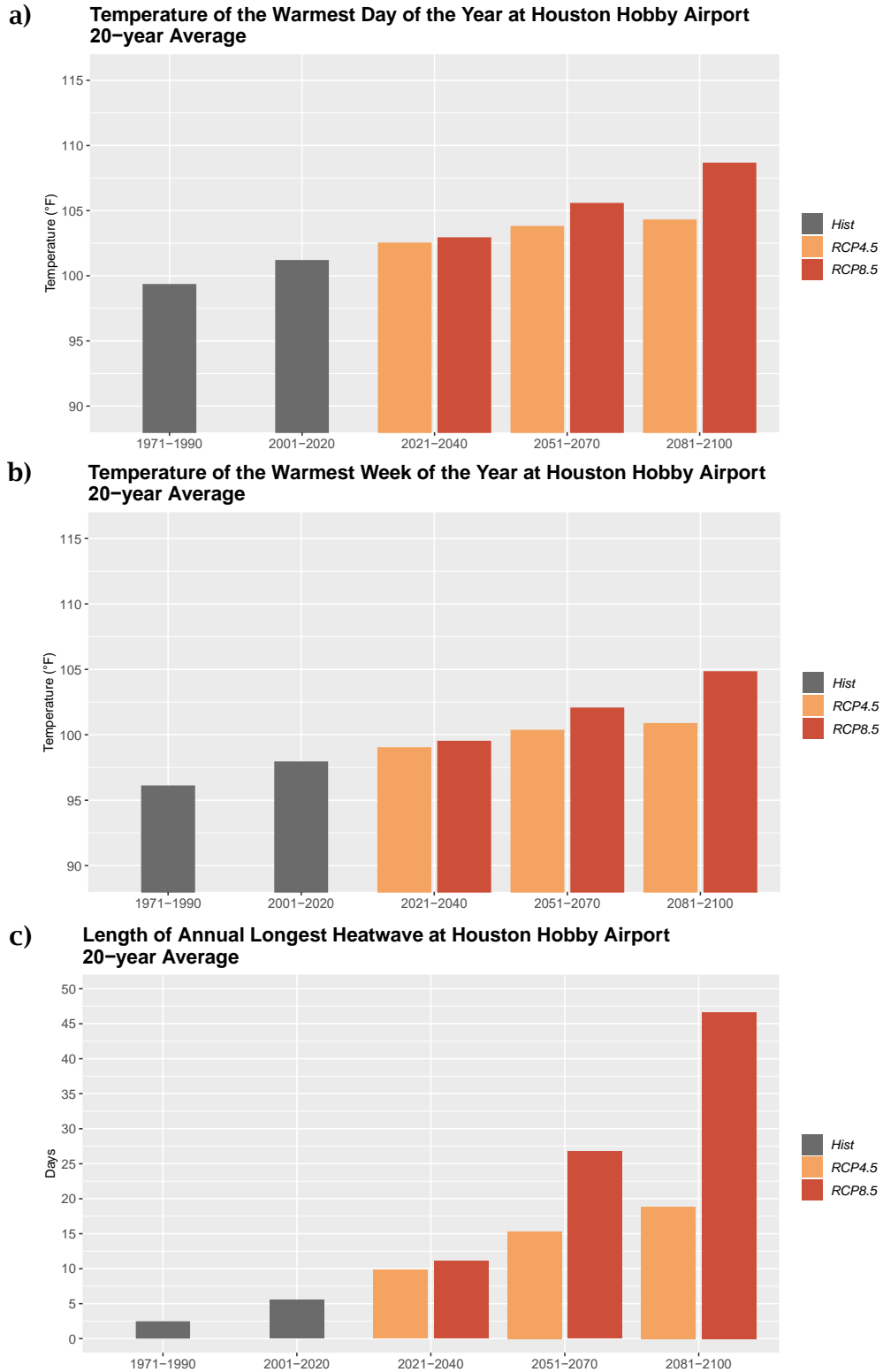


Figure 18 Observed and projected changes in a) temperature of the hottest day of the year, b) temperature of the hottest week of the year, and c) length of the average annual longest heatwave at Houston William P. Hobby Airport for five 20-year periods. The gray bars show the average historical values, the orange and red bars are the means of 22 GCMs for the lower (RCP4.5) and higher (RCP8.5) scenarios, respectively.

THREE. Changes in Annual and Seasonal Precipitation and Dry Days

The Greater Houston area is not projected to experience significant changes in **total annual precipitation** (Figure 19a and Figure 20a) under either the lower or higher scenarios. The model projections underestimate the total annual precipitation slightly, which is most likely due to the proximity of the area to the ocean, which may hinder accurate precipitation simulations to a certain degree. Observed annual total precipitation for the 1971-1990 period was 51 inches. For the most recent 20-year period (2001-2020) the average is 49 inches and this value does not change significantly by the middle of the century, with a projected total annual precipitation remaining at about 49 inches on average for the coming 20-year period.

By the middle of the century, average model projections indicate no real change in the annual total precipitation amounts with about 50 inches projected annual for the lower scenario and about 49 inches projected for the higher scenario. The model average values remain largely the same by the end of the century (Figure 19a and Figure 20a); for the lower scenario the projected total annual precipitation is about 50 inches while for the higher scenario decreases slightly to about 48 inches.

Figure 19b and Figure 20b show the historical values and projected changes in the number of **dry days per year**. During the 1971-1990 period, observations show an average of 266 dry days per year. For the most recent 20-year period the average is nearly identical, 267 days per year. Over the coming 20 years projections show a few more dry days per year with about 270 dry days, averaged over all the climate models, for that period.

By the middle of the century, projections show very little change for either scenario with 271 dry days projected per year, on average, for the lower scenario and 273 annual dry days for the higher scenario. Toward the end of the century the model average projects no change for the lower scenario with the model average projected at 270 dry days per year. There is a slight increase in the model average for the higher scenario with 277 dry days per year.

It is important to note that the spread between models is quite large for these two indicators, with some models projecting annual total precipitation values of less than 20 inches in some years while select models project total precipitation amounts of above 100 inches per year, while dry days per year range between 220 and 315. Some of this is due to higher uncertainty for these indicators, but part of the spread in models is also due to models not aligning on which years are very wet and which are very dry. The lines shown in Figure 19 and the bars in Figure 20 are averaged over all 22 global climate models for each scenario, and do not show interannual variations which will naturally occur, with some years being abnormally dry and others abnormally wet. This natural variation is expected to continue, and the individual models do in fact project this variability, but because they do not agree on exactly which years will be very wet or dry, the variability is muted in the average values.

Similarly to total annual precipitation, what is most notable in the **seasonal precipitation totals** is the trend in precipitation amounts, or lack thereof (Figure 21 and Figure 22). Consistent with the regional projections, none of the four seasons show any significant change or trend in seasonal precipitation between the two historical periods (1971-1990 and 2001-2020).

Projections show no significant changes for total winter precipitation under either the lower or higher scenario, with the average total seasonal winter precipitation remaining between 10 and 11 inches throughout the end of the century for both the lower and higher scenario. For the lower scenario, spring is not projected to experience significant changes in precipitation, with the seasonal total precipitation projected to be very close to 11 inches, on average, for every 20-year period, while the higher scenario shows a very slight decrease from 11 to 10 inches per year in spring precipitation toward the end of the century. Average summer

precipitation projections show a slight decrease for both the lower and higher scenarios toward the end of the century, with a larger decrease for the higher scenario. However, the change is small; on the order of 2 inches decrease, or less, by the end of the century. For both the lower and higher scenarios model projections show a slight increase in fall precipitation. By the middle of the century, the global climate model average shows an increase of about 1 inch in fall precipitation for both the lower and higher scenario, compared to the 1971-1990 period, and by the end of the century the total fall rainfall increases by 1.5 inches for both scenarios.

As with annual total precipitation, seasonal precipitation amounts vary from year to year with some years being exceptionally wet and others exceptionally dry. This natural variability will continue but is not reflected in the model average nor the 20-year period averages.

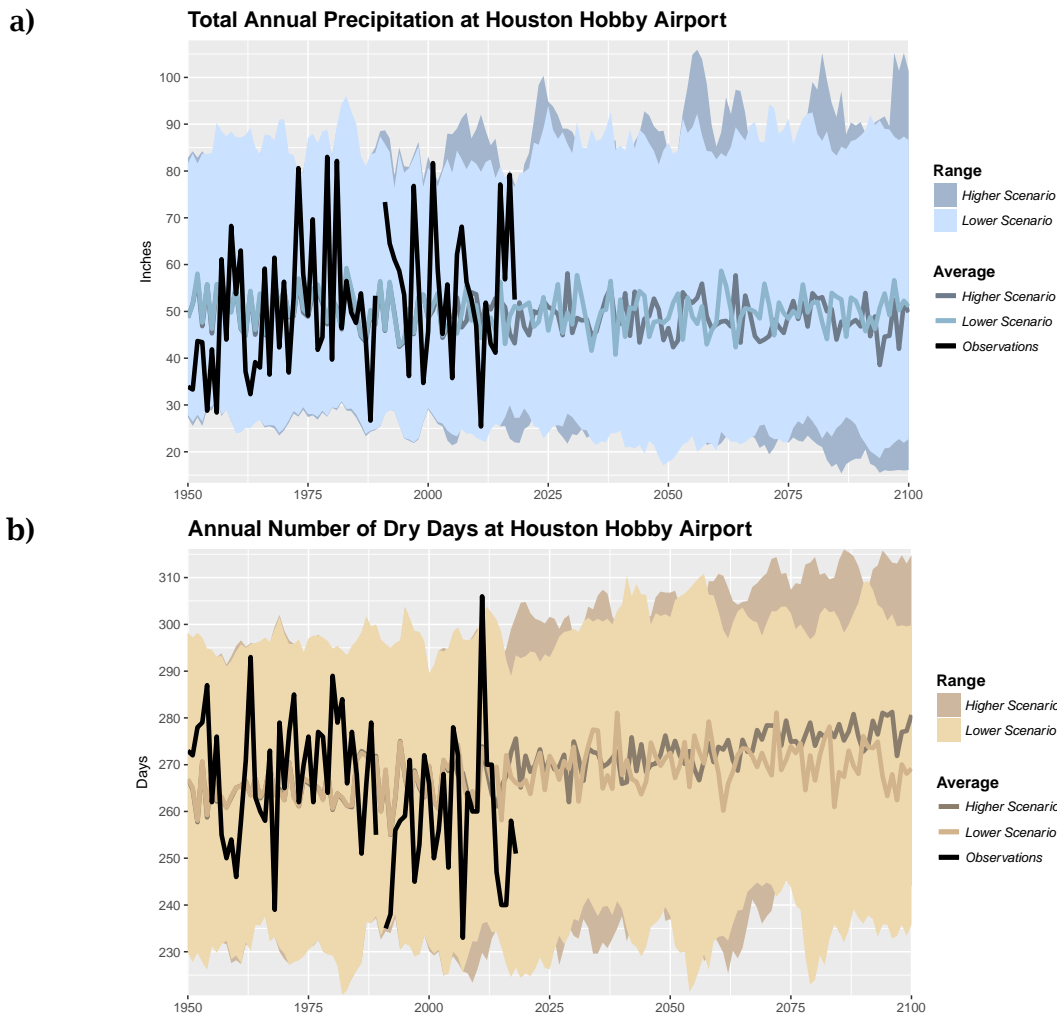


Figure 19 Observed and projected a) total annual precipitation and b) annual number of dry days at Houston William P. Hobby Airport. The black line shows observations, the light blue in a) and the tan line in b) are the means of 22 GCMs for the lower (RCP4.5) scenario and the dark blue line in a) and the dark brown line in b) are the means for the higher (RCP8.5) scenarios, respectively, and the shaded areas are the ranges among the 22 GCMs for the lower and higher scenarios.

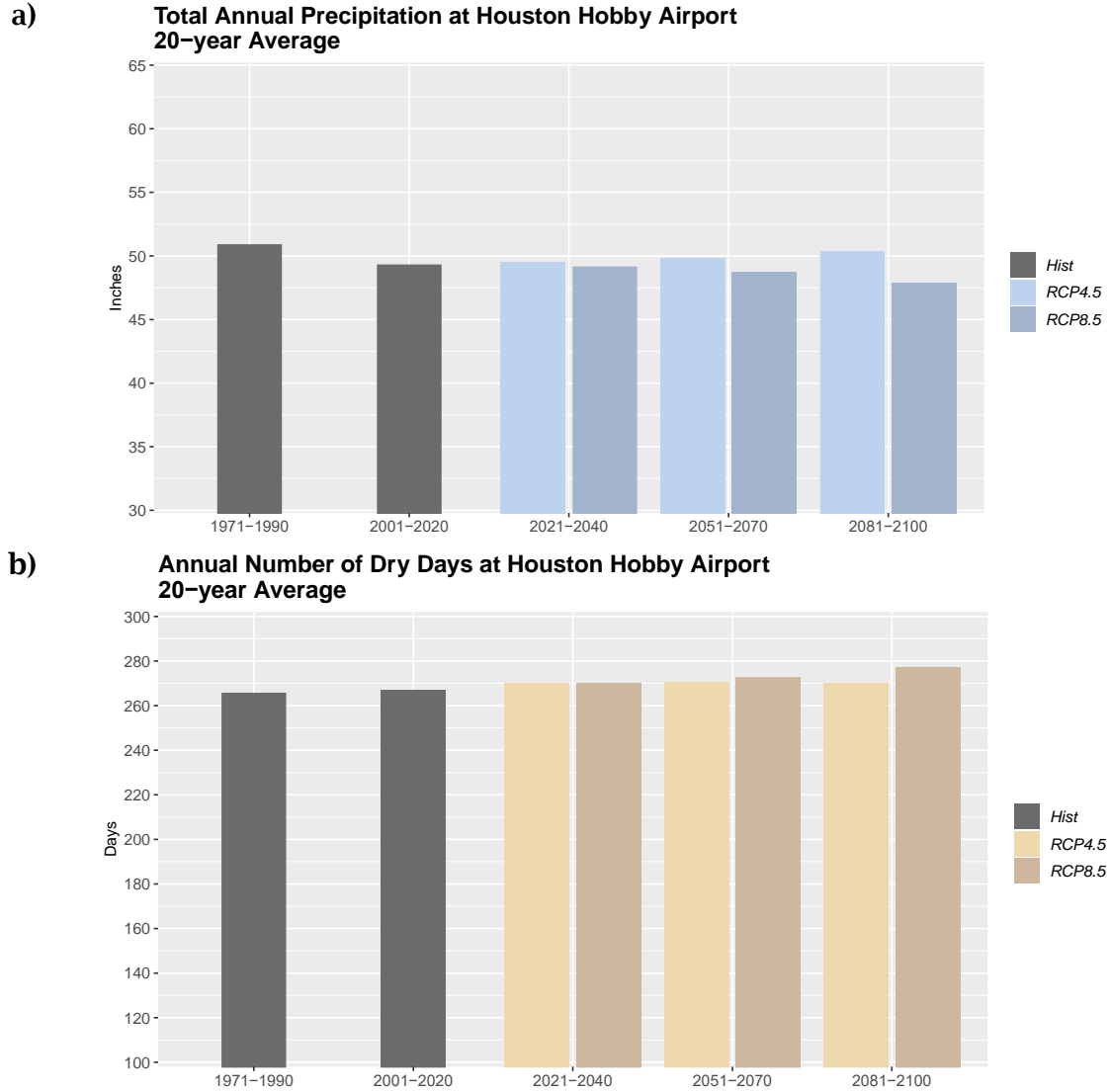


Figure 20 Observed and projected a) total annual precipitation and b) annual number of dry days at Houston William P. Hobby Airport for four 20-year periods. The gray bars show the average historical values, the lighter and darker bars are the means of 22 GCMs for the lower (RCP4.5) and higher (RCP8.5) scenarios, respectively.

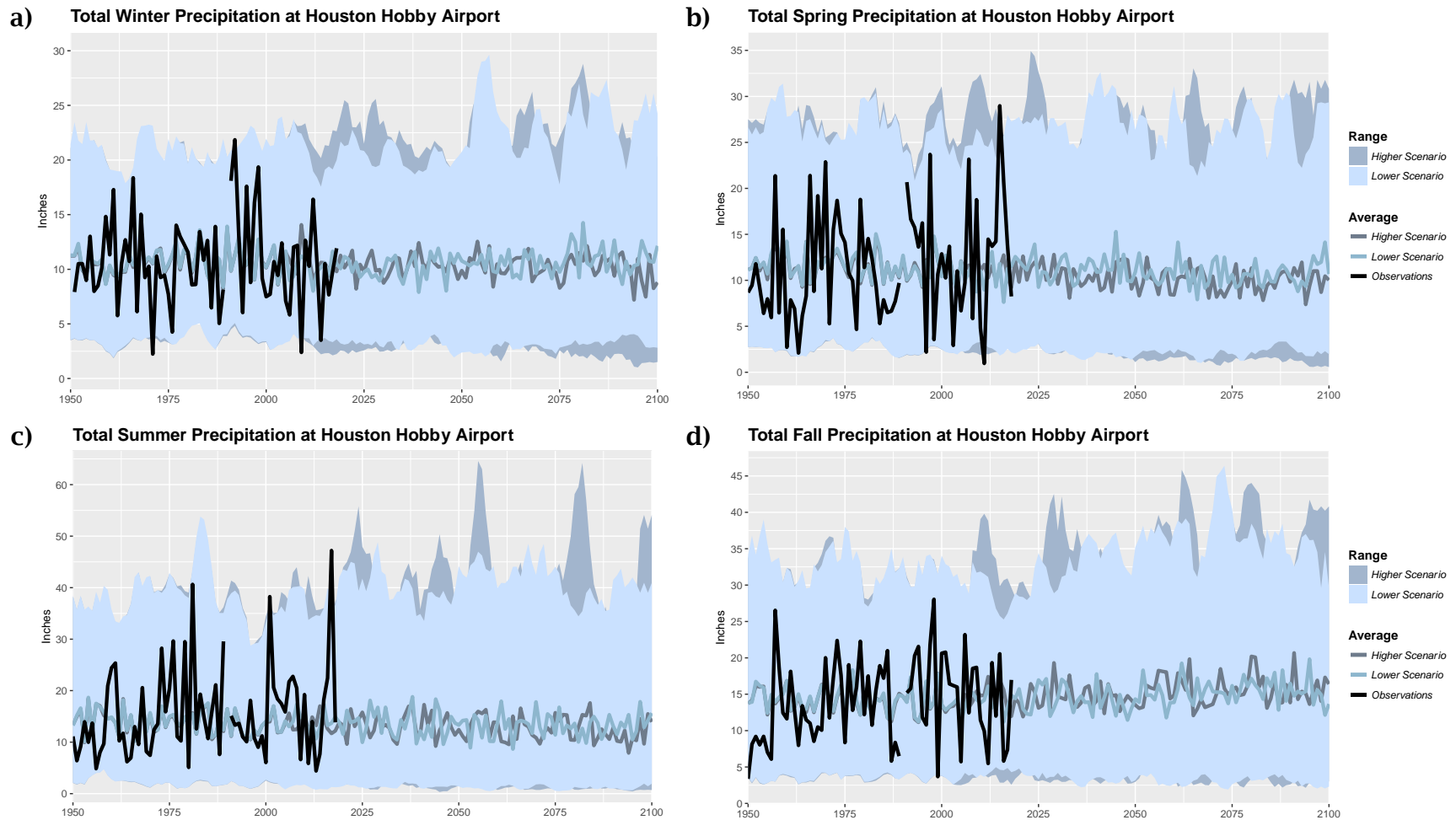
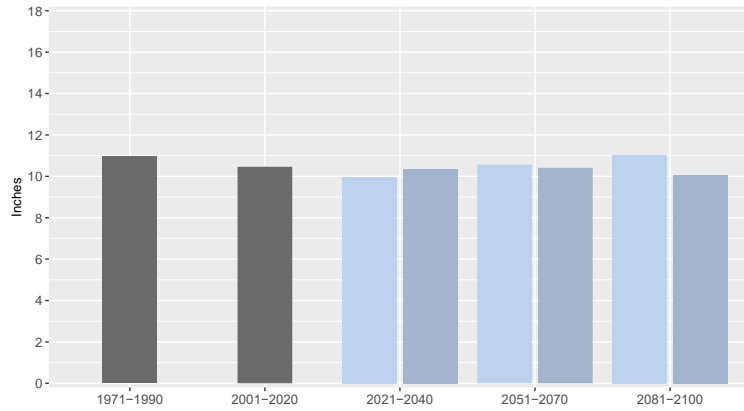
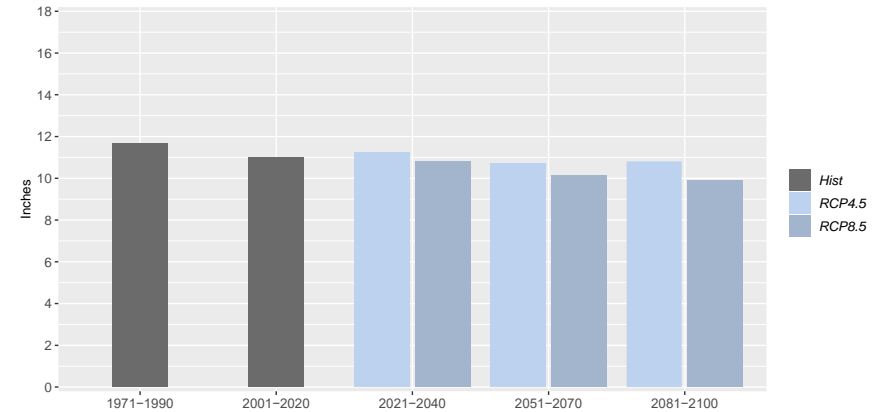


Figure 21 Observed and projected a) winter, b) spring, c) summer, and d) fall seasonal total precipitation at Houston William P. Hobby Airport. The black line shows observations, the light and dark blue lines are the means of 22 GCMs for the lower (RCP4.5) and higher (RCP8.5) scenarios, respectively, and the shaded areas are the ranges among the 22 GCMs for the lower (light blue) and higher (dark blue) scenarios.

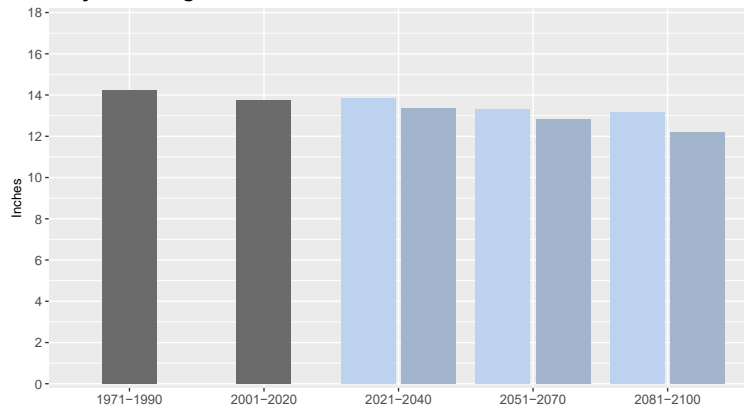
**a) Total Winter Precipitation at Houston Hobby Airport
20-year Average**



**b) Total Spring Precipitation at Houston Hobby Airport
20-year Average**



**c) Total Summer Precipitation at Houston Hobby Airport
20-year Average**



**d) Total Fall Precipitation at Houston Hobby Airport
20-year Average**

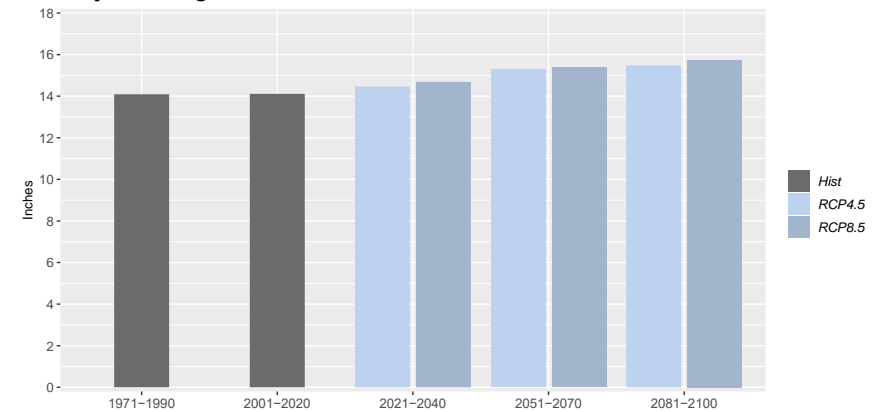


Figure 22 Observed and projected a) winter, b) spring, c) summer, and d) fall seasonal total precipitation at Houston William P. Hobby Airport. The gray bars show the average historical values, the light blue and dark blue bars are the means of 22 GCMs for the lower (RCP4.5) and higher (RCP8.5) scenarios, respectively.

FOUR. Changes in Extreme Precipitation

Although the total annual precipitation is not projected to change, the average of the 22 global climate models does show slight increases in extreme precipitation events for both the lower and higher scenarios. For the earlier observed period (1971-1990), observations at William P. Hobby Airport show that the annual wettest 3-day precipitation event accumulated 6.4 inches of rain, on average for the 20-year period (not shown), whereas the global climate models simulated average for the same period is higher at 7.8 inches. Since these values deviate slightly from each other it is more important to examine the projected trend.

Future projections show a slight increase in the amount of precipitation falling in the **wettest 3-day event** for the lower scenario in the coming 20-year period and then no further change until the end of the century. Projections for the higher scenario show a slight positive trend in this indicator (Figure 23a and Figure 24a). By the middle of the century the average for both scenarios is 8.6 inches for both the lower and higher scenario, and by the end of the century the amounts are projected to increase further to 9 inches under the higher scenario. Figure 23 shows that there is a wide range in the global climate model projections, which means there is higher uncertainty in the amounts. One reason for the spread is that global climate models do not match day-to-day or even year-to-year observed variability, therefore events such as a large storm passing through the Houston area will not happen in the same year for every global climate model, and when events are averaged over several models the resulting mean dampens the very heavy events. The spread in projections (Figure 23a) can tell us something about the severity of singular events, according to individual global climate models.

Single day events with **precipitation above four inches** are also projected to increase slightly toward the end of the century for both scenarios (Figure 23b and Figure 24b). The observations for the 1971-1990 period show that days with precipitation above four inches occurred about 19 times during that period. During the most recent 20-year period (2001-2020) the global climate model average did not change much with 18 such events during that period. In the coming 20 years these heavy events are projected to increase slightly to about 20 four-inch precipitation events. By the middle of the century projections for the model average shows an increase to 22 four-inch precipitation events for the lower scenario and 21 for the higher scenario. By the end of the century these events are projected to increase to about 23 days with precipitation above four inches for both the lower and higher scenario during this period. Again, there is a wide range in the global climate models (Figure 23b) and the model average dampens individual model projections, which are higher in some years.

According to the National Oceanic and Atmospheric Administration (NOAA) ATLAS-14¹ precipitation frequency estimates for William P. Hobby Airport, the current 24-hour 100-year precipitation depth is 17.6 inches. Figure 24c shows the projected changes in the frequency of this, currently, **100-year storm event**. The numbers are very small because a 100-year event should theoretically only occur once every 100 years, which results in a theoretical average occurrence of 0.01 days per year. The values shown are 20-year total number of events averaged over 22 global climate models. Only some global climate models project future events exceeding the historical 100-year storm event. Over the coming two decades between two and three models project one such event for this location, depending on the scenario; by mid-century, the projections are similar, for the lower scenario two models project two events each for this period and for the higher scenario, two models project one event to occur and one model project two events during this 20-year period (not shown). By the end of the century there are three models that project one event each during the 2081-

¹ https://hdsc.nws.noaa.gov/hdsc/pfds/pfds_map_cont.html, accessed March 2020

2100 period for the lower scenario at this location, while for the higher scenario, three models project one event each exceeding the historical 100-year storm level and one model projecting that two such events will occur during this period. The GFDL-ESM2G climate model stands out projecting five events exceeding the historical 100-year storm level between now and the end of the century for the higher scenario. Although not all climate models project occurrences of the historical 100-year precipitation event at William P. Hobby Airport, the few that do show that these events may increase toward the end of the century. Projections for some of the other locations included in this analysis show a larger increase in the recurrence of the 100-year storm. Figures showing projections of the 100-year storm event for individual downscaled global climate models are available in Appendix C.

It is important to note that these projections do not incorporate the effect of hurricanes on the frequency of a 100-year rain event. As noted earlier, for example, Emanuel (2019) found that a hurricane like Harvey that would be considered a 100-year event for the period 1981-2000 would be more likely to be a one-in-five or one-in-six event before the end of the century.

Finally, the potential for changes in drought can be estimated by examining the **Standardized Precipitation-Evapotranspiration Index (SPEI)**. Extended periods of positive SPEI values indicate a water surplus and negative values indicate periods of drought. Figure 25 shows the observed and global climate model simulated SPEI index for the higher and lower scenario. The observed SPEI curve is highly fluctuating, much more so than the model average as well as the full range of global climate models. The global climate model ensemble average shows a slight negative trend for both the lower and higher scenarios, with no significant difference between the two scenarios. This suggests the risk of drought increases in the future for both scenarios toward the end of the century, consistent with other studies (e.g. Ryu and Hayhoe 2017, Ryu et al. 2018).

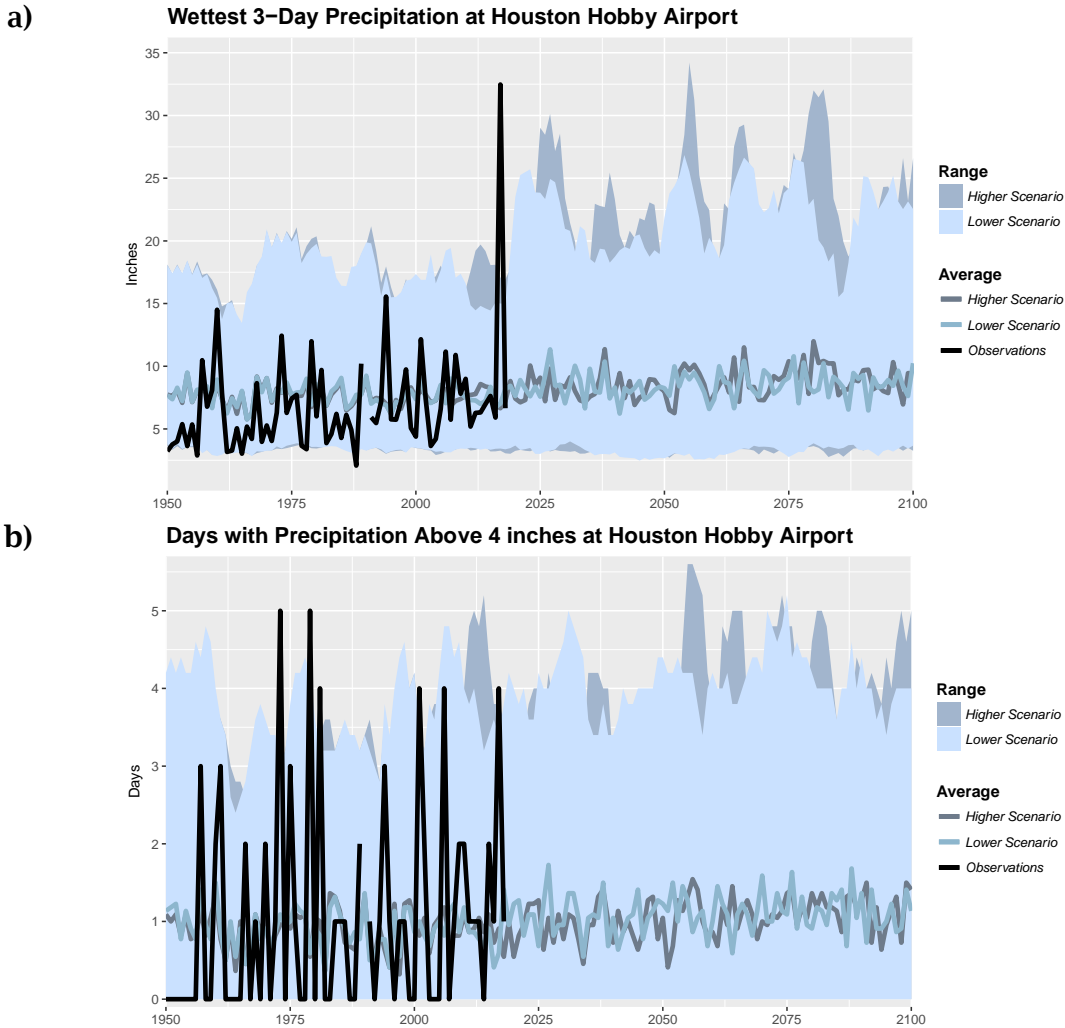


Figure 23 Observed and projected a) wettest 3-day precipitation amounts and b) the number of days per year with precipitation above 4 inches at Houston William P. Hobby Airport. The black line shows observations, the light blue lines are the means of 22 GCMs for the lower (RCP4.5) scenario and the dark blue lines are the means for the higher (RCP8.5) scenarios, respectively. The shaded areas are the ranges among the 22 GCMs for the lower and higher scenarios.

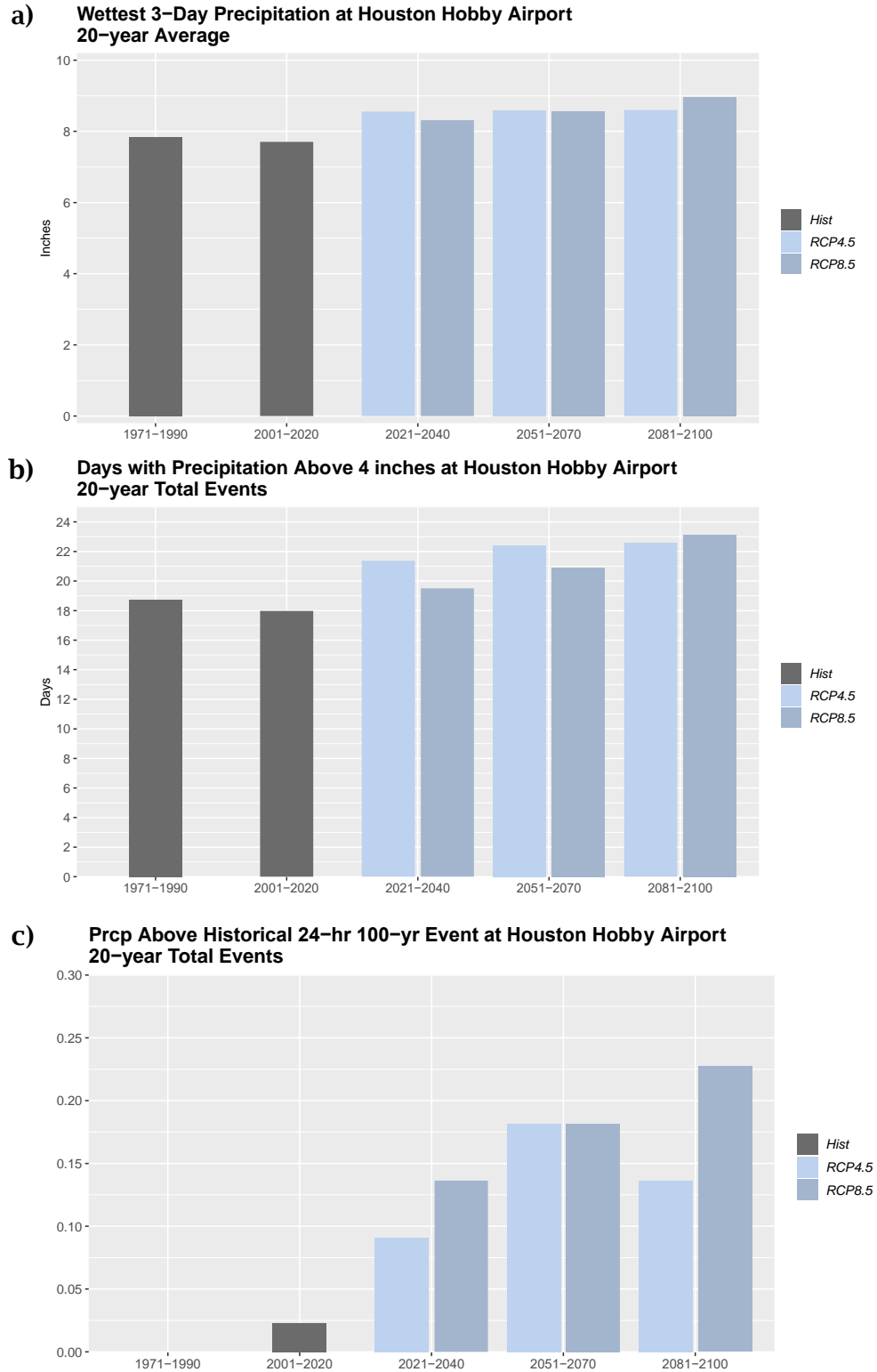


Figure 24 Observed and projected a) wettest 3-day precipitation amounts, b) the number of days per year with precipitation above 4 inches, and c) the total number of days with precipitation exceeding the historical 24-hour 100-year precipitation event for four 20-year periods at Houston William P. Hobby Airport. The gray bars show the average historical values, the light blue and dark blue bars are the means of 22 GCMs for the lower (RCP4.5) and higher (RCP8.5) scenarios, respectively.

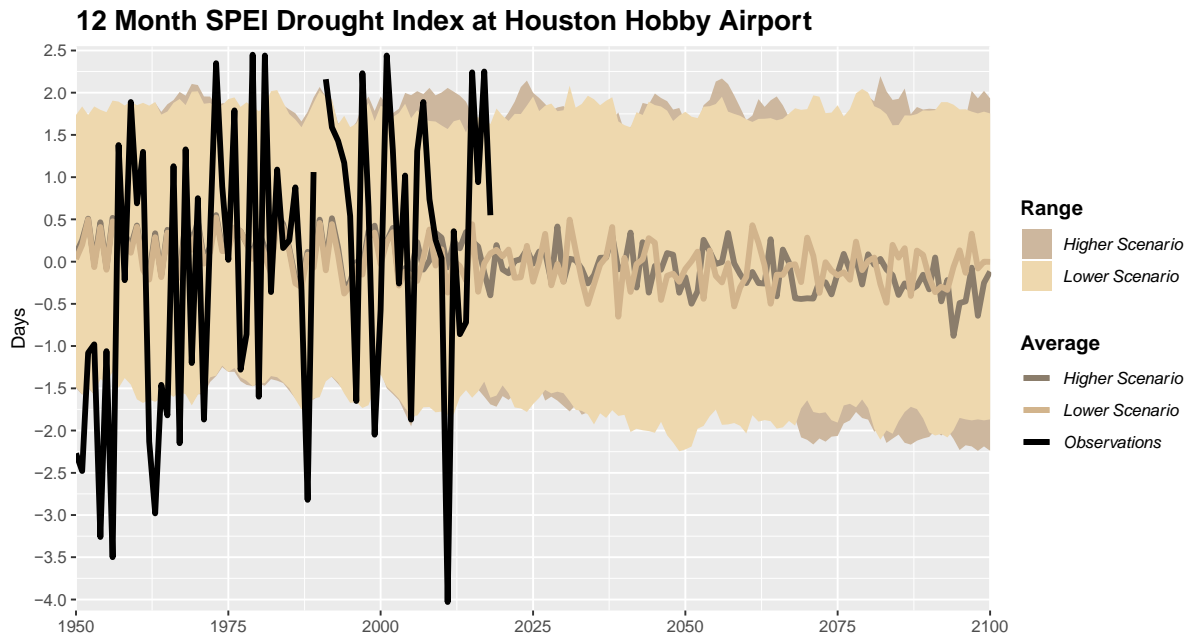


Figure 25 Observed and projected 12-month SPEI drought index at Houston William P. Hobby Airport. The black line shows observations, the tan line is the mean of 22 GCMs for the lower (RCP4.5) scenario and the dark brown line is the mean for the higher (RCP8.5) scenario, respectively, and the shaded areas are the ranges among the 22 GCMs for the lower and higher scenarios.

FIVE. Regional Variability

The 11 weather stations included in this study are listed in Table 1 and shown in Figure 26 in the **Data, Models, and Methods** section below. Although the region these stations cover is a smaller area that includes the City of Houston as well as the surrounding area there is some geographical variability in some of the indicators, mainly due to the proximity of the ocean for several of the stations, which can have a cooling effect during the hotter part of the year and a warming effect in the cooler part of the year, whereas other stations are further inland and do not benefit from this moderating effect of the water.

The start, end, and length of summer do not vary significantly across the area; all stations exhibit similar trends. Hot extreme temperatures such as the number of days above 100°F do vary, with coastal locations having fewer observed and projected days above 100°F and inland stations seeing higher numbers. For example, Galveston, which is surrounded by water on both sides, has only rarely experienced days with temperature above 100°F and is not projected to see much of an increase toward the end of the century, whereas Columbus, located further inland, historically has observed more than 20 days per year, on average, above 100°F and is projected to see dramatic increases in this indicator under both the lower and higher scenario, with projections at the end of the century, for the lower and higher scenario, suggesting between 50 and 100 days per year above this threshold are possible.

Wintertime temperatures also vary across the area due to proximity to the ocean for some stations. Locations that are on or very near the coast generally experience slightly warmer cold season temperatures compared to sites further inland. This is evident in the annual heating degree-days, indicating the amount of heating needed, which historically has been between 1100 and 1200 HDDs for Galveston and are projected to decrease for both scenarios to between 500 and 800 HDDs by the end of the century, depending on scenario;

whereas Cleveland, which is further inland and not so much affected by the warmer ocean surface water in winter, historically has observed heating degree-days between 1800 and 2000, is also projected to see decreases in this indicator although not as dramatically as Galveston, but to values between 1000 and 1400 HDDs, depending on the scenario.

Regional precipitation patterns vary as well, although they are not affected in the same manner as temperature by proximity to the ocean. Annual precipitation amounts are lowest at the southwestern locations of Palacios Airport and Columbus, which both historically have seen average annual precipitation amounts between 40 and 42 inches per year. Annual precipitation amounts generally increase toward the north and east, with the Houston NWS Office location reporting the highest 20-year average annual precipitation amounts with historical values on average between 60 and 63 inches. The northeastern stations of Beaumont Research Center and Port Arthur Airport have slightly lower amounts but are also in the higher end of the range between stations. None of the locations are projected to see a significant change in the annual total precipitation amounts.

There is no clear geographical pattern in the spatial variability of extreme precipitation. Some of the southwestern locations, such as Palacios Airport and Columbus, have slightly lower observed precipitation amounts in the wettest 3-day events, with historical values between 6.5 to 8 inches, on average for the 1971-1990 period. Projections show slight increases toward the end of the century to between 7 and 8.5 inches for these stations. The Houston NWS Office station, just southeast of the city has the highest historical wettest 3-day precipitation amounts of 10.8 inches, averaged over the 1971-1990 period. This location is also projected to see very slight increases for both the lower and higher scenario to between 11 and 12 inches, on average, by the end of the century. As noted previously, however, urbanization can significantly impact the risks of flooding due to a given amount of rain. Thus, even if extreme precipitation does not vary significantly across the region, flood risk may.

In addition, as Houston residents experienced during Hurricane Harvey in 2017, extreme precipitation often occurs as localized events, with areas not far from one another receiving very different amounts of precipitation. Extreme precipitation is difficult for global climate models to simulate, and climate models differ in their projections of when and how often extreme events may happen. That is partly due the fact that each model is independently simulating natural variability and does not align on which years are more or less prone to have, for example, large, destructive hurricanes than other years. It is also due to the fact that most global models do not currently resolve hurricanes and none of them resolve the microphysics of clouds and precipitation processes; higher-resolution, specialized models are required for hurricane modeling, but precipitation processes are still parameterized (i.e. represented by equations that capture the behavior of the process at the spatial and temporal scale of the model resolution) rather than explicitly resolved by even the highest-resolution models at this time.

Precipitation projections in the annual wettest 3-day event do not vary much across the region. In some years, for example, the northeastern side of the City of Houston may receive more extreme rain events than the southwest, while in other years it will be the opposite. This variability in spatial distribution will continue to occur as part of the natural variability of the weather and climate.

Projections in the exceedance of the historical 24-hour 100-year storm event vary significantly across the region. Projections for William P. Hobby Airport, discussed in the previous section, show that only a handful of climate models project exceedance of the 100-year event in the future. For many other locations, the number of global climate models that project events exceeding the historical 100-year storm is much larger and in some cases

with many occurrences during each 20-year period. For the Houston NWS Office location, for example, almost all 22 global climate models project events exceeding the 100-year storm through the end of the century, with the INMCM4 model projecting as many as 32 events exceeding the 100-year storm, for the lower scenario, between now and the end of the century (see Appendix C). For the higher scenario, several models also project multiple events exceeding the historical 100-year precipitation event at the Houston NWS Office location, with the GFDL-ESM2G model projecting as many as nine events by the end of the century, with eight of them happening in the 2051-2070 period (not shown).

SIX. Conclusions and Summary

Climate in Houston is already changing: all seasons are warming; hot days are becoming more frequent; heavy precipitation is becoming more frequent; and heatwaves and hot days have increased in intensity. Although little changes are seen in the total annual precipitation amounts, precipitation patterns are changing, with more extreme rain events becoming more intense and an increasing number of dry days.

In the future, climate is expected to continue to change. While natural factors continue to affect the Earth's climate, the main driver of climate change today and over the remainder of this century is human emissions of carbon dioxide and other heat-trapping gases. As a result, the human choices that determine emissions are the primary uncertainty in future projections. For that reason, this assessment quantifies projections under two different scenarios: a higher scenario where fossil fuel dependence continues and heat-trapping gases continue to increase, and a lower scenario characterized by a rapid transition to clean energy and a reduction in heat-trapping gas emissions that is consistent with the goal of the Houston Climate Action Plan. The lower scenario quantifies what the city will have to adapt to, even with significant emission reductions world-wide; the higher scenario shows what impacts may be avoided by reducing emissions.

Projected changes for Houston's climate include:

- Increases in the average temperature of all seasons and lengthening of summer, with summer beginning earlier and ending later. By the middle of the century summer is expected to last 41 or 55 days longer for the lower and higher scenarios, respectively, and by the end of the century 47 or 81 days longer, compared to the 1971-1990 historical period.
- Increases in energy demand for cooling buildings for the spring, summer, and fall seasons. By the middle of the century CDD is projected to increase by 351 or 487 CDDs for the lower and higher scenario, respectively, and 396 or 729 CDDs by the end of the century for summer compared to the historical period.
- Decreases in the energy demand for heating buildings in the colder months. Annual cumulative values are projected to decrease by 394 or 534 HDDs by the middle of the century and 460 or 739 HDDs by the end of the century for the lower and higher scenarios, respectively.
- Increases in the number of days per year with temperature above 100°F. For the middle of the century the Houston area can expect to experience approximately 12 or 23 days per year above 100°F for the lower and higher scenarios, respectively, and as many as 14 or 54 days for the lower and higher scenarios by the end of the century.
- Increasing number of very warm nights above 80°F. Projections indicate that Houston can expect more warm nights, with 22 or 50 nights per year, on average, for the lower and

higher scenario respectively by the middle of the century, whereas by the end of the century it can expect 30 or 96 warm nights per year.

- Increasing extreme hot temperatures. The temperature of the hottest day of the year is projected to increase to 104°F or 106°F for the lower and higher scenarios, respectively, by the middle of the century, and to 104°F or 109°F by the end of the century, compared to 99.4°F for the 1971-1990 average hottest day of the year.
- Increases in the average temperature of the hottest week of the year. Values are projected to increase from 96.1°F during the 1971-1990 period to 100°F or 102°F by the middle of the century for the lower and higher scenarios, respectively, and to 101°F or 105°F by the end of the century.
- Longer heatwaves. During the 1971-1990 period a heatwave lasted on average 2.5 days but their average length is projected to increase by 15.3 or 26.7 days by the middle of the century for the lower and higher scenarios, respectively, and by 18.8 or 46.6 days by the end of the century.
- No significant changes in the annual total precipitation. Seasonal changes are projected for summer and fall, with a slight decreasing trend in summer and an increasing trend in fall.
- Increase in the number of dry days per year. During the 1971-1990 period, observations show an average of 266 dry days per year and by the middle of the century, projections show a slight increase for both scenarios with 271 or 273 annual dry days for the lower and higher scenarios, respectively, and 270 or 277 days per year by the end of the century.
- Decreasing trend in the SPEI drought index for both the lower and higher scenarios, indicating a higher risk of droughts in the future, including extended periods of drought.
- Increases in the amount of precipitation falling in the wettest 3-day event. By the middle of the century the wettest 3 days are projected to average 8.6 inches for both scenarios, compared to 7.8 inches in the earlier historical period. By the end of the century there is no change projected for the lower scenario but an increase to 9 inches for the higher scenario.
- Slight increases in the number of days with precipitation above 4 inches. By the middle of the century numbers are projected to increase slightly to 22 or 21 total number of events for that 20-year period for the lower and higher scenarios, respectively, compared to 19 days for the historical period, and by the end of the century to 22 or 23 events for the later 20-year period.
- Significant increases in the return period of the 100-year rain event under both the higher and lower scenarios.

Table 1 shows a summary of the findings as well as the range in projections, which depends on individual years and individual climate model projections. There is greatest certainty in projected increases in seasonal temperatures, increases in the length of summer, and changes in cooling and heating degree-days. These are changes that are already occurring (see Appendix B) and are projected to continue over the remainder of the century.

There is moderate certainty in projected seasonal precipitation and increases in heavy precipitation and very wet days. Observed trends and projected future increases in heavy precipitation events are consistent across North America and have formally been attributed to the impacts of human-induced climate change. There is also moderate certainty in

projected changes in drier conditions, as a result of increased temperatures rather than changes in precipitation.

There is less certainty in projected changes in extreme precipitation. Although observed trends and regional projections indicate an increase, for the city of Houston itself there is a wide spread in models and less data available from which to estimate more extreme conditions. However, local factors such as urbanization can increase the risk of flooding for a given amount of rain; and this analysis does not include hurricanes, which are becoming more intense, with more rainfall associated with them, as a result of a changing climate.

The observed and projected future changes documented in this report have the potential to affect Houston's economy, ecosystems, energy demand, infrastructure, and more. Decreasing number of cold days and increased risk of extreme heat and heavy precipitation have the potential to affect both public and private infrastructure, with implications for a broad range of sectors, from insurance to energy demand for heating and cooling residential and commercial buildings.

The projections described in this report are intended to enable assessment of these impacts and inform efforts to build resilience to future change. The sections that follow provide detailed information regarding the data, models, and methods used in developing these projections, as well as the products and outputs available from this analysis.

Table 1. Summary of future projections for the lower and higher scenarios for the mid- and end-of-century time periods compared to averages for the 1971-1990 historical period. Values in parentheses are the lowest to highest value depending on year and/or climate model.

Indicator	1971-1990 (Observed)	2051-2070 (lower)	2051-2070 (higher)	2081-2100 (lower)	2081-2100 (higher)
Days per year above 100 °F	1 day (0-8 days)	12 days (0-51 days)	23 days (0-80 days)	14 days (0-53 days)	55 days (5-122 days)
Nights per year above 80 °F	<1 night (0-3 nights)	20 nights (1-73 nights)	50 nights (7-110 nights)	30 nights (1-78 nights)	95 nights (32-143 nights)
Temperature of the hottest day	99 °F (95-103 °F)	104 °F (98-112 °F)	106 °F (98-115 °F)	104 °F (98-113 °F)	109 °F (102-118 °F)
Length of the longest heatwave	2.5 days (1-5 days)	15 days (2-48 days)	27 days (3-79 days)	19 days (4-53 days)	47 days (8-111 days)
First day of summer	June 13 th (May 29 th -Jul 1 st)	May 22 nd (Apr 22 nd -Jun 19 th)	May 14 th (Apr 5 th -Jun 17 th)	May 19 th (Apr 16 th -Jun 13 th)	May 1 st (Mar 17 th -Jun 2 nd)
Last day of summer	Sept 18 th (Sept 3 rd -Oct 7 th)	Oct 7 th (Sept 14 th -Nov 3 rd)	Oct 13 th (Sept 18 th -Nov 14 th)	Oct 9 th (Sept 9 th -Nov 9 th)	Oct 26 th (Sept 30 th -Dec 2 nd)
Length of summer	97 days (70-119 days)	137 days (97-177 days)	152 days (107-206 days)	144 days (105-189 days)	177 days (137-240 days)
March to November cooling degree-days (CDDs)	3050 CDDs (2475-3575 CDDs)	3925 CDDs (2875-4950 CDDs)	4300 CDDs (3250-5600 CDDs)	4075 CDDs (3125-5175 CDDs)	4975 CDDs (3400-6300 CDDs)
Annual heating degree-days (HDDs)	1350 HDDs (1000-1975 HDDs)	950 HDDs (550-1400 HDDs)	825 HDDs (375-1450 HDDs)	900 HDDs (450-1450 HDDs)	600 HDDs (200-1150 HDDs)
Total annual precipitation	51 inches (27-83 inches)	50 inches* (18-92 inches)	49 inches* (21-106 inches)	50 inches* (19-92 inches)	48 inches* (15-105 inches)
Annual number of dry days	266 days (251-289 days)	271 days (221-311 days)	273 days (225-311 days)	270 days (227-309 days)	277 days (233-316 days)
Average wettest 3-day precipitation event	Observed: 6.4 inches [†] (2.1-12.4 inches) Simulated: 7.8 inches [†] (3.1-21.1 inches)	8.6 inches [†] (2.5-26.8 inches)	8.6 inches [†] (2.7-34.2 inches)	8.6 inches [†] (2.8-25.2 inches)	9 inches [†] (2.8-32.1 inches)
Total 20-year precipitation events above 4 inches	19 events (0-100 events)	22 events [§] (0-88 events)	21 events [§] (0-112 events)	23 events [§] (0-92 events)	23 events [§] (0-100 events)

* There is significant variability in the climate model projections for this indicator, with values for individual years and models ranging between less than 20 inches in some years to more than 100 inches in other years.

† The historical simulated values for this indicator are slightly higher than observations, which likely means that future projections have a small positive bias.

§ There is a lot of variability in the climate model projections for this indicator, with values for individual years and models ranging between zero and 6 events per year with precipitation above four inches.

Data, Models, and Methods

ONE. Observed Data

Observed daily maximum and minimum temperature and precipitation were obtained from 11 **long-term weather stations** across the Houston region with at least 30 years' worth of daily temperature and precipitation recorded between 1950 and 2019 from the Global Historical Climatology Network (GHCN) maintained by the U.S. National Centers for Environmental Information. GHCN is an integrated database of daily climate summaries from over 100,000 land surface stations across 180 countries that includes daily climate records from numerous sources that have been integrated and subjected to a common suite of quality assurance reviews. The stations used in this report consist of Angleton, Beaumont Research Center, Cleveland, Columbus, Freeport, Galveston, George Bush Intercontinental Airport, William P. Hobby Airport, Houston National Weather Service Office, Palacios Airport, Port Arthur Airport (Table 2 and Figure 26). Source: <https://www.ncdc.noaa.gov/gHCN-daily-description>.

Table 2. City or location names, GHCN ID numbers, latitude and longitude for the 11 long-term weather stations used in this analysis.

Location	GHCN ID	Latitude	Longitude
Angleton	USC00410257	29.1573	-95.4593
Beaumont Res. Center	USC00410613	30.0688	-94.2927
Cleveland	USC00411810	30.3637	-95.084
Columbus	USC00411911	29.699	-96.573
Freeport	USC00413340	28.9845	-95.3809
Galveston	USW00012944	29.33333	-94.77167
G. Bush Int. Airport	USW00012960	29.98	-95.36
W.P. Hobby Airport	USW00012918	29.63806	-95.28194
Houston NWS Office	USC00414333	29.4718	-95.0832
Palacios Airport	USW00012935	28.72472	-96.25361
Port Arthur Airport	USW00012917	29.95056	-94.02056

TWO. Climate Indicators

Daily temperature and precipitation observations for the station-based data were then used to calculate a set of **climate indicators** relevant to potential impacts on the Houston area.

This analysis includes 15 temperature-based indicators, 9 precipitation-based indicators, and 1 hybrid temperature-precipitation indicator. The climate indicators are defined and listed in Tables 3A (temperature), 3B (precipitation), and 3C (hybrid variables).

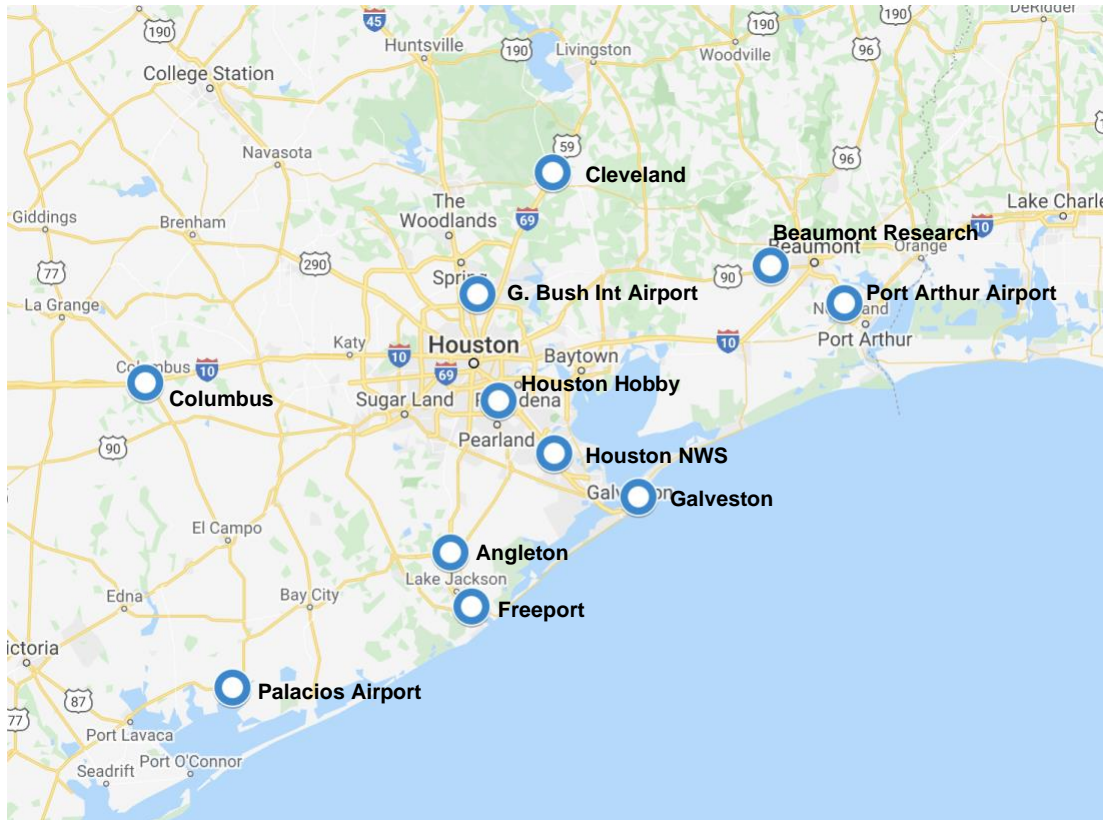


Figure 26 Map of the 11 weather stations included in the City of Houston Climate Assessment.

Table 3A. These climate indicators have been calculated from daily **temperature** observations and model simulations, for 11 weather stations in the Houston area.

Indicator	Definition	Units
Onset of summer	First day in spring with 10-day average temperature above the 75 th quantile historical temperature	Day of Year (Julian Date)
End of summer	Last day in fall with 10-day average temperature above the 75 th quantile historical temperature	Day of Year (Julian Date)
Length of summer	The number of days between onset and end of summer	Days
Cooling Degree-Days	Cumulative days in spring, summer, and fall with average temperature above 65°F	Degree-Days
Heating Degree-Days	Cumulative days in winter, spring, fall, and annually with average temperature below 65°F	Degree-Days
Days per Year Above 100°F	Number of days per year with maximum temperature above 100°F	Days per Year
Nights per Year Above 80°F	Number of nights per year with minimum temperature above 80°F	Days per Year
Hottest Day of the Year	Maximum temperature on the hottest day of the year	°F
Hottest Week of the Year	Maximum temperature of the hottest week of the year	°F
Longest Heatwave	Length of the longest heatwave	Days

Table 3B. These climate indicators have been calculated from daily **precipitation** observations and model simulations, for 11 weather stations in the Houston area.

Precipitation-Related Indicator	Definition	Units
Annual Precipitation	Cumulative precipitation for January through December	inches
Seasonal Precipitation	Cumulative precipitation for a) Dec-Jan-Feb, b) Mar-Apr-May, c) Jun-Jul-Aug, and d) Sep, Oct, Nov	inches
Annual Dry Days	Number of days between each year with less than 0.01 inches of precipitation	Days per Year
Wettest 3-day Event	Cumulative Precipitation in the wettest three consecutive days of the year	Inches
Very Wet Days	Number of days per year with precipitation above 4 inches in one day.	Days per Year
Return period of historical 100-year storm	How often will the 1-in-100-year rain event be exceeded in the future.	Days per Year

Table 3C. This climate indicator has been calculated from daily **temperature** and **precipitation** observations and model simulations, for 11 weather stations in the Houston area.

Hybrid Indicator	Definition	Units
SPEI Drought Index	12-month SPEI drought index.	Unit-less

THREE. Future Scenarios

At the local scale, how much and how fast climate will change in the future is uncertain due to multiple factors that are described in detail in Section 5 below. At the regional to global scale, however, given that human emissions of carbon dioxide and other heat-trapping gases are the primary driver of climate change today, one of the most important sources of uncertainty in future projections is the choices humans will make that determine future emissions. This uncertainty is particularly relevant to quantifying the magnitude of projected changes in average annual and seasonal temperature, and many extreme temperature and precipitation indicators, for mid-century and beyond.

To account for scenario uncertainty, future projections were developed for two very different scenarios, or Representative Concentration Pathways (RCPs), that span a broad range of possible changes over the coming century (Moss et al. 2010; Figure 27a). The **lower scenario** used here (RCP 4.5) represents a future in which the world shifts to clean energy sources in the coming decades, reducing carbon emissions from human activities to 1970 levels by around 2080. (This report does not include projections for the lowest scenario, RCP2.6, as only a few years' worth of emissions at present-day rates remain to be emitted before the carbon budget required to meet RCP2.6 is exceeded. See Hayhoe et al. 2017 for more details.) The **higher scenario** used here (RCP 8.5) represents a future in which people continue to depend heavily on fossil fuels, and emissions of heat-trapping gases continue to grow. The numbers in the scenario labels (RCP4.5 and RCP8.5) refer to the projected change in radiative forcing (+4.5 and +8.5) in units of watts per square meter. Radiative forcing is a measure of the extent to which humans have artificially enhanced the magnitude of the naturally

occurring greenhouse effect that already maintains the temperature of the planet at an average temperature of more than 85°F above what it would be without an atmosphere.

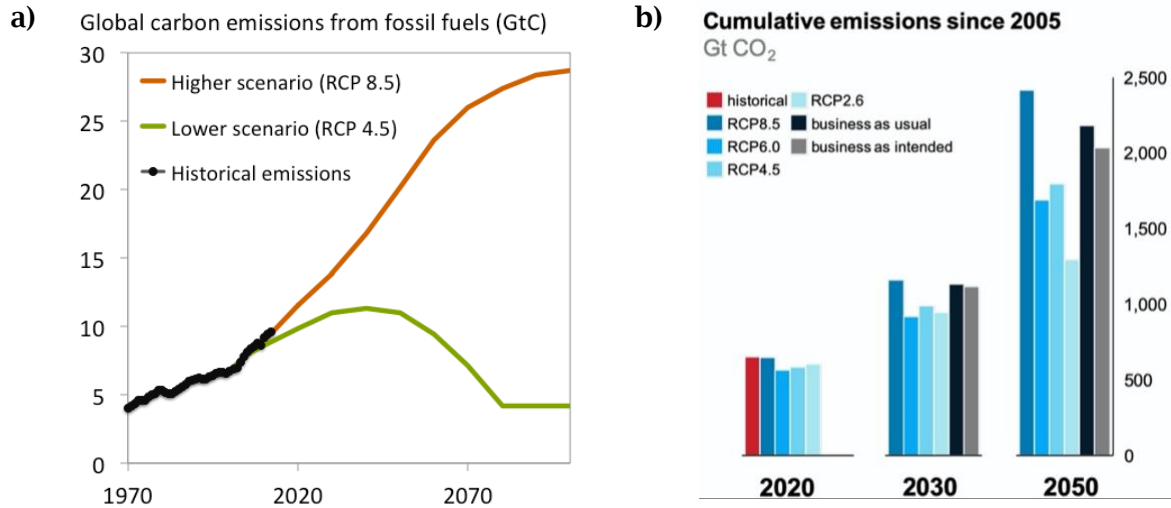


Figure 27 a) Historical carbon emissions (black) continue to increase from one decade to the next. This assessment examines how the Houston climate might change if the world follows Representative Concentration Pathway (RCP) 8.5, a higher scenario with continued dependence on carbon-intensive fossil fuels (orange) or RCP 4.5, a lower scenario where replacing fossil fuels with zero-carbon alternatives reduces and ultimately stabilizes global carbon emissions (green). Data: CDIAC, IIASA. b) Recent historical cumulative emissions are tracking the RCP8.5 scenario (from Schwalm et al., 2020).

Each scenario is treated equivalently in this analysis, with no likelihood assigned to either. Results from the higher and a lower future scenario are used equally. However, given that the RCP scenarios begin in 2006, the *Fourth U.S. National Climate Assessment* analyzed emissions from 2006 through 2016 and concluded that, currently, “the observed increase in global carbon emissions over the past 15–20 years has been consistent with higher scenarios (very high confidence).” (Hayhoe et al. 2017) and a more recent study finds that “emissions consistent with RCP8.5 [are] in close agreement with historical total cumulative CO₂ emissions (within 1%), [and] RCP8.5 is also the best match out to midcentury under current and stated policies with still highly plausible levels of CO₂ emissions in 2100.” (Schwalm et al., 2020; Figure 27b). However, a significant amount of future change can be avoided by reducing and eventually eliminating carbon emissions from human activities, compared to continuing to rely on fossil fuels, but it requires that the majority of the world meets its Paris targets as the City of Houston is doing and follows the City of Houston’s leadership.

FOUR. Global Climate Models and Empirical-Statistical Downscaling

As described in NCA4 Vol. 1, “global climate models are mathematical frameworks that were originally built on fundamental equations of physics. They account for the conservation of energy, mass, and momentum and how these are exchanged among different components of the climate system. Using these fundamental relationships, global climate models are able to simulate many important aspects of Earth’s climate: large-scale patterns of temperature and precipitation, general characteristics of storm tracks and extratropical cyclones, and observed changes in global mean temperature and ocean heat content as a result of human emissions. The complexity of climate models has grown over time, as they incorporate additional

components of Earth's climate system. For example, global climate models were previously referred to as "general circulation models" when they included only the physics needed to simulate the general circulation of the atmosphere. Today, global climate models simulate many more aspects of the climate system: atmospheric chemistry and aerosols, land surface interactions including soil and vegetation, land and sea ice, and increasingly even an interactive carbon cycle and/or biogeochemistry." (Hayhoe et al. 2017)

Regarding the use of these models for future projections, it states that "confidence in the usefulness of the future projections generated by global climate models is based on multiple factors. These include the fundamental nature of the physical processes they represent, such as radiative transfer or geophysical fluid dynamics, which can be tested directly against measurements or theoretical calculations to demonstrate that model approximations are valid (e.g., IPCC 1990). They also include the vast body of literature dedicated to evaluating and assessing model abilities to simulate observed features of the earth system, including large-scale modes of natural variability, and to reproduce their net response to external forcing that captures the interaction of many processes which produce observable climate system feedbacks (e.g., Flato et al. 2013)." And it concludes, "**there is no better framework for integrating our knowledge of the physical processes in a complex coupled system like Earth's climate.**" (Hayhoe et al. 2017)

This is not intended to imply that global climate models are perfect. They are not, and the differences between them represent the limitations of scientific ability to simulate the climate system. These differences are an important source of uncertainty in determining the magnitude and sometimes even the direction of projected changes in average and seasonal precipitation, as well as the magnitude of the more extreme indicators of temperature and precipitation. In most cases, it is not possible to identify a single "best" model or small subset of such models; rather, research has shown that the ensemble or average of multiple models is typically better able to simulate long-term climate than any individual model, though the multi-model mean can be optimized by a weighting scheme that takes into account the extent to which various models are related and thereby should not be treated as independent sources (Knutti, 2017).

For that reason, future projections for this report were based on simulations from 22 different global climate models from phase 5 of the Coupled Model Intercomparison Project (CMIP5). The global climate models used to generate future projections, and their country of origin, are: ACCESS1-0 (Australia), ACCESS1-3 (Australia), BCC-CSM-1-1 and BCC-CSM1-1-M (China), BNU-ESM (China), CanESM2 (Canada), CCSM4 (USA), CNRM-CM5 (France), CSIRO-Mk3-6-0 (Australia), GFDL-ESM2G and GFDL-ESM2M (USA), HadGEM2-ES and HadGEM2-CC (UK), INMCM4 (Russia), IPSL-CM5A-LR, IPSL-CM5A-MR, and IPSL-CM5B-LR (France), MIROC5 (Japan), MPI-ESM-LR and MPI-ESM-MR (Germany), MRI-CGCM3 (Japan) and NorESM1-M (Norway). Results from other global climate models were not included if required daily outputs were not available, they had not been downscaled, and/or known issues precluded their use in this application.

Global climate model output is typically too coarse to be applied at the scale of a major city, let alone an individual weather station. For that reason, global climate model outputs are typically downscaled using a statistical or dynamical method (Figure 28; for more information, see Section 5 and Kotamarthi et al. 2016). This report used projections that had been downscaled using an **empirical statistical downscaling model** that combines global climate model simulations with historical records of daily observations (using at least 30 years if not more, to cover a range of weather conditions) to produce locally relevant projections of temperature and precipitation. The downscaling models are "trained" using these observational datasets to increase the spatial resolution of the future projections and

to remove or correct the bias in global climate model simulations relative to observations, producing high-resolution projections at the same temporal and spatial scale of the original observations.

This report used daily maximum and minimum temperature and precipitation projections for the lower RCP4.5 and higher RCP8.5 scenarios that were statistically downscaled using a nonparametric empirical statistical downscaling method that uses a kernel density estimator to map observed distributions to those simulated by the global climate models for that region. The first version of the ARRM is described in Stoner et al. (2012); an updated description of this downscaling model that includes the newer nonparametric method and improved treatment of extremes that was applied to the temperature projections used in this report is presented Hayhoe et al., 2020.

Temperature and precipitation had been downscaled to the 11 long-term *weather stations* across the Houston area with at least 30 years' worth of daily data recorded between 1950 and 2016 listed in Table 1. Before being used to downscale global climate model simulations, all GHCN station data undergoes a quality control process that uses a nearest neighbor approach to remove any anomalously extreme temperature and/or precipitation values that are not verified by data recorded by a neighboring station within twenty four hours of the day of the anomalous observation.

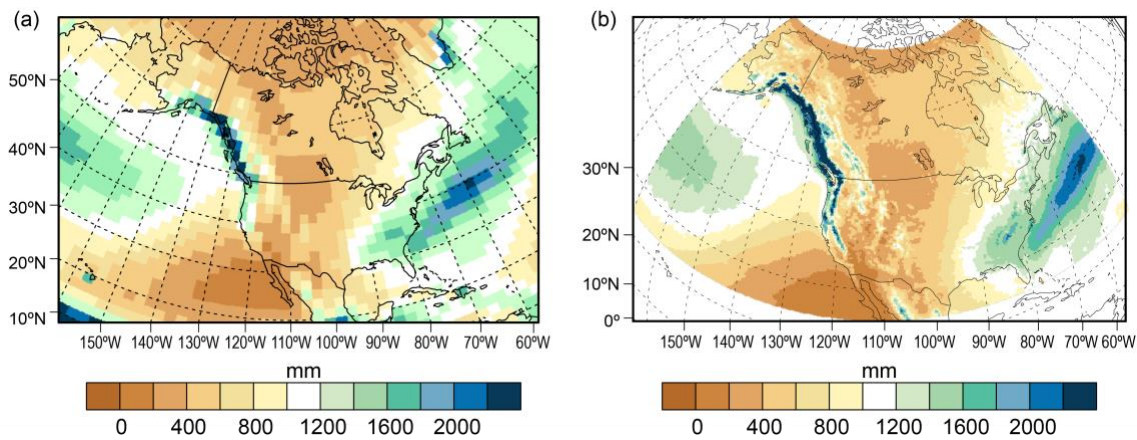


Figure 28 CMIP5 global climate models typically operate at coarser horizontal spatial scales on the order of 30 to 200 miles (50 to 300 km). This figure compares annual average precipitation (in millimeters) for the historical period 1979-2008 using (a) a resolution of 250 km or 150 miles with (b) a resolution of 15 miles or 25 km to illustrate the importance of spatial scale in resolving key topographical features, particularly along the coasts and in mountainous areas. Source: Fourth U.S. National Climate Assessment, Volume 1, Chapter 4, Figure 4.4 (Hayhoe et al. 2017).

FIVE. Sources of Uncertainty in Future Projections

There are four main sources of uncertainty in future climate projections:

1. Natural variability, which causes temperature, precipitation, and other aspects of climate to vary from year to year and even decade to decade.

The Earth's climate is extremely complex. Interactions between the various components of the system can be non-linear, making it difficult to determine direct cause-and-effect. The response of the climate system to internal variability can be chaotic, meaning that predictions of day-to-day and even year-to-year variations in temperature and precipitation can be extremely sensitive to the initial conditions.

This source of uncertainty is particularly important over *shorter time frames*. As NCA4 states, "over the next two decades, global temperature increase is projected to be between 0.5°F and 1.3°F (0.3°–0.7°C) (medium confidence). *This range is primarily due to uncertainties in natural sources of variability that affect short-term trends. In some regions, this means that the trend may not be distinguishable from natural variability* (high confidence)." (Hayhoe et al. 2017)

However, although the internal variability of the climate system is highly non-linear, *the response of the climate system to a given external forcing* (e.g., from changes in energy from the Sun, or from increasing heat-trapping gases due to human activities) *is predictable over longer timescales*. So even though it is not possible to predict the weather beyond two weeks, it is very possible to reliably simulate the long-term, large-scale response of the climate system to changes in energy from the Sun, volcanic eruptions, natural cycles, and increasing emissions of heat-trapping gases from human activities.

To address the first source of uncertainty, **natural variability**, simulations from 22 different climate models, each with a different pattern of natural variability based on different initial conditions, are used to calculate the statistics of climate and weather at each site.

Natural variability is an important source of uncertainty over shorter time scales. However, averaged over longer time scales of multiple decades, the contribution of natural variability to overall uncertainty decreases significantly for most variables, including those related to temperature and extreme precipitation.

2. Scientific and model uncertainty, including exactly how much the Earth will warm in response to human emissions and whether global climate models accurately represent important and relevant aspects of Earth's climate.

Climate sensitivity is defined as the increase in global temperature when carbon dioxide doubles relative to pre-industrial times. Its value likely lies between 2 to 4.5°C [3.6 to 8.1°F], but it is impossible to determine it exactly as it depends on the initial conditions of the planet and the rate, magnitude, and the type of forcing that is driving the change. As Kopp et al. (2017) indicates, the current initial conditions + forcing of the planet are unprecedented in at least the last 50 million years. This is the first source of scientific uncertainty in future projections.

The second source of uncertainty is *structural*. Are the climate models correctly representing every part of the Earth system? What if there are processes important to regional or global change, such as the radiative effects of black carbon, or possible changes in the circulation and carbon uptake of the Southern Ocean due to global warming, which are not yet included in the models?

The third source of uncertainty arises due to the fact that global climate models have limited resolution in time and space. Many processes, including cloud formation, precipitation, and the effects of dust on the atmosphere, occur at scales smaller than the model can resolved.

Scientists use lab experiments, observations, and high-resolution modeling to try and understand how these processes appear in aggregate, at the scale of a global model. Using these empirical relationships, or parameterizations, introduces *parametric* uncertainty.

Although scientific uncertainty is usually distributed evenly relative to the mean or best guess value, it is important to note that the uncertainty in model structure and climate sensitivity is asymmetric. Certain aspects of the climate system and lower bounds to climate sensitivity tend to be better-understood and therefore smaller than higher bounds. As a result, by using mid-range values, global climate models are more at risk of under-estimating than over-estimating scientific uncertainty. As NCA4 concludes, “while climate models incorporate important climate processes that can be well quantified, they do not include all of the processes that can contribute to feedbacks, compound extreme events, and abrupt and/or irreversible changes. For this reason, future changes outside the range projected by climate models cannot be ruled out (very high confidence). [This is referring to structural uncertainty.] Moreover, *the systematic tendency of climate models to underestimate temperature change during warm paleoclimates suggests that climate models are more likely to underestimate than to overestimate the amount of long-term future change* (medium confidence). [This is referring to climate sensitivity.]” (Hayhoe et al. 2017)

To address the second source of uncertainty, **scientific and model uncertainty**, the future projections used in this report are based on simulations from multiple global climate models and the range of projections resulting from these simulations are presented. Scientific or model uncertainty tends to be an important source of uncertainty in determining the magnitude and sometimes even the direction of projected changes in average precipitation.

3. Scenario or human uncertainty, as future climate change will occur largely in response to emissions from human activities that have not yet occurred.

Scenarios are intended to cover a wide range of plausible futures. Their purpose is to illustrate differences in the extent and severity of the global warming that would result from different choices, depending on factors such as:

- how human societies and economies evolve;
- how quickly technological advances occur;
- how new energy sources are developed; and
- how policies are enacted that affect heat-trapping gas emissions.

Factors not under human control, such as the response of natural emissions of greenhouse gases to a warming Arctic, for example, or the response of clouds to a warming planet, are not explicitly included in these scenarios. Natural factors such as these contribute to the uncertainty in climate sensitivity described above.

The further into the future projections extend, the more important the role of scenario or human uncertainty becomes in quantifying the rate and magnitude of future change. NCA4 concludes that, “beyond the next few decades, the magnitude of climate change depends primarily on cumulative emissions of greenhouse gases and aerosols and the sensitivity of the climate system to those emissions (high confidence).” (Hayhoe et al. 2017).

To address the third source of uncertainty, that of **human activities** and heat-trapping gas emissions, future projections in this report are based on two very different plausible pathways for the future, a higher and a lower scenario. Climate model simulations using these two scenarios present what the future may look like depending on the actions we take as humans to reduce emissions. The two scenarios are not bounding what is possible, emissions could be even lower if drastic action is taken now to curb emissions, or they could be higher

if none are taken, but they are likely paths if considerable action is taken in the next few decades to reduce emissions (lower scenario) and if little to no action is taken to reduce emissions (higher scenario).

NCA4 analyzed emissions from 2006 through 2016 and concluded that, currently, “the observed increase in global carbon emissions over the past 15–20 years has been consistent with higher scenarios (very high confidence).” (Hayhoe et al. 2017) However, if most of the world follows the example of the City of Houston in meeting its Paris Agreement targets, the lower scenario is achievable.

4. Local uncertainty, which results from the many factors that interact to determine how the climate of one specific location, such as individual sites or weather stations in the Houston area, will respond to global-scale change over the coming century.

NCA4 states that, “combining output from global climate models and dynamical and statistical downscaling models using advanced averaging, weighting, and pattern scaling approaches can result in more relevant and robust future projections. For some regions, sectors, and impacts, these techniques are increasing the ability of the scientific community to provide guidance on the use of climate projections for quantifying regional-scale changes and impacts (*medium to high confidence*).” (Hayhoe et al. 2017) However, the application of a downscaling model adds an additional layer of uncertainty as well.

An empirical-statistical model, such as used in this report, develops a statistical relationship between global climate model output and observations assuming that the conditions experienced in a given city or location tend to be part of a larger pattern of weather systems and air masses affecting the entire region. Statistical methods don't resolve the physical processes responsible for this relationship (although some of these relationships may be implied by the predictors chosen from the global model). For this reason, statistical methods are based on the fundamental assumption that the relationship between large-scale climate and local climate remains stationary over decades. If climate change alters local feedback processes that affect the relationship between local and large-scale climate, statistical methods will not be able to simulate these changes.

Statistical methods are limited by observations. It is only possible to develop projections for variables that have already been observed for a number of years, and for the scale at which they were observed. Statistical downscaling also assumes the observations provide a perfectly accurate representation of actual conditions. In reality, all kinds of factors, from observer error to long-term trends in the data due to equipment decay, can bias data. Therefore, a statistical model may end up incorporating observational error into future projections, if that error was unintentionally built into the statistical relationship between observed local variables and large-scale climate.

To address the fourth source of uncertainty, that of **local change**, global climate model simulations were statistically downscaled to individual long-term weather station observations covering the Houston area, to incorporate observed records of variability and change. The assumptions of stationarity that underlie the specific statistical method used in this report have been evaluated using the perfect model approach and shown to provide reliable information, compared to that of a fully dynamic global model, through 2100 under a higher RCP8.5 scenario for daily wet day precipitation out to the 99.9th percentile of the distribution and maximum and minimum temperature out to the 99.9th percentile (Dixon et al. 2016). They are furthermore only as precise as the observational data.

Products

This analysis has produced a range of outputs and products that are appropriate for scientific analysis, future planning, and public outreach. They are described here in order, from most technical to least technical.

ONE. Daily Station-Based Climate Projections - Data

Station-based statistically downscaled maximum and minimum temperature and precipitation for 11 long-term weather stations from 1950 to 2100, for 22 global climate models and 2 future scenarios. These station-based projections are daily and are available for the long-term weather stations listed in Table 2.

Station downscaled projections are available in CSV format and are appropriate for use in scientific analysis by researchers and practitioners who are familiar with climate data and projections.

The archive consists of 66 individual station files (11 stations x 2 scenarios x 3 variables) that each contain downscaled projections for the 22 global climate models as well as historical values.

TWO. Annual Station-Based Climate Indicators - Data

The primary daily temperature and precipitation outputs from Product One have been used to calculate a set of *climate indicators* from the observations and from each individual model simulations that are relevant to potential impacts on Houston. The climate indicators are listed in Tables 2A (temperature), 2B (precipitation), and 2C (hybrid variables).

Indicators were calculated using both observed and model-simulated data for the historical period, so that it is possible to compare observations with model simulations over the historical period. They were also calculated using model projections for the period 1950 to 2100.

Station downscaled projections are available in CSV format and are appropriate for use in scientific analysis by researchers and practitioners who are familiar with climate data and projections.

The archive consists 550 station files (11 stations x 2 scenarios x 25 indicators) that each contain annual indicator values calculated for observations and each of the 22 global climate models.

In the archive of annual climate indicators, each file covers the period 1950 to 2100. Since observations are only available for the historical period, their values are set to "NA" for the future.

THREE. Multi-Model Mean and Ranges of Station-Based Climate Indicators for the Higher and Lower Future Scenarios – Data and Time Series Plots

The station-based *climate indicators* calculated from the observations for each of the 11 long-term weather stations listed in Table 2, and from each individual model simulation in Product Two, have also been summarized as annual values from 1950-2100 for the higher and lower scenarios described in the Data, Models, and Methods section, as well as for the length of the observed historical record. These values have been archived in a single CSV file

for each weather station that can be opened in Excel. The format of a sample file is shown in Table 4.

Table 4. Sample output file format for station-based projections of changes by year. The first column contains the year. Subsequent columns are grouped in sevens, one set of seven for each climate indicator listed in Table 3. The first column gives the observed value. Values are set to NA if observations are not available for that year. The second and third columns give the multi-model mean value for the lower scenario (RCP4.5) and the higher scenario (RCP8.5) for that year. The fourth and fifth columns give the multi-model minimum and maximum value, defined as the extremes of the multi-model ensemble for that year smoothed by a 5-year running mean, for the lower scenario. The sixth and seventh columns give the multi-model minimum and maximum value for the higher scenario. There is one output file for each of the 11 weather stations. In the actual files, the indicators' name also appears in the header of each column; they have been removed here for clarity.

Years	OBS	RCP4.5 mean	RCP8.5 mean	RCP4.5 min	RCP4.5 max	RCP8.5 min	RCP8.5 max
1950	96.98	99.20	99.03	93.07	104.30	93.27	104.53
1951	100.04	99.56	99.66	93.98	103.84	94.14	103.96
1952	98.06	98.01	98.02	93.07	104.40	93.89	104.41
...
2099	NA	104.43	108.52	98.67	110.41	103.44	117.33
2100	NA	104.47	108.80	99.01	110.62	103.56	117.81

The data has been used to create time series plots and bar charts – one for each of the 25 climate indicators listed in Tables 3A, B and C. The complete set of time series for individual weather stations is available as a PDF file in *Appendix A: Climate Indicator Time Series for Weather Stations*. Bar charts are available for individual weather stations as a PDF file in *Appendix B: Climate Indicator Bar Charts for Weather Stations*.

Four sample plots are shown in Figure 29. Each plot is labelled with the city, the variable, and the units (e.g. “Annual Heating Degree-Days at Houston Hobby Airport”). Each plot contains three lines: a black line indicating observations for that location; a darker line indicating the multi-model mean for the higher scenario; and a lighter line indicating the multi-model mean for the lower scenario. The length of the observed data will vary from one station to the next, based on the years available in the historical record. The multi-model averages extend from 1950 to 2100. Each plot also contains two shaded areas: a lighter area indicating the multi-model range for the lower scenario, and a darker area indicating the top (for a variable that is increasing over time) or bottom (for a variable that is decreasing) end of the range for the higher scenario.

The time series plots are color-coded, with orange referring to warm temperatures (e.g. warmest day of the year or degree-days), purple to cold temperatures (e.g. winter heating degree-days), blue to precipitation (e.g. total annual precipitation), and brown for dry days and drought.

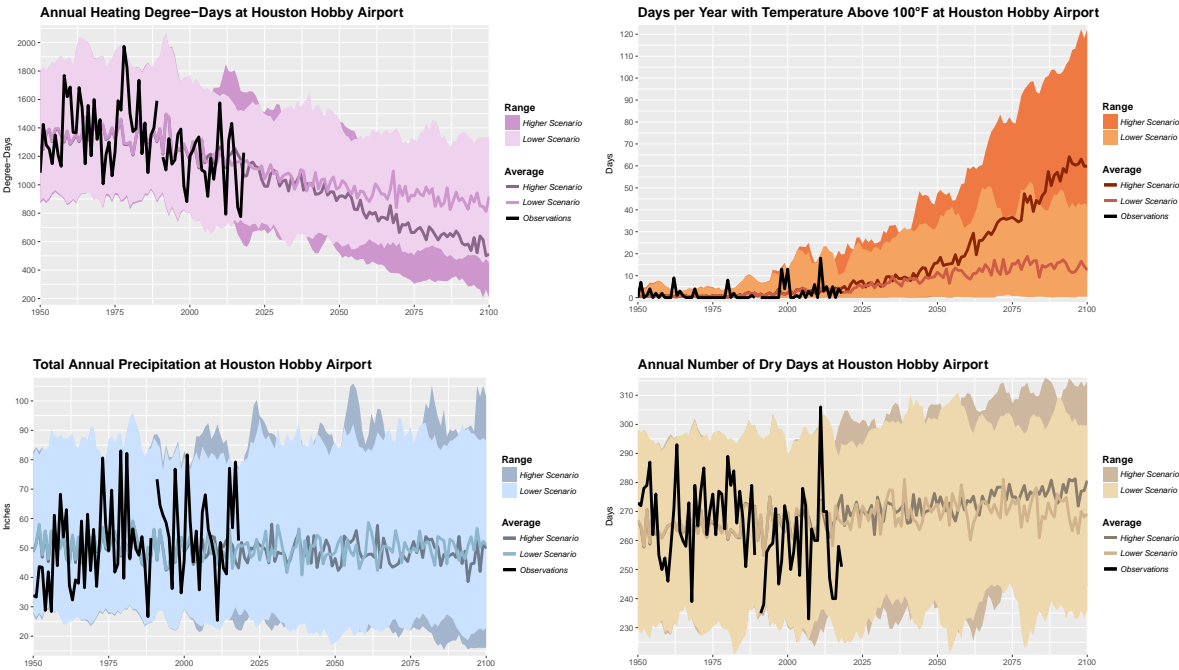


Figure 29 Projected changes in four different climate indicators for the Houston William P. Hobby Airport weather station, for the variables listed at the top of each chart. Values shown are the projected multi-model mean for the higher (darker line) and lower (lighter line) future scenarios as well as the observations (black line). The multi-model range for the higher (dark) and lower (light) future scenarios is indicated by the shaded areas. 24 figures, one for each of the climate indicators listed in Tables 3A, B and C, with the exception of 100-year precipitation return indicator, are available in a PDF file for each of the 11 long-term weather stations listed in Table 2.

Appendices

Appendix A: Climate Indicator Time Series for Weather Stations

This appendix consists of 11 PDF files, one for each of the weather stations listed in Table 2. Each file contains 24 time series plots, one for each climate indicator listed in Table 3 (except for the 100-year precipitation return indicator). Each time series shows the observed values for the duration of the historical record, and projected *change* corresponding to the higher and lower future scenarios, from 1950 to 2100.

Appendix B: Climate Indicator Bar Charts for Weather Stations

This appendix consists of 11 PDF files, one for each of the weather stations listed in Table 2. Each file contains 24 bar charts, one for each climate indicator listed in Table 3 (except the SPEI drought indicator). Each bar chart shows the observed value for 1971-1990 and 2001-2020 and projected values three 21st century periods: 2021-2040, 2051-2070, and 2081-2100, for each future scenario.

Appendix C: Climate Indicator Bar Charts for Weather Stations – Return Frequency of the 24-hour 100-year Precipitation Event

This appendix consists of 2 PDF files, one for the lower scenario and one for the higher scenario. Each file contains 11 bar charts, one for each of the weather stations listed in Table 2. Each bar chart shows the simulated value for the 24-hour 100-year precipitation event for 1971-1990 and 2001-2020 and projected values for three 21st century periods: 2021-2040, 2051-2070, and 2081-2100, for each global climate model that has projections of this event. Models not included in the bar charts or in certain periods do not simulate future precipitation events of this magnitude for that location. Each bar is the total number of events in each 20-year period.

References

- Brauer, N.S., J.B. Basara, C.R. Homeyer, G.M. McFarquhar, and P.E. Kirstetter. 2020. Quantifying Precipitation Efficiency and Drivers of Excessive Precipitation in Post-Landfall Hurricane Harvey. *J. Hydrometeorol.*, 21, 433-452, doi: 10.1175/JHM-D-19-0192.1.
- Combs, S. 2012. The Impact of the 2011 Drought and Beyond. Texas Comptroller of Public Accounts. https://texashistory.unt.edu/ark:/67531/metaph542095/m2/1/high_res_d/txc-0790.pdf.
- Dixon, K.W., J.R. Lanzante, M.J. Nath, K. Hayhoe, A. Stoner, A. Radhakrishnan, V. Balaji, and C.F. Gaitán. 2016. Evaluating the Stationarity Assumption in Statistically Downscaled Climate Projections: is Past Performance and Indicator of Future Results? *Climatic Change*, 135, 395-408, doi: 10.1007/s10584-016-1598-0.
- Easterling, D.R., K.E. Kunkel, J.R. Arnold, T. Knutson, A.N. LeGrande, L.R. Leung, R.S. Vose, D.E. Waliser, & M.F. Wehner. 2017. Precipitation change in the United States. In: *Climate Science Special Report: Fourth National Climate Assessment, Volume I* [Wuebbles, D.J., D.W. Fahey, K.A. Hibbard, D.J. Dokken, B.C. Stewart, and T.K. Maycock (eds.)]. U.S. Global Change Research Program, Washington, DC, USA, pp. 207-230, doi: 10.7930/JOH993CC.
- Emanuel, K. 2017. Assessing the Present and Future Probability of Hurricane Harvey's Rainfall. *PNAS*, 114, 12681-12684, doi: 10.1073/pnas.1716222114.
- Feulner, G. and S. Rahmstorf. 2010. On the effect of a new grand minimum of solar activity on the future climate on Earth. *Geophysical Research Letters*, 37(5), doi: 10.1029/2010GL042710.
- Flato, G., J. Marotzke, B. Abiodun, P. Braconnot, S.C. Chou, W. Collins, P. Cox, F. Driouech, S. Emori, V. Eyring, C. Forest, P. Gleckler, E. Guilyardi, C. Jakob, V. Kattsov, C. Reason and M. Rummukainen. 2013. Evaluation of Climate Models. In: *Climate Change 2013: The Physical Science Basis. Contribution of Working Group I to the Fifth Assessment Report of the Intergovernmental Panel on Climate Change* [Stocker, T.F., D. Qin, G.-K. Plattner, M. Tignor, S.K. Allen, J. Boschung, A. Nauels, Y. Xia, V. Bex and P.M. Midgley (eds.)]. Cambridge University Press, Cambridge, United Kingdom and New York, NY, USA
- Frame, D.J., M.F. Wehner, I. Noy, and S.M. Rosier. 2020. The Economic Costs of Hurricane Harvey Attributable to Climate Change. *Climatic Change*, 160, 271-281, doi: 10.1007/s10584-020-02692-8.
- Gowda, P., J.L. Steiner, C. Olson, M. Boggess, T. Farrigan, and M.A. Grusak. 2018: Agriculture and Rural Communities. In *Impacts, Risks, and Adaptation in the United States: Fourth National Climate Assessment, Volume II* [Reidmiller, D.R., C.W. Avery, D.R. Easterling, K.E. Kunkel, K.L.M. Lewis, T.K. Maycock, and B.C. Stewart (eds.)]. U.S. Global Change Research Program, Washington, DC, USA, pp. 391-437, doi: 10.7930/NCA4.2018.CH10.
- Hartmann, D.L., A.M.G. Klein Tank, M. Rusticucci, L.V. Alexander, S. Brönnimann, Y. Charabi, F.J. Dentener, E.J. Dlugokencky, D.R. Easterling, A. Kaplan, B.J. Soden, P.W. Thorne, M. Wild & P.M. Zhai. 2013. Observations: Atmosphere and Surface. In: *Climate Change 2013: The Physical Science Basis. Contribution of Working Group I to the Fifth*

- Assessment Report of the Intergovernmental Panel on Climate Change [Stocker, T.F., D. Qin, G.-K. Plattner, M. Tignor, S.K. Allen, J. Boschung, A. Nauels, Y. Xia, V. Bex and P.M. Midgley (eds.)]. Cambridge University Press, Cambridge, United Kingdom and New York, NY, USA.
- Hayhoe, K. & R. Kopp. 2016. What surprises lurk within the climate system? *Environmental Research Letters*, 11 (12), 120202, doi: 10.1088/1748-9326/11/12/120202.
- Hayhoe, K., D.J. Wuebbles, D.R. Easterling, D.W. Fahey, S. Doherty, J. Kossin, W. Sweet, R. Vose, and M. Wehner. 2018. Our Changing Climate. In *Impacts, Risks, and Adaptation in the United States: Fourth National Climate Assessment, Volume II* [Reidmiller, D.R., C.W. Avery, D.R. Easterling, K.E. Kunkel, K.L.M. Lewis, T.K. Maycock, and B.C. Stewart (eds.)]. U.S. Global Change Research Program, Washington, DC, USA, pp. 72-144. doi: 10.7930/NCA4.2018.CH2.
- Hayhoe, K., J. Edmonds, R.E. Kopp, A.N. LeGrande, B.M. Sanderson, M.F. Wehner, & D.J. Wuebbles. 2017. Climate models, scenarios, and projections. In: *Climate Science Special Report: Fourth National Climate Assessment, Volume I* [Wuebbles, D.J., D.W. Fahey, K.A. Hibbard, D.J. Dokken, B.C. Stewart, and T.K. Maycock (eds.)]. U.S. Global Change Research Program, Washington, DC, USA, pp. 133-160, doi: 10.7930/J0WH2N54.
- Hayhoe, K., I. Scott-Fleming, and A. Stoner. 2020. STAR-ESDM: High-Resolution Station- and Grid-Based Climate Projections. Presented at the American Meteorological Society Annual Meeting, Boston, MA, 2020, <https://ams.confex.com/ams/2020Annual/meetingapp.cgi/Paper/367184>.
- IPCC. 1990. *Climate Change: The IPCC Scientific Assessment*. Cambridge University Press, 212 pp.
- Knutson, T., J.P. Kossin, C. Mears, J. Perlwitz, & M.F. Wehner. 2017. Detection and attribution of climate change. In: *Climate Science Special Report: Fourth National Climate Assessment, Volume I* [Wuebbles, D.J., D.W. Fahey, K.A. Hibbard, D.J. Dokken, B.C. Stewart, and T.K. Maycock (eds.)]. U.S. Global Change Research Program, Washington, DC, USA, pp. 114-132, doi: 10.7930/J01834ND.
- Kloesel, K., B. Bartush, J. Banner, D. Brown, J. Lemery, X. Lin, C. Loeffler, G. McManus, E. Mullens, J. Nielsen-Gammon, M. Shafer, C. Sorensen, S. Sperry, D. Wildcat, and J. Ziolkowska. 2018: Southern Great Plains. In *Impacts, Risks, and Adaptation in the United States: Fourth National Climate Assessment, Volume II* [Reidmiller, D.R., C.W. Avery, D.R. Easterling, K.E. Kunkel, K.L.M. Lewis, T.K. Maycock, and B.C. Stewart (eds.)]. U.S. Global Change Research Program, Washington, DC, USA, pp. 987-1035. doi: 10.7930/NCA4.2018.CH23.
- Knutti, R., J. Sedláček, B. M. Sanderson, R. Lorenz, E. M. Fischer, and V. Eyring. 2017. A climate model projection weighting scheme accounting for performance and interdependence. *Geophysical Research Letters*, 44, 1909-1918, doi: 10.1002/2016GL072012.
- Kossin, J.P., T. Hall, T. Knutson, K.E. Kunkel, R.J. Trapp, D.E. Waliser, and M.F. Wehner. 2017: Extreme storms. In: *Climate Science Special Report: Fourth National Climate Assessment, Volume I* [Wuebbles, D.J., D.W. Fahey, K.A. Hibbard, D.J. Dokken, B.C. Stewart, and T.K. Maycock (eds.)]. U.S. Global Change Research Program, Washington, DC, USA, pp. 257-276, doi: 10.7930/J07S7KXX.

- Kotamarthi, R., L. Mearns, K. Hayhoe, C. Castro & D. Wuebbles. 2016. *Use of Climate Information for Decision-Making and Impacts Research: State of Our Understanding*. U.S. Dept. of Defense Technical Report AD1029525, Available online at: <http://www.dtic.mil/dtic/tr/fulltext/u2/1029525.pdf>
- Lall, U., T. Johnson, P. Colohan, A. Aghakouchak, C. Brown, G. McCabe, R. Pulwarty, and A. Sankarasubramanian. 2018: Water. In *Impacts, Risks, and Adaptation in the United States: Fourth National Climate Assessment, Volume II* [Reidmiller, D.R., C.W. Avery, D.R. Easterling, K.E. Kunkel, K.L.M. Lewis, T.K. Maycock, and B.C. Stewart (eds.)]. U.S. Global Change Research Program, Washington, DC, USA, pp. 145-173, doi: 10.7930/NCA4.2018.CH3.
- Lindsey, R. 2020. Climate Change: Global Sea Level. <https://www.climate.gov/news-features/understanding-climate/climate-change-global-sea-level>, Accessed August 2020.
- Lipton, D., M. A. Rubenstein, S.R. Weiskopf, S. Carter, J. Peterson, L. Crozier, M. Fogarty, S. Gaichas, K.J.W. Hyde, T.L. Morelli, J. Morissette, H. Moustahfid, R. Muñoz, R. Poudel, M.D. Staudinger, C. Stock, L. Thompson, R. Waples, and J.F. Weltzin. 2018: Ecosystems, Ecosystem Services, and Biodiversity. In *Impacts, Risks, and Adaptation in the United States: Fourth National Climate Assessment, Volume II* [Reidmiller, D.R., C.W. Avery, D.R. Easterling, K.E. Kunkel, K.L.M. Lewis, T.K. Maycock, and B.C. Stewart (eds.)]. U.S. Global Change Research Program, Washington, DC, USA, pp. 268-321, doi: 10.7930/NCA4.2018.CH7.
- Marsooli, R., N. Lin, K. Emanuel, and K. Feng. 2019. Climate Change Exacerbates Hurricane Flood Hazards along US Atlantic and Gulf Coasts in Spatially Varying Patterns. *Nature Communications*, 10, 3785, doi: 10.1038/s41467-019-11755-z.
- Masson-Delmotte, V., M. Schulz, A. Abe-Ouchi, J. Beer, A. Ganopolski, J.F. González Rouco, E. Jansen, K. Lambeck, J. Luterbacher, T. Naish, T. Osborn, B. Otto-Bliesner, T. Quinn, R. Ramesh, M. Rojas, X. Shao and A. Timmermann. 2013. Information from Paleoclimate Archives. In: *Climate Change 2013: The Physical Science Basis. Contribution of Working Group I to the Fifth Assessment Report of the Intergovernmental Panel on Climate Change* [Stocker, T.F., D. Qin, G.-K. Plattner, M. Tignor, S.K. Allen, J. Boschung, A. Nauels, Y. Xia, V. Bex and P.M. Midgley (eds.)]. Cambridge University Press, Cambridge, United Kingdom and New York, NY, USA.
- Maxwell, K., S. Julius, A. Grambsch, A. Kosmal, L. Larson, and N. Sonti. 2018: Built Environment, Urban Systems, and Cities. In *Impacts, Risks, and Adaptation in the United States: Fourth National Climate Assessment, Volume II* [Reidmiller, D.R., C.W. Avery, D.R. Easterling, K.E. Kunkel, K.L.M. Lewis, T.K. Maycock, and B.C. Stewart (eds.)]. U.S. Global Change Research Program, Washington, DC, USA, pp. 438-478, doi: 10.7930/NCA4.2018.CH11.
- Moss, R. H., J. A. Edmonds, K. A. Hibbard, M. R. Manning, S. K. Rose, D. P. van Vuuren, T. R. Carter, S. Emori, M. Kainuma, T. Kram, G. A. Meehl, J. F. B. Mitchell, N. Nakicenovic, K. Riahi, S. J. Smith, R. J. Stouffer, A. M. Thomson, J. P. Weyant, and T. J. Wilbanks. 2010. The next generation of scenarios for climate change research and assessment. *Nature*, 463, 747-756, doi:10.1038/nature08823.

- NASA. 2001. Global Effects of Mount Pinatubo. Available online at: <https://earthobservatory.nasa.gov/images/1510/global-effects-of-mount-pinatubo>
- NWS. 2017. <https://www.weather.gov/hgx/hurricaneharvey>. Accessed August 2017.
- van Oldenborgh G.J., K. van der Wiel, A. Sebastian, R. Singh, J. Arrighi, F. Otto, K. Haustein, S. Li, G. Vecchi, and H. Cullen. 2017. Attribution of Extreme Rainfall from Hurricane Harvey, August 2017. *Environmental Research Letters*, 12, 124009, doi: 10.1088/1748-9326/aa9ef2.
- Risser, M., and M. Wehner. 2017. Attributable Human-Induced Changes in the Likelihood and Magnitude of the Observed Extreme Precipitation during Hurricane Harvey. *Geophysical Research Letters*, doi: 10.1002/2017GL075888.
- Ryu, J.-H., K. Hayhoe. 2017. Observed and CMIP5 Modeled Influence of Large-Scale Circulation on Summer Precipitation and Drought in the South-Central United States. *Climate Dynamics*, 49, 4293-9310, doi: 10.1007/s00382-017-3534-z.
- Ryu, J.-H., K. Hayhoe, S.-L. Kang. 2018. Projected Changes in Summertime Circulation Patterns Imply Increased Drought Risk for the South-Central United States. *Geophysical Research Letters*, 45, 11447-11455, doi: 10.1029/2018GL080593.
- Schwalm, C.R., S. Glendon, and P.B. Duffy. 2020. RCP8.5 tracks cumulative CO2 emissions. Proceedings of the National Academy of Sciences of the United States of America, doi: 10.1073/pnas.2007117117.
- Shepherd, A., E. Ivins, E. Rignot et al. (86 more authors). 2020. Mass Balance of the Greenland Ice Sheet from 1992 to 2018. *Nature*, 579, 233-239, doi: 10.1038/s41586-019-1855-2.
- Shiva, J.S., D.G. Chandler, and K.E. Kunkel. 2019. Localized Changes in Heatwave Properties Across the United States. *Earth's Future*, 7, 300-319, doi: 10.1029/2018EF001085.
- Smith, A.B. 2020. U.S. Billion-dollar Weather and Climate Disasters, 1980 - present (NCEI Accession 0209268). NOAA National Centers for Environmental Information. Dataset. doi: 10.25921/stkw-7w73. Accessed August 2020.
- Stoner, A. M. K., K. Hayhoe, X. Yang, and D. J. Wuebbles. 2012. An asynchronous regional regression model for statistical downscaling of daily climate variables. *International Journal of Climatology*, 33, 2473-2494, doi: 10.1002/joc.3603.
- Sweet, W.V., R. Horton, R.E. Kopp, A.N. LeGrande, & A. Romanou. 2017. Sea level rise. In: *Climate Science Special Report: Fourth National Climate Assessment, Volume I* [Wuebbles, D.J., D.W. Fahey, K.A. Hibbard, D.J. Dokken, B.C. Stewart, and T.K. Maycock (eds.)]. U.S. Global Change Research Program, Washington, DC, USA, pp. 333-363, doi: 10.7930/J0VM49F2.
- Taylor, P.C., W. Maslowski, J. Perlwitz, & D.J. Wuebbles. 2017. Arctic changes and their effects on Alaska and the rest of the United States. In: *Climate Science Special Report: Fourth National Climate Assessment, Volume I* [Wuebbles, D.J., D.W. Fahey, K.A. Hibbard, D.J. Dokken, B.C. Stewart, and T.K. Maycock (eds.)]. U.S. Global Change Research Program, Washington, DC, USA, pp. 303-332, doi: 10.7930/J00863GK.

- Trenberth, K.E., L. Cheng, P. Jacobs, Y. Zhang, J. Fasullo. 2018. Hurricane Harvey Links to Ocean Heat Content and Climate Change Adaptation. *Earth's Future*, 6, 730-744, doi: 10.1029/2018EF000825.
- Vose, R.S., D.R. Easterling, K.E. Kunkel, A.N. LeGrande, & M.F. Wehner. 2017. Temperature changes in the United States. In: *Climate Science Special Report: Fourth National Climate Assessment, Volume I* [Wuebbles, D.J., D.W. Fahey, K.A. Hibbard, D.J. Dokken, B.C. Stewart, and T.K. Maycock (eds.)]. U.S. Global Change Research Program, Washington, DC, USA, pp. 185-206, doi: 10.7930/JON29V45.
- Wehner, M.F., J.R. Arnold, T. Knutson, K.E. Kunkel, and A.N. LeGrande. 2017: Droughts, floods, and wildfires. In: *Climate Science Special Report: Fourth National Climate Assessment, Volume I* [Wuebbles, D.J., D.W. Fahey, K.A. Hibbard, D.J. Dokken, B.C. Stewart, and T.K. Maycock (eds.)]. U.S. Global Change Research Program, Washington, DC, USA, pp. 231-256, doi: 10.7930/JOCJ8BNN.
- World Meteorological Organization (WMO). 2014. "Climate Data and Data Related Products". World Meteorological Organization. Archived from the original on 1 October 2014. Available online at: http://web.archive.loc.gov/all/20141001233620/https%3A/www.wmo.int/pages/themes/climate/climate_data_and_products.php
- Wuebbles, D.J., D.R. Easterling, K. Hayhoe, T. Knutson, R.E. Kopp, J.P. Kossin, K.E. Kunkel, A.N. LeGrande, C. Mears, W.V. Sweet, P.C. Taylor, R.S. Vose, & M.F. Wehner. 2017. Our globally changing climate. In: *Climate Science Special Report: Fourth National Climate Assessment, Volume I* [Wuebbles, D.J., D.W. Fahey, K.A. Hibbard, D.J. Dokken, B.C. Stewart, and T.K. Maycock (eds.)]. U.S. Global Change Research Program, Washington, DC, USA, pp. 35-72, doi: 10.7930/J08S4N35.
- Zamuda, C., D.E. Bilello, G. Conzelmann, E. Mecray, A. Satsangi, V. Tidwell, and B.J. Walker. 2018: Energy Supply, Delivery, and Demand. In *Impacts, Risks, and Adaptation in the United States: Fourth National Climate Assessment, Volume II* [Reidmiller, D.R., C.W. Avery, D.R. Easterling, K.E. Kunkel, K.L.M. Lewis, T.K. Maycock, and B.C. Stewart (eds.)]. U.S. Global Change Research Program, Washington, DC, USA, pp. 174-201. doi: 10.7930/NCA4.2018.CH4.
- Zhang, W., G. Villarini, G.A. Vecchi, and J.A. Smith. 2018. Urbanization Exacerbated the Rainfall and Flooding caused by hurricane Harvey in Houston. *Nature*, 563, 384-388, doi: 10.1038/s41586-018-0676-z.